SOIL WATER INTERACTIONS IN SOUTHERN AFRICAN AGROFORESTRY SYSTEMS

SVENJA-MARIA HOFFMEISTER

SOIL WATER INTERACTIONS IN SOUTHERN AFRICAN AGROFORESTRY SYSTEMS

Zur Erlangung des akademischen Grades einer

DOKTORIN DER NATURWISSENSCHAFTEN
(Dr. rer. nat.)

von der KIT-Fakultät für
Bauingenieur-, Geo- und Umweltwissenschaften
des Karlsruher Instituts für Technologie (KIT)
genehmigte

DISSERTATION

von
M. Sc. Svenja-Maria Hoffmeister
aus Dinslaken

Tag der mündlichen Prüfung:
24. April 2025

REFERENT: Prof. Dr. Erwin Zehe
KORREFERENT: Prof. Dr. Anke Hildebrandt

Karlsruhe 2025

Dedicated to Life

"The ideal state of equilibrium, like human happiness, may never be achieved in practise, but its natural pursuit is a universal rule."

Hillel (2004). Introduction to Environmental Soil Physics,chap. 8, p. 150

CONTENTS

LIST OF FIGURES

LIST OF TABLES

ABSTRACT

Over 61% of Southern Africa's population relies heavily on agriculture in order to support their livelihoods (Dixon et al., 2001). However, climate change has reduced agricultural productivity by over 34 % during the last 60 years and is expected to negatively impact growth conditions due to shorter seasons and increased water stress (Trisos et al., 2022). Regional shifts in precipitation, soil nutrient depletion, and erosion further threaten food security (Niang et al., 2014; Mbow et al., 2014; Montanarella et al., 2016; Olsson et al., 2019). Sustainable agroecological and agroforestry systems (AFSs) offer promising solutions by enhancing food security and ecosystem health while providing water, nutrition, income, and recreation (Trisos et al., 2022). However, the introduction of trees into monoculture systems may lead to competition over resources.

This thesis aimed to enhance the understanding of soil-water-plant processes in AFSs in the light of their potential to mitigate climate change challenges in agriculture. The specific objectives of the thesis were to (I) improve understanding of the impacts of AFSs on soil water dynamics and how to monitor key processes of soil water dynamics, (II) evaluate the influence of carbon addition on soil structure and stability and therefore on soil hydrological properties and dynamics, and (III) to explore process-based hydrological modelling of soil water dynamics under dry conditions and their potential use for AFS management decisions.

The study in chapter 2 investigated the hydrological and pedological impacts of an Italian Alder windbreak on a blackberry orchard in South Africa's Western Cape, a region facing water scarcity. Specifically, the influence of the AFS on the water balance was targeted by combining measurement campaigns (soil sampling for nutrient analyses, soil physical and hydrological properties, laser scanning to describe the windbreak in great detail) with high-frequency monitoring (meteorological variables together with soil water content and matric potential to analyses soil water responses to rain events and dry periods through analyses of soil water storage and root water uptake) over a six-month period.

Chapter 3 addresses how soil C accumulation in two Malawian Gliricidia-maize intercropping systems influences soil structure and stability and subsequently soil water properties and dynamics. Two long-term experimental sites with each a Gliricidia-maize plot and sole-maize control plot were extensively sampled (nutrients, soil carbon, density fractionation, porosity, bulk density, conductivity, water retention) and for a period of three months monitored (air temperature

and relative humidity, precipitation, soil water content and soil matric potential).
Chapter 4 describes how soil water retention models and variations in the permanent wilting point (PWP) influence the results of physically-based hydrological modelling under dry conditions. The data obtained during the field work of chapter 2 were used to parametrise the domain and as driving forces for the model.
The results of all three chapters can be summarized as followed:

I The studies demonstrated the versatile influences of trees on monoculture fields. Accumulation of soil nutrients improves soil fertility but also impacts soil structure and stability. Root channels, enhanced biological activity and improved soil stability influence soil infiltration and water retention capacities. Furthermore, trees influence microclimatic patterns through wind shielding effects or interception. While competition over resources like water and nutrients may occur, strategies minimizing this are available, and a considerate combination of plant and trees can prevent such competition.

II Diverse measurement combinations such as campaign based sampling for soil physical properties covering the spatial variation alongside soil hydrological monitoring for the temporal dimension aid in capturing dominant ecohydrological processes. Careful planning and testing of sensor networks is crucial for successful acquisition of high-quality data. Despite challenges in technology limitations (accuracy, communication issues) and related to working in the field (maintenance difficulties, power interruptions), innovative setups and advancements in technologies will improve ecohydrological measurements and data-reliability.

III The physically-based model struggled in accurately representing soil drying processes as well as variability in the rain events. The choice of the soil hydraulic model and the assumption of a constant PWP strongly impact water availability, which in turn may influence water management in the form of e.g. irrigation timing and amounts. The selection of the PWP not only affects plant water availability but also determines when soil water becomes insufficient to sustain evapotranspiration and related latent heat fluxes. The incoming radiation is then only transformed into sensible heat, which further impacts land-surface modelling even at larger scales.

Key findings highlight the importance of tailored AFS designs, interdisciplinary collaboration, and improved observational methods, such as integrating sap flow sensors and matric potential measurements, particularly in water-limited regions. Long-term research trials like those in Malawi are vital for studying slow-developing systems

and soil changes, while holistic models incorporating wind and sun shielding, distributed root water uptake, and energy dynamics are necessary for accurate predictions and better management. Addressing uncertainties in transpiration estimates and shifts in dominant processes between wet and dry conditions is critical for advancing water resource management in AFSs.

ZUSAMMENFASSUNG

Mehr als 61 % der Bevölkerung aus der Region des südlichen Afrikas sind stark von der Landwirtschaft als Lebensgrundlage abhängig (Dixon et al. 2001). Der Klimawandel hat jedoch die landwirtschaftliche Produktivität in den letzten 60 Jahren um mehr als 34 % verringert und wird Wachstumsbedingungen mit hoher Wahrscheinlichkeit aufgrund kürzerer Vegetationszeiten und erhöhten Wassermangels verschlechtern (Trisos et al. 2022). Zudem bedrohen regionale Verschiebungen in Niederschlägen zusammen mit Nährstoffverarmung und erhöhter Erosionsanfälligkeit die Nahrungsmittelsicherheit (Niang et al. 2014; Mbow et al. 2014; Montanarella et al. 2016; Olsson et al. 2019). Nachhaltige agrarökologische und agroforstwirtschaftliche Systeme (AFS), also die Integration von Bäumen auf landwirtschaftlichen Flächen, bieten vielversprechende Lösungen, indem sie die Sicherheit der Nahrungsgrundlage und die Gesundheit der Ökosysteme verbessern und gleichzeitig Wasser, Einkommen und Erholung bieten (Trisos et al. 2022). Die Einführung von Bäumen in Monokulturen kann jedoch zu einem Wettbewerb um Ressourcen führen.
Zielsetzung dieser Arbeit ist es, Boden-Wasser-Pflanzen-Prozesse in AFS im Hinblick auf ihr Potenzial, den Herausforderungen des Klimawandels in der Landwirtschaft entgegenwirken zu können, zu verstehen. Die spezifischen Ziele sind (I) ein verbessertes Verständnis über die Auswirkungen von AFS auf die Bodenwasserdynamik und wie Schlüsselprozesse des Bodenwasserhaushaltes gemessen werden können, (II) die Evaluierung des Einflusses von Kohlenstoffzunahme auf die Bodenstruktur und -stabilität und somit auf die bodenhydrologischen Eigenschaften und Dynamiken sowie (III) die Erprobung prozessbasierter hydrologischer Modellierung unter trockenen Bedingungen und deren potenzieller Einsatz für AFS-Managemententscheidungen.
Die Studie in Kapitel 2 untersuchte hydrologische und bodenkundliche Auswirkungen einer Windschutzhecke auf eine Brombeerplantage am Western Cape, Südafrika, eine von Wasserknappheit betroffene Region. Konkret wurde der Einfluss von einem AFS auf den Wasserhaushalt durch die Kombination von Messkampagnen (Bodenproben für Nährstoffanalysen, bodenphysikalische und hydrologische Eigenschaften, Laserscanning zur detaillierten Beschreibung der Windschutzhecke) mit hochfrequenten Messungen (meteorologische Parameter kombiniert mit Bodenwassergehalt und Matrixpotenzial zur Untersuchung von Bodenreaktionen auf Regenereignisse und Trockenperioden durch Betrachtung der Bodenwasserspeicherung und der Wurzelwasseraufnahme) über einen Zeitraum von sechs Monaten untersucht.

Kapitel 3 befasst sich mit den Auswirkungen der Anreicherung von Kohlenstoff im Boden in zwei malawischen Gliricidia-Mais-AFSs auf die Bodenstruktur und -stabilität und damit auf die Bodenwassereigenschaften und -dynamik. Zwei Langzeitversuchsflächen mit je einer Gliricidia-Mais-Fläche und einer Kontrollfläche mit ausschließlich Maisbepflanzung wurden umfassend beprobt (Nährstoffe, Kohlenstoffgehalt, Dichtefraktionierung, Porosität, Lagerungsdichte, Leitfähigkeit, Wasserretentionseigenschaften) und über einen Zeitraum von drei Monaten mit Hochfrequenzmessungen (Lufttemperatur und relative Luftfeuchtigkeit, Niederschlag, Bodenwassergehalt und Bodenwasserpotenzial) beobachtet.
In Kapitel 4 geht es um den Einfluss von Wasserretentionsmodellen und Veränderungen des permanenten Welkepunktes (PWP) auf die Ergebnisse der physikalischbasierten hydrologischen Modellierung unter trockenen Bedingungen. Die gewonnen Daten aus Kapitel 2 dienen als Grundlage zur Parametrisierung des Gebiets und als Treiber für das Modell.
Die Ergebnisse der drei Kapitel lassen sich wie folgt zusammenfassen:

I Die Studien zeigten die vielfältigen Einflüsse von Bäumen auf Monokulturfelder. Die Anreicherung von Bodennährstoffen verbessert die Bodenfruchtbarkeit, wirkt sich aber auch auf die Struktur und Stabilität des Bodens aus. Wurzelkanäle, erhöhte biologische Aktivität und verbesserte Bodenstruktur beeinflussen die Wasserinfiltration in den Boden und dessen Speicherungsvermögen. Darüber hinaus verändern Bäume das Mikroklima, indem sie z.B. Windgeschwindigkeiten reduzieren oder Niederschlag abfangen. Auch wenn es zu Konkurrenz um Ressourcen kommen kann, gibt es Strategien, diese zu minimieren und durch angemessene Kombinationen von Pflanzen und Bäumen möglicherweise ganz zu verhindern.

II Vielfältige Messkombinationen wie z.B. Kampagnen zur Entnahme von Bodenproben zur Analyse bodenphysikalischer Eigenschaften, die die räumliche Varianz abdecken, und bodenhydrologische Langzeitbeobachtungen für die zeitliche Dimension helfen bei der Erfassung der wichtigsten ökohydrologischen Prozesse. Sorgfältige Planung und Prüfung von Sensornetzen ist entscheidend für eine erfolgreiche Erfassung hochwertiger Daten. Trotz der Herausforderungen, die sich aus den technologischen Beschränkungen (Genauigkeit, Kommunikationsprobleme) und der Arbeit im Feld (Wartungsschwierigkeiten, Stromausfälle) ergeben, werden innovative Einrichtungen und Fortschritte bei den Technologien die ökohydrologischen Messungen und die Zuverlässigkeit der Daten verbessern.

III Das physikalischbasierte Modell hatte Schwierigkeiten, die Trocknungsprozesse im Boden sowie die Variabilität der Regenereignis-

se genau darzustellen. Die Wahl des bodenhydraulischen Modells und die Annahme eines konstanten PWP wirken sich stark auf die Wasserverfügbarkeit aus, was wiederum das Wassermanagement beeinflussen kann, z.B. in Form von Bewässerungszeitpunkten und -mengen. Die Wahl des PWP beeinflusst nicht nur die Pflanzenwasserverfügbarkeit, sondern auch, ab wann latente Wärmeflüsse unterbunden werden, wodurch sich die sensiblen Wärmeflüsse erhöhen, was wiederum Auswirkungen auf die Landoberflächenmodellierung auch auf größeren Skalen hat.

Die Ergebnisse unterstreichen die Bedeutung angepasster AFS-Konzepte, interdisziplinärer Zusammenarbeit und verbesserter Beobachtungsmethoden wie z.B. die Integration von Saftflusssensoren und Messungen des Matrixpotenzials, insbesondere in wasserarmen Regionen. Langfristige Forschungsversuche wie in Malawi sind für die Untersuchung von sich langsam entwickelnden Systemen und Bodenveränderungen unerlässlich. Ganzheitliche Modelle, die Windschutz, Schattenwurf, tiefenverteilte Wurzelwasseraufnahme sowie Energiedynamiken mit einbeziehen, sind für genauere Vorhersagen und eine bessere Bewirtschaftung notwendig. Die Verringerung von Unsicherheiten in Transpirationsschätzungen sowie die Berücksichtigung, dass unter nassen und trockenen Bedingungen unterschiedliche Prozesse überwiegen, sind entscheidend für erfolgreiches resourcenschonendes AFS-Management.

Part I

INTRODUCTION

1

INTRODUCTION

It has been suggested that the livelihoods of more than half of southern Africa's population (61 %) strongly depend on agriculture for their livelihoods through active engagement (Dixon et al., 2001). However, recent developments have led to a decrease in crop yields and agricultural productivity (more than 34 % since 1961) in Africa due to climate change. Further negative impacts are expected, which may be attributed to shorter growing seasons and increased water stress (Trisos et al., 2022). Near future climate change impacts may result in changes in regional precipitation amounts and distribution (Niang et al., 2014), which will influence plant water availability (Trisos et al., 2022), and hence, directly impact the food supply for local populations. The importance of soil is evident in the summary by Lal et al. (2021) of the role of soil in achieving the Sustainable Development Goals (SDGs). Soil health and soil water dynamics directly address some of the SDGs, while others address them indirectly through e.g. plant production. Soils are threatened by nutrient depletion (Mbow et al., 2014) and erosion (Montanarella et al., 2016; Olsson et al., 2019), again directly affecting food production (e.g Tumushabe, 2018; World Food Programme, 2019).

Agroecological and agroforestry systems (AFSs) offer sustainable opportunities for food security in the light of climate change and a growing population (Kwesiga et al., 2003; Nair, 2007; Mbow et al., 2014; Kuyah et al., 2019; Sileshi et al., 2020; Trisos et al., 2022). An improved understanding of these environmental systems from an interdisciplinary perspective allows more sustainable and effective management of land use units, providing, among other factors, water, nutrition, income, and recreation benefits while promoting healthy and functional ecosystems. AFSs have been shown to carry numerous benefits, such as preventing erosion, improving biodiversity and soil fertility, and providing additional income sources (Sheppard et al., 2020a).

Since trees also require water and nutrients, their influence on soil-water interactions may result in competition over these resources. Approximately 40 % of the world is classified as dry regions fighting severe water limitations at least part of the year (Cherlet et al., 2018). This situation, therefore, requires a thorough understanding of soil water and plant interactions to properly inform about water management in such systems.

Investigating different plant combinations under varying pedological and climatic conditions helps to learn about beneficial and competing

consequences. Interdisciplinary approaches are necessary to improve our understanding of AFSs through field observations and modelling of key processes.
AFSs play an important role in shaping a more resilient and sustainable agricultural landscape (also outside of southern Africa). They have the potential to improve soils and optimise water use efficiency, therefore representing sustainable solutions also based on traditional cultivation techniques, which have, however, not yet been sufficiently investigated using quantitative approaches. In line with Sheppard et al. (2020a), I apply the term "southern Africa" orientated on the Southern African Development Community (SADC) member states, and part of the commonly nominated sub-Saharan African (SSA) region".

This thesis begins with an introduction to AFSs (section 1.1), followed by a theoretical background on soil, water, and plant dynamics (section 1.2), focussing on dominant processes in AFSs, methods for their quantification (section 1.3) through measurements and modelling. After stating the thesis's objectives (section 1.4), the following three chapters (chapters 2, 3 and 4) consist of one published paper and two manuscripts, respectively. In chapter 5, I will synthesis the key findings of the three studies and discuss them together with observational and modelling methods before ending with concluding remarks and an outlook.

1.1 AGROFORESTRY CONCEPT AND BENEFITS

Multifunctional land use concepts such as AFSs have been promoted as a mitigation strategy to overcome challenges arising from changing climatic conditions (Nair, 2012; Pachauri, 2012). AFSs consist of at least two different plant types, of which one is always a woody perennial, or a combination with livestock interacting on the same land management unit in space or time (Nair, 1993; Leakey, 1996). A suitable combination and arrangement of plant species for the respective climate and site can provide a variety of benefits (Sheppard et al., 2020a) such as protection against soil erosion, excessive evapotranspiration, or nutrient depletion (Cleugh, 1998; Littmann and Veste, 2008; Makate et al., 2019). Furthermore, AFSs promote a more sustainable and diversified land use in contrast to monocropping systems (Jose, 2009; Mbow et al., 2014; Wilson and Lovell, 2016; Rosenstock et al., 2019).

Definition AFS

AFS benefits

Water availability

Competition for water and nutrients is often feared when implementing AFSs and the hydrological effect of the introduction of trees can range from mutual benefit to critical competition based on location, environment, and availability of resources. Different studies found more soil water in plots without trees than in the ones with trees; further, the soil water content decreased the closer approaching a tree

(Odhiambo et al., 2001; Siriri et al., 2013). Several factors determine the availability of water within AFSs. Aside from the plants involved, the most critical aspects are soil characteristics and climatic conditions (e.g. precipitation, air temperature, wind speed and direction), which control plant evapotranspiration.

Water management

Different management strategies were developed to reduce the competition between trees and crops in AFSs. One such method is pruning or coppicing, because shoot removal results in less transpiration of trees (Burgess, 2011). Trees often need to develop a deeper root system as a result of ploughing, which cuts the roots near the surface, and therefore, leaves more space in the topsoil for shallower rooting agricultural crops (Singh et al., 1989; Korwar and Radder, 1994). Further, Sekiya et al. (2011) pruned deep-rooted forage plants and showed that the plants continued nursing surrounding crops by lifting up water from deeper soil layers. Leffler et al. (2005) showed that roots can transport water even if undergoing senescence. Analogous to nutrient safety-nets, this is referred to as "water-safety net" (Burgess, 2011). This complementary use of water from different depths or at different times increases the overall water use efficiency of a unit area. The concept of coexistent water use of different plant species has also been studied using the term "hydrological niches" (Silvertown et al., 2015).

1.2 SOIL-WATER-PLANT INTERACTIONS

1.2.1 *Basic concepts of soil water in the partially saturated zone*

Soils form as weathering products from regoliths and are a mixture of mineral particles, water, and air. The composition, soil particle distribution, and ratio between water and air in voids, determine water movement and availability in the soil. Soil and water are, next to light, of primary importance for plant growth. The interplay between soil and water in the unsaturated zone, expanding between the soil surface to the water table, is complex, and several aspects will be addressed in this chapter.

Soil water

The term soil water describes the content of water in the soil. Soil water content or soil moisture is considered to be the water amount (expressed in volume or weight), which can be removed by oven drying at 105-110 °C (DIN EN ISO 17892-1:2022-08, 2022).

Soil water flow

The movement of water in the soil under unsaturated conditions is expressed using the Darcy equation:

$$q(\theta) = -K(\theta)\frac{\partial \Psi_m(\theta) + z}{\partial z} \tag{1.1}$$

with the soil water flux density q [m s^{-1}], the hydraulic head $H = \Psi_m(\theta) + z$ [m], the gravitational head z [m], and the hydraulic conductivity $K(\theta)$ [m s^{-1}], which is dependent on the volumetric soil water content (θ) and the matric potential (Ψ_m) [m].

Hydraulic conductivity

Both the matric potential and the hydraulic conductivity are functions of the water content (eq. 1.1), which is a crucial aspect of water flow in the unsaturated zone. The hydraulic conductivity expresses the rate at which water moves through a porous medium and is dictated by pore size and soil water content. Hydraulic conductivity increases with increasing water content and pore size.

Matric potential

The matric potential, takes negative values in unsaturated conditions. Its absolute values increase with declining water content and declining pore size. It is linked to attractive forces between the soil and liquid water, which bind water within the pores or capillaries. These forces determine how strongly water is retained in the soil. This is the main reason why it is critically important for the plant and crop system as it is the force or tension that plants must overcome in order to extract water from the soil.

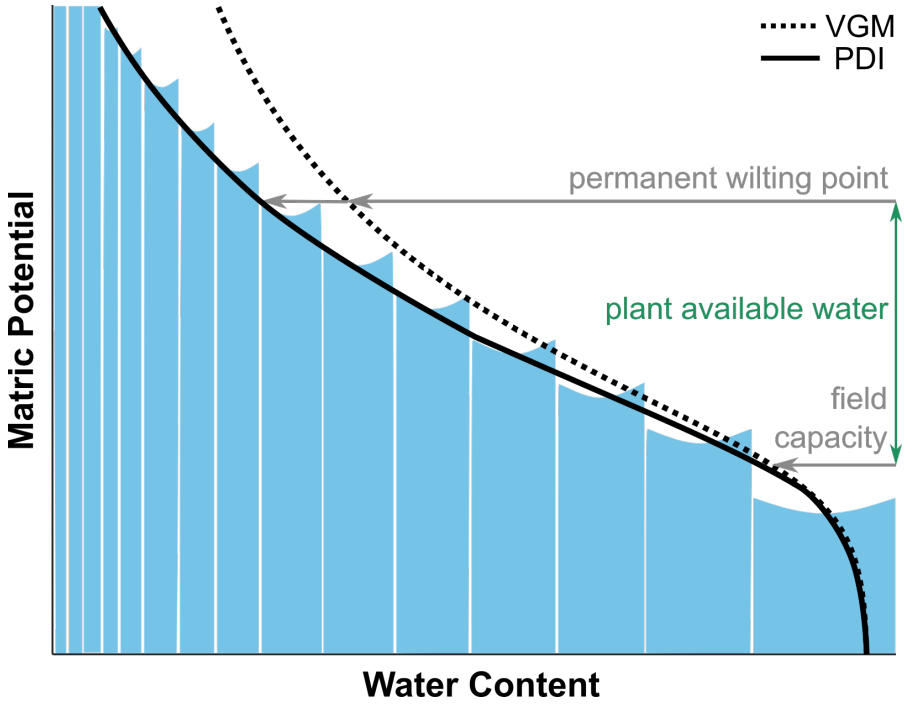

Figure 1.1: Soil water retention curve and pore size relationship for the Van Genuchten/Mualem (VGM) and Peters-Durner-Iden (PDI) soil hydraulic models (adapted from Dyck and Peschke, 1995)

Soil water retention curve

The non-linear relationship between soil water content and matric potential is decribed by the soil water retention curve (Fig. 1.1). It is a fundamental physical property describing the time- and space-variability of a given soil. The matric potential is zero when the soil is saturated (water content = porosity). The water content changes little with increasing matric potential until a point of infliction is reached, when significant volumes of air start appearing in the soil pores (air-entry pressure/point, equation 1.2). Beyond the air-entry pressure water drains rapidly from the larger pores until successively depleting the smaller ones. Extracting residual water under dry conditions requires sufficient pressure to exceed the water's molecular forces of attraction, which hold it in the mostly air-filled pores through surface tension and electrochemical forces (Scott, 2000). The curve is also influenced by the drying and wetting history of the soil (Rubin, 1967; Perrens and Watson, 1977).

Soil texture

At low matric potential, the soil water retention curve is strongly influenced by soil texture. Soil texture describes the relative fractions of particles (clay, other minerals, rock fragments) of different size ranges contained within a given soil (Scott, 2000) and is considered a static variable considering human lifespans but can change over long timescales. Different soil textural classes draw distinct soil water retention curves, particularly in the wet range. Typically, sandy soils allow for air to enter the soil at high soil water contents permitting rapid water drainage (Scott, 2000). The air-entry point of clayey soils occurs at a higher water content and the change in the curve slope is slower, indicating the larger water volumes retained in this type of soil.

Soil structure

Two soils of a similar texture may still show different behaviours due to distinct differences in the way the particles are arranged. Soil structure describes how particles and pores are arranged or organised into complex and irregular patterns (Scott, 2000; Hillel, 2004). Particles are bound together by physical-chemical (freezing/drying, attraction of metallic oxides or carbonates) and biological processes (organic matter, organic glues of e.g. fungi). Intensive land management with heavy machinery such as ploughing or harvesting deteriorates the soil structure, for example, through compaction. At high matric potentials, the water retention curve is greatly influenced by the soil structure. This was observed, for instance, by Jackisch et al. (2017), who demonstrated strong influences on estimated retention parameters as a result of aggregated fine material presented in a network of highly conductive course pores.

1.2.2 *The influence of plants on soil water dynamics in AFSs*

S:P:A:C

Water movement in the environment occurs interdependently between the pedosphere, the atmosphere and biosphere, which form a "physic-

ally unified and dynamic system" (Scott, 2000). Water flows within the so called "soil-plant-atmosphere continuum" (S:P:A:C) from regions of higher total potential to regions of lower total potential (Philip, 1966). Figure 1.2 summarises the dominant processes involved in soil-water-plant dynamics on the plot scale, which comprise precipitation, infiltration, redistribution, runoff and evapotranspiration. Focusing primarily on AFSs, I draw examples from this context.

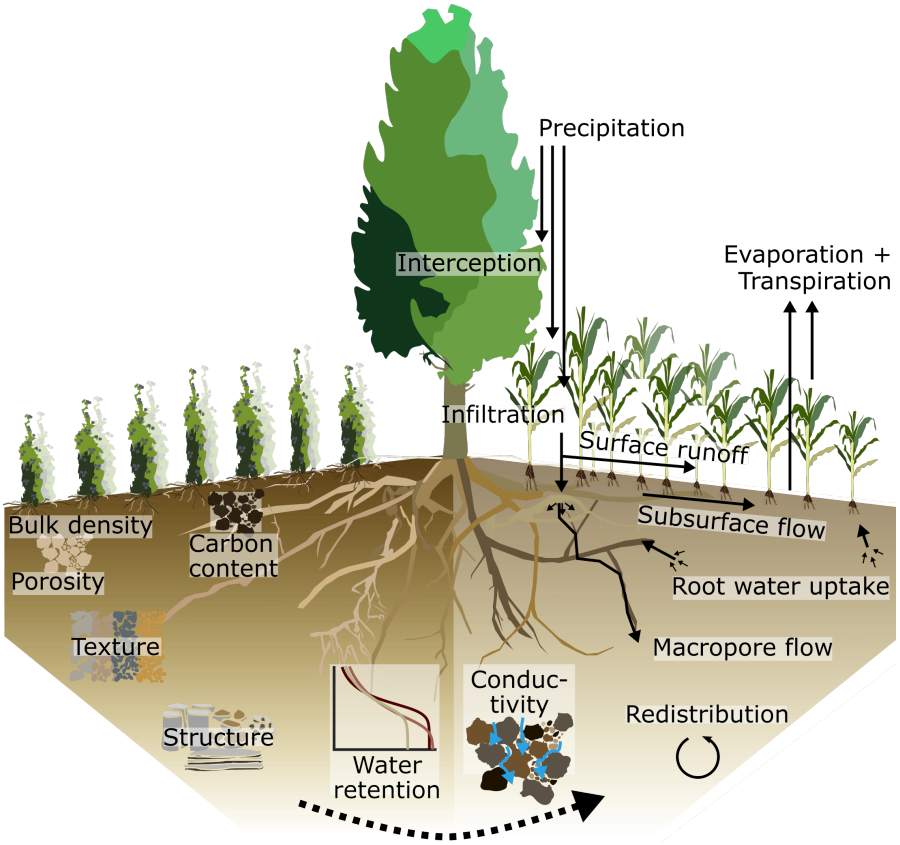

Figure 1.2: Illustration of key processes involved in soil-water-plant interactions exemplified in an AFS. The left-hand side depicts soil characteristics that influence the water movement processes on the right-hand side, mainly connected through the characteristics in the middle column (water retention and conductivity)

Precipitation and interception

The amount of precipitation reaching the soil varies depending on the presence and type of vegetation. Two effects are taking place (1) microclimatic effects and (2) interception. Larger structures, such as windbreaks, have the dominant effect of reducing low frequency high impact storm events. A turbulent mixing-layer forming above the windbreak determines the air flow behind the windbreak. These turbulences influence microclimatic patterns such as temperature, heat or relative humidity as well as the evapotranspiration in the vicinity (Cleugh, 1998; Veste et al., 2020; Jacobs et al., 2022).
Vegetation can create or alter precipitation throughfall patterns by interception depending on plant species and arrangement, which in

turn influences together with trunkflow the local infiltration, and therefore, the soil moisture (Tietjen et al., 2010). Fischer-Bedtke et al. (2023) found that throughfall patterns in a mixed-beech forest (70 % *Fagus sylvatica*) correspond to soil moisture dynamics, i.e. increases in soil water storage occurred at locations with more throughfall.

Infiltration

Infiltration determines how much water enters the soil and how much remains at the surface either ponding or forming surface runoff, the main driver for soil erosion by water. Its is quantitively described by the infiltration rate and the cumulate infiltration amount and is governed by either the precipitation rate as long as it does not exceed the infiltrability or hydraulic conductivity. Infiltration occurs either directly into deeper layers through macropore flow, rapid flow of water in large pores bypassing large fractions of the soil matrix, or by slow percolation or matrix flow which stores it near the soil surface. It is one of the processes strongly influenced by soil characteristics as coarse-textured soils have a higher conductivity and, similarly, a higher infiltrability. The relation between soil water content and conductivity remains unchanged for a stable soil structure (Scott, 2000). Tree roots develop to larger rooting depths than agricultural crops. Root growth favours soil structure development, thereby increasing soil water infiltration rate and capacity (Dalland et al., 1993; Anderson et al., 2009; Mwangi et al., 2016; Rosenstock et al., 2019). Roots and biological organisms (earthworms, insects) create channels through which macropore flow significantly contributes to infiltration (Jarvis, 2007; Beven and Germann, 2013;). If not infiltrated, moisture is redistributed as surface runoff along topographic gradients, which can have an important feedback on the habitat of soil fauna (worms) and plants (e.g. Zehe and Blöschl, 2004; Schaik et al., 2014).

Redistribution

Water in the soil is redistributed by following gradients in the total potential, moving from wetter to drier regions within the soil profile. The direction of flow can therefore be downward or lateral, but also upward from deeper wetter layers to drier shallower soils. The so called ”hydraulic lift” within the root system was first observed in the field by Richards and Caldwell (1987), who found a larger nocturnal increase of soil water potential in the topsoil than could be solely explained by water movement in the soil. During the night, the root system transported water from deeper wetter soils upwards and lost the water to the drier topsoil, who lost water due to daytime transpiration. This way more soil moisture can be stored and used by plants during the day (Burgess et al., 1998), potentially hindering full stomatal closure and supporting nutrient uptake and cycling (Domec et al., 2004). Hydraulic lift from deeper to shallower depths in the soil favours shallow rooting plants including many annual agricultural crops. It makes that water fraction available, which is especially important during dry periods in arid regions (Burgess, 2011; Bayala and Prieto, 2019). As the water movement through the root

system can also be downward or lateral Burgess et al. (1998) suggested to name it hydraulic redistribution. The presence of the root system additionally affects bulk density and aggregate stability. Sileshi et al. (2014) summarized in their review concerning a number of African countries, that fertilizer trees also improve soil physical properties including bulk density and aggregate stability, which is directly linked to soil water flow.

Evapotranspiration

The largest sink of soil water is evaporation and transpiration, or evapotranspiration. It describes the movement of water from the soil or plant surface into the atmosphere, where it can be further redistributed over larger regions. Evaporation is a two-stage process in regions with deep water tables. In the first stage, evaporation is governed by the energy input (radiation) and atmospheric conditions (relative humidity and wind speed) and soil surface characteristics. Due to their capability of storing more water and higher unsaturated hydraulic conductivities, will fine-textured soils persist longer in this stage than coarser ones. Soil hydraulic conductivity controls the second stage of evaporation by supplying water from below to the soil surface, thus reducing the importance of radiative energy (Scott, 2000). Similarly, transpiration is governed by meteorological, plant, and soil factors. The more the soil dries out, the higher the pressure that plants need to overcome in order to extract water from the soil.

RWU

Root water uptake (RWU) and evapotranspiration connect the water cycle between the pedosphere and the atmosphere (Schneider et al., 2010; Seneviratne et al., 2010; Asbjornsen et al., 2011; Guderle et al., 2018). Knowledge of these fluxes is key to understanding plant-soil-water relations, in particular when interested in plant water use, water redistribution and competition over resources (Davis and Mooney, 1986; Chirwa et al., 1994; Hildebrandt and Eltahir, 2007; Arnold et al., 2009; Everson et al., 2009; Guderle and Hildebrandt, 2015; Wu et al., 2016). It has also frequently been used as a proxy to estimate transpiration fluxes (Jarvis, 1989; Guderle and Hildebrandt, 2015; Guderle et al., 2018; Jackisch et al., 2020). RWU is determined by plant characteristics including size, extension of the root system, transpiration rate and soil properties. Demir et al. (2024) showed that RWU patterns were rather dominated by soil water distribution and characteristics of neighbouring trees than soil characteristics.

PWP

The water content at which the leaves of a plant reached a wilting stage from which they cannot recover is called the permanent wilting point (PWP). The work of Richards and Weaver (1943) was central to the adoption of the widely distributed wilting point concept, which defines the PWP as the water content retained in the soil under a matric potential of -15000 hPa. Experiments to measure the wilting point are tedious work, but several studies were conducted showing that the PWP contains a rather high variability. Cotton (*Gossypium hirsutum L.*) under field conditions wilted at -15000 hPa (Savage et al.,

1996) while maize (*Zea mays L.*) wilted within -22000 to -30000 hPa in the root hair zone (Hsieh et al., 1972) and greenhouse pepper (*Capsicum spp.*) at -37000 hPa (Rawlins et al., 1968). The water content at field capacity (FC, -330 hPa) describes the maximum of water stored in the soil against gravity.

PAW

The effective field capacity, which is the difference in water content between FC and PWP, is commonly interpreted as plant-available water (PAW). Close to FC (Fig. 1.1), small changes in matric potential correspond to high fluctuations in the water content as the slope of the water retention curve is very steep in that range.

It is critical to gain deeper understanding of the complex interactions of water fluxes, their quantities and interactions with the surrounding environment to successfully and sustainably manage AFSs. There are some studies (e.g. Kuyah et al., 2019) that have started disentangling this issue by comparing environmental conditions of AFSs with water availability and yield gains. For instance, the review by Jacobs et al. (2022) summarizes the impacts of trees on microclimate and the water balance in temperate regions. As many factors are involved in AFSs, this is a difficult task and often suitable studies and modelling exercises are missing that systematically approach this question.

1.3 QUANTIFICATION OF SOIL-WATER-PLANT INTERACTIONS

1.3.1 *Measurements*

Soil-water-plant dynamics involve many different processes 1.2, of which some are easier and some harder to observe. High-resolution data in the spatial domain, the temporal domain, or both, are required depending on the flux or property of interest to quantify the processes and expand process understanding. To this point, no established or standardized measurement protocol exists to reliably measure the different components of the soil-water-plant interactions in general or specifically in AFSs. Existing measurements can be divided into campaign-based techniques, usually covering the spatial extent at one point in time, and long-term monitoring at fewer locations, comprising temporal high-resolution techniques. Campaign-based measurements usually provide information concerning soil characterisation (e.g. soil texture, bulk density, nutrients, soil hydraulic conductivity) while monitoring stations inform on meteorological or water dynamics (e.g. precipitation, wind speed, soil storage changes, root water uptake).

Campaign-based

In soil science, soil samples are being taken in the field of interest to draw conclusions about spatial patterns in soil properties alongside a soil profile pit analysis to classify soil horizons. Due to the great small-scale spatial heterogeneity of soil properties, it is necessary to take sufficient samples and replicates to be able to quantify the variab-

ility and to improve data reliability. Laboratory analyses are, however, costly and time consuming. These typically include, among others, the analysis of soil colour, texture, bulk density, porosity, nutrients and carbon content, pH, or cations. Choosing adequate sampling designs (e.g. stratified, nested or geostatistical) can help to reduce the amount of samples while still covering enough soil variability to ensure representativeness of the data set. Soil properties develop over long time spans, therefore, a high temporal resolution is not necessary.
Likewise, in the field of hydrology, soil sampling is a common technique to determine specific soil water characteristics including water retention curves or the saturated hydraulic conductivity.

Monitoring

In recent years the development of new sensing techniques has progressed (Bogena et al., 2022; Zhang et al., 2024). It is nowadays common to install high-frequency instruments to observe water movements, which is of critical importance to capture not only variations in space but also in time as changes in intensities and return times are to be expected (Niang et al., 2014). Often, meteorological stations are equipped with instruments to measure air temperature, atmospheric pressure, relative humidity, wind speed and direction, solar radiation and precipitation amount. These data are critical for a comprehensive assessment of soil water and plant interactions.
Soil water cannot be measured directly in the field, but a number of sensors exist that measure an electrical property (e.g. relative electric permittivity or the capacitance), which can be related to soil water content. Matric potential is often measured by tensiometers, but can also be inferred from, for example, water content measured within ceramic cells in equilibrium with the surrounding soil. All methods have different advantages and disadvantages as tested and discussed by Durner et al. (2017). Disadvantages of indirect measurements are that they are often influenced by other environmental conditions such as temperature or salt conditions and produce only accurate data within certain measurement ranges. Field-specific calibrations are usually recommended by manufacturers to increase data accuracy.

1.3.2 *Modelling*

Measured time series are often not representative over larger spatial scales due to heterogeneities in e.g. soil characteristics or topography. Models imitating ecosystem processes, taking into account various influences such as soil properties, can be used to learn something about either the model by comparing it with observations, or about the ecosystem by varying certain aspects of the model parameters, so that not everything needs to be measured. One could, for instance, test varied AFS scenarios under different precipitation patterns. If a model is able to predict differences between scenarios, it would be a very helpful decision support tool for the planning or improvement of

AFSs.

AFS models

Models are also used and developed in AFS research, however, not much implemented in planning. They mostly focus on distinguished aspects such as yields and financial outcomes or nutrient cycling (e.g. Burgess and Rosati, 2018). Among the furthest developed and known AFS models are the yield and growth model YIELD-SAFE (Werf et al., 2007), Hydro-SVAT (Soil Vegetation Atmosphere Transfer), which combines basin-reservoir dynamics with eco-physiological cycles to explore ecosystem services at the landscape scale (Gómez-Delgado et al., 2011;Kay et al., 2018), and WaNulCAS, which models water, nutrient and light (Van Noordwijk and Lusiana, 1998). Soil hydrological model development in the context of AFSs has increased in recent years, but such models are often not implemented at the plot scale. Many factors determine the successful functionality of agroecosystems (e.g. plant-water availability, nutrient supply) and are therefore challenging to generalize. For management and planning strategies, such information is critical. If dominant processes such as evapotranspiration can be represented adequately in hydrological models on the plot scale, they can provide useful tools for practitioners.

Physically-based models in AFS context

Physically-based models grounded on conservation laws are capable of simulating relevant soil water process such as infiltration, lateral water flow, or evapotranspiration. After calibration to a well-monitored system, the verified model can perform virtual experiments to explore different aspects, such as e. g. the relationship between soil characteristic and bedrock topography on runoff formation (Hopp et al., 2009; Wienhöfer and Zehe, 2014; Loritz et al., 2017) or infiltration and solute dynamics (Klaus and Zehe, 2010; Klaus and Zehe, 2011). In addition to forcing data (for instance time series detailing precipitation, air temperature and wind velocity), they usually require numerous input data to characterise the pedosphere and land-use. Under dry conditions, there are especially two factors of critical importance, which will be focused on in the following paragraphs.

Soil hydraulic models

The soil water retention curve introduced in section 1.2.1 (Fig. 1.1) is a critical component in hydrological modelling. Several empirical models exist that parametrise the relationship between soil water content and matric potential (R. H. Brooks and A. T. Corey, 1964; Fredlund et al., 1994; Kosugi, 1996). The most commonly used formulation is the van Genuchten/Mualem (VGM) soil hydraulic model (Van Genuchten, 1980; Mualem, 1976) (Fig. 1.1):

$$\theta(\psi) = \theta_r + \frac{\theta_s - \theta_r}{[1 + (\alpha|\psi|)^n]^{1-1/n}} \tag{1.2}$$

with the residual water content θ_r ($cm^3\ cm^{-3}$), the saturated water content θ_s ($cm^3\ cm^{-3}$) , the scaling parameter inverse to the air-entry point α (cm^{-1}), the matric potential ψ (hPa) and the dimensionless shape parameter n.

The importance of the soil hydraulic model on modelling results was presented by Novick et al. (2022), demonstrating the huge uncertainty imposed by these parameters on the results achieved.
Peters et al. (2024) suggested an improved version for the VGM model, which differentiates between capillary and non-capillary water, promising to yield better representation of water retention parametrisation in the dry moisture range. This might be of critical importance for working under dry conditions, where the focus lies on different hydrological processes than if working with, for example, flash-floods. In paper 4, a comparison of the VGM and PDI model is performed.

Relevance of PWP

Another important but in the modelling context so far not recognised aspect, is the assumption of a universal PWP for all plants and soil types. In water-limited regions, the PWP is a key threshold that determines when soil water becomes insufficient to sustain evapotranspiration and the related latent heat flux. The incoming radiation is therefore only transformed into sensible heat, which increases surface and air temperatures at this specific location.

PWP in modelling

While the PWP is recognised as a plant and soil texture-dependent variable in the "field experimental" context, it is a static parameter in the "modelling" environment. One likely reason is the difficulty of implementing the interactions of soil properties and mechanisms of plant tolerance to water deficits in determining the wilting of a plant (Groenevelt et al., 2001; Asgarzadeh et al., 2010; Wiecheteck et al., 2020). Experiments have shown, however, that the PWP may vary substantially with soil texture and plants species as demonstrated above (Wiecheteck et al., 2020). The variability in PWP might not be so critical in determining plant-available water as the uncertainties in FC exceed the uncertainties of the PWP. Nevertheless, due to the above mentioned influence of the PWP on the energy budget, it is important to ascertain the uncertainties related to the PWP's variability. In chapter 4, variation of PWP is analysed with modelling.

1.4 PROJECT BACKGROUND AND OBJECTIVES

The work presented in this thesis was embedded in the project ASAP ("Agroforestry in Southern Africa – new Pathways of innovative land use systems under a changing climate" funded by the German Federal Ministry of Education and Research, BMBF, final Asap final report, 2023), which aimed at exploring ecosystem services and environmental benefits of AFS in southern Africa. The field work presented in chapters 2 and 3 was part of the working package on water fluxes in AFSs, in which soil water data were collected in three AFSs in South Africa and Malawi and combined with time series of basic weather data, soil moisture and soil water potential sensors.

The overall objective of this thesis closely aligns with the working package aims: Improving the understanding of soil water and plant interactions and how the key processes of these interactions (Fig. 1.2) can be observed and quantified, in the field or laboratory as well as in the modelling context.
The specific objectives of the thesis were to evaluate:

I dominant soil water processes in AFSs and the influence of trees on monocultural fields;

II comprehensive yet parsimonious measurement options to capture these dominant soil water processes in AFSs;

III challenges encountered when modelling these processes in AFSs under dry conditions.

The following three chapters consist of one published paper and two manuscripts (summarized in Fig. 1.3). They relate to the above mentioned objectives of the thesis, but touch upon several aspects of the objectives. The aim of the separate chapters were as follows:
Chapter 2: to understand the hydrological and pedological interactions of a windbreak in a blackberry orchard in a water scarce environment (South Africa) better. The suitability of capturing soil water interactions in a comprehensive way by combining campaign-based measurements and high-frequency monitoring was tested on soil (objective I and II).
Chapter 3: to evaluate the impact of Gliricidia-maize intercropping on soil C accumulation and water fluxes compared to sole maize control in two long-term experiments in Malawi. Indications for changes in soil water dynamics and soil hydraulic properties due to soil structure and stability improvement through soil C accumulation were investigated. (objective I and II).
Chapter 4: to explore process-based hydrological modelling of soil water dynamics under dry conditions and their potential use for AFS management (objective I and III). Special emphasis lies on the sensitivity of the water balance (particularly soil evaporation, plant

transpiration and storage changes) to the choice of the soil hydraulic model and to uncertainties in the PWP. Comparisons were evaluated in the frequency domain to avoid temporal shifts between signals leading to low correlation metrics (NSE or coefficient of determination (R^2) despite signals similarities (Ehret and Zehe, 2011; Seibert et al., 2016).

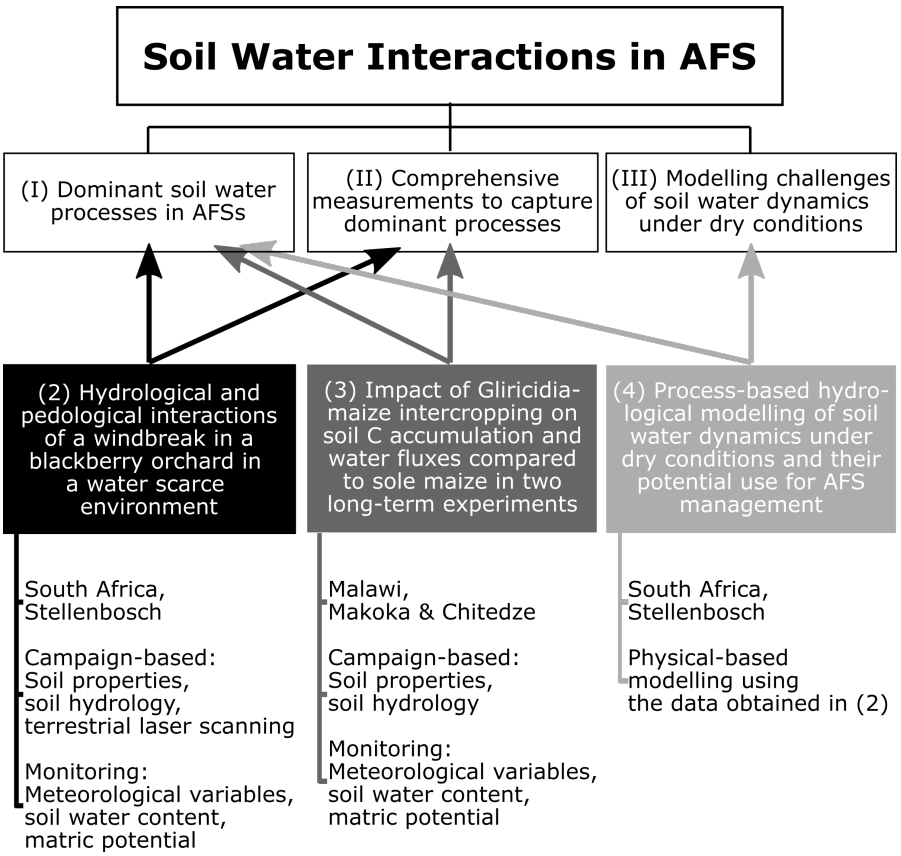

Figure 1.3: Overview of the aims of the thesis and how they relate to the chapters and methods.

Part II

HYDROLOGICAL AND PEDOLOGICAL EFFECTS IN A WINDBREAK AFS

This study is published in the scientific journal Hydrology and Earth System Science (HESS). The remainder of this part is a reprint of:

Hoffmeister, S., Bohn Reckziegel, R., du Toit, B., Hassler, S. K., Kestel, F., Maier, R., Sheppard, J. P., and Zehe, E. (2024). "Hydrological and pedological effects of combining Italian alder and blackberries in an agroforestry windbreak system in South Africa." In: Hydrology and Earth System Sciences 28.17, pp. 3963–3982. https://doi.org/10.5194/hess-28-3963-2024.

2

HYDROLOGICAL AND PEDOLOGICAL EFFECTS OF COMBINING ITALIAN ALDER AND BLACKBERRIES IN AN AGROFORESTRY WINDBREAK SYSTEM IN SOUTH AFRICA

ABSTRACT

The Western Cape in South Africa is a water scarce region which will likely receive less rainfall and higher air temperatures under projected climate change scenarios. The integration of trees within agricultural systems provides an effective measure for improving water retention on agricultural land. Studying an established and irrigated agroforestry system (AFS) combining alder (*Alnus cordata* (Loisel.) Duby) as a linear windbreak with a blackberry (*Rubus fructicosus* L.) crop, we explore the water use dynamics of the intercrop as influenced by the windbreak element by combining methods from hydrology, soil science and forestry disciplines. Our objective is to explore whether the AFS positively impacts the water balance by combining measurement campaigns to characterise the spatial variability of various key system properties with continuous monitoring.

The campaigns encompassed extensive soil sampling to determine soil characteristics (nutrient concentrations, hydraulic conductivity, texture, water retention) in the laboratory as well as terrestrial laser scans of the field site, especially of the windbreaks. The continuous measurements covered meteorological, soil water content and soil water potential observations over a 6-month period (in summer). These were applied to understand soil water dynamics during rainstorms and dry spells, including root water uptake as well as soil water storage. We recorded a total of 13 rainfall events delivering 2.5 – 117.6 mm of rainfall with maximum intensities of 4.1 to 82.6 mm h^{-1}. Further analyses showed that infiltration is likely dominated by preferential flow, with root water uptake potentially occurring in two depth zones corresponding to different plant communities. While soil water content varied by depth and was influenced by physical and environmental factors, it was generally higher in the intercrop zone than within the windbreak-influenced zone. During dry spells, soil water content did not drop below the water content of the permanent wilting point ($<$ – 1500 kPa). Values corresponding to soil water tensions above 1000 kPa were recorded on several occasions; these were mitigated by irrigation and, thus, did not result in water stress. Nutrient distribution and soil physical properties differed near the windbreak in comparison to the blackberry crop, and the carbon sequestration potential is great in

comparison to monoculture farming.
We could demonstrate positive effects of the windbreak on the water balance and dynamics in the blackberry field site, even though questions remain as to the extent of these benefits and how they compared to disadvantageous aspects brought about by the presence of the trees (e.g. increased water usage). Irrigation did, in fact, shift the AFS from a water-limited regime to an energy-limited one.

2.1 INTRODUCTION

In a changing world, agricultural flexibility and adaptation measures are required to uphold and enhance global living standards while protecting and restoring ecosystems, as well as to ensure agricultural productivity amid more frequent water shortages, particularly in the global south (Douville et al., 2021). A promising mitigation measure to address these pressing challenges is the reintegration and improvement of agroforestry systems (AFSs). AFSs describe the combination of woody perennial species with crops and/or livestock components. These system have the potential to deliver multiple benefits and offer new perspectives for existing agricultural systems including their greater resilience and productivity (Sheppard et al., 2020a). AFSs can modify existing agricultural land and take many temporal and spatial forms, differing in both composition and arrangement. Examples of commonly practised systems include alley cropping (crops/plants are grown between rows of trees or shrubs), hedgerows and windbreaks, multi-strata agroforestry (multiple layered trees and crops), parklands, boundary planting, and planted fallows (Kuyah et al., 2019). The benefits of incorporating woody perennials into agricultural systems encompass non-timber forest products, animal fodder and building materials, alongside increased household resilience (Kuyah et al., 2019; Sheppard et al., 2020a; Sheppard et al., 2020b). Simultaneously, AFSs promote a more sustainable and diversified land use (Mbow et al., 2014; Rosenstock et al., 2019; Wilson and Lovell, 2016; Jose, 2009) in contrast to conventional modern monocropping systems (Kuyah et al., 2019; Sheppard et al., 2020a). Multiple on-site environmental benefits include soil conservation, nitrogen fixation, nutrient input, improved water infiltration capacity, enhanced water quality, reduced evapotranspiration, reduced surface runoff and erosion, and stable soil fertility, leading to sustainable agricultural land use (Mbow et al., 2014; Rosenstock et al., 2019).

Tree shelterbelts and windbreaks have various impacts on the microclimate within their zone of influence, which in turn affect the water balance. The maximum zonal effect may extend 5 times the height of the windbreak downwind and for a short distance upwind (Campi et al., 2009; McNaughton, 1988). The reduction of wind speed and shading influence evapotranspiration as well as air temperature and promote dew formation, while the leaves and branches intercept rainfall. Dew formation is increased by up to 80 %, resulting in an increase in precipitation by up to 20 % and soil water content by up to 10 % (Nägeli, 1943; Van Eimern et al., 1964). Windbreaks have been found to reduce wind speed and potential evaporation on the leeward side by up to 70 % and 30 %, respectively (Veste et al., 2020; Hintermaier-Erhard and Zech, 1997; Häckel, 1999). Such windbreak effects result in reduced wind erosion and consequently less reduction

in soil quality; the wind would otherwise transport the finest topsoil fractions (alongside any nutrients) away (Shi et al., 2018; Shao, 2008). Besides reducing erosion losses, windbreaks also improve nutrient cycling efficiency (Sileshi et al., 2020). Due to their small footprint, windbreaks may only contribute moderately to direct carbon and nutrient enrichment, although the increased presence of woody biomass and related litterfall provide a benefit compared to a treeless landscape (Sheppard et al., 2024). Indirectly, however, windbreaks can increase carbon storage and soil conservation through improved crop productivity (Albrecht and Kandji, 2003). In a comprehensive review on US windbreaks, Smith et al. (2021) found that the main drivers leading to windbreak removal are the poor conditions of the trees, the age of vegetation, conflicts with irrigation and machinery, and competition with crops. The first two points highlight the importance of proper windbreak maintenance, intrinsically coupled with additional time and labour. The latter two points demonstrate how important it is to design windbreaks appropriately, so that resource competition between tree and crop can be limited by, for example, suitable spacing and choice of species in combination. Within this concert, however, the windbreak's effect on the local water balance remains a critical research challenge.

Water availability for plants is affected by many factors. While precipitation and potential evapotranspiration determine the climatic water supply and demand (Lal, 2020), the supply to demand ratio can substantially be altered by irrigation management. The most important terrain characteristics are land use, soil infiltration and soil-water-holding properties. Soil texture, organic matter content and aggregation state are important factors controlling soil hydraulic parameters, alongside climatic and vegetation factors. Soil water retention curves characterise the strength of capillary forces acting on soil water and are, thus, useful to assess both its binding status and availability to plants, especially in water-limited regions. While the corresponding soil water content at field capacity (FC) determines the maximum water storage against gravity, the water content at tensions less than the permanent wilting point (PWP = – 1500 kPa) is not plant available anymore. The effective field capacity, i.e. the difference between both values, can be interpreted as the plant-available water stock. Note that, especially around FC, small fluctuations in matric potential amount to large variations in water content due to the steep slope of the water content curve.

Our rationale is to explore the promise of AFSs of an improved water and nutrient status, using an established irrigated AFS combining alder as a linear windbreak with a blackberry crop as a benchmark system. South Africa, particularly the Western Cape region, is a water-scarce region facing severe challenges in sustaining agricultural productivity in the future due to projected increases in air temperature

and longer dry spells as a consequence of climate change (e.g. Faucher-eau et al., 2003). The high wind speeds along the coastal region result in high potential evapotranspiration (PET) and, thus, a strong atmospheric demand. The steady-state connection between the PET and the actual evapotranspiration (AET) can be assessed with the Budyko framework (Budyko, 1974). This relates the actual to potential evapotranspiration (release over demand) to the dryness index (precipitation supply over potential evaporation demand). The Budyko curve is often used to characterise the long-term average water and energy balance at catchment or regional scales and can, therefore, be used to categorise areas into different climate regimes:

1. Energy-limited settings with an aridity index (precipitation / PET) $>$ 1. More water could evaporate if more energy were available. AET is limited by the radiative energy supply (AET = PET).

2. Water-limited settings with the aridity index $<$ 1. ET is limited by the water supply (AET $<$ PET).

Windbreaks carry the potential to reduce the necessary water supply by precipitation and irrigation, ensuring sufficient water availability for crop plant growth. However, field and simulation studies investigating system-level feedbacks between trees, crops and microclimate are lacking, especially for drylands (Sheppard et al., 2020a). For this reason, we tested whether a multidisciplinary and multi-method approach to characterise an established irrigated fruit orchard in South Africa is able to close this gap and deliver a holistic system perspective on the processes affecting water availability and fluxes. Specifically, we combined various campaign-based measurements from multiple disciplines with high-frequency, long-term monitoring of water and energy balance components to capture both spatial variability and temporal dynamics. We used terrestrial laser scanning (TLS) as a novel method for investigating three-dimensional structures of trees and their shade patterns (Bohn Reckziegel et al., 2021; Raumonen et al., 2013). We took undisturbed soil samples to analyse soil physical properties, such as the site-specific water retention curve and soil hydraulic conductivity, which are key to determine the plant-available soil water storage. Transects of surface soil samples were analysed to assess the influence of the windbreak on nutrient distribution. The long-term monitoring included high-frequency soil water content and soil water potential to provide information on temporal dynamics of potential water limitation for transpiration. This was combined with meteorological records of precipitation, solar radiation, air temperature, relative humidity and wind speed, thus allowing for the characterisation of both water supply and potential evaporation demand and the related energy limitation. By merging the different methods, we could infer processes such as infiltration through the combination of nutrient

analyses with soil water dynamics during rain events or by reflecting on the energy budget through shade-cast simulations and evapotranspiration estimates. The main objective of this study was to synthesise dominant controls on water availability from these observations and to particularly evaluate the positive and negative effects of the windbreak on the water and nutrient balance and cycling in the AFS.

2.2 MATERIALS AND METHODS

2.2.1 *Site description*

The field site is located in the Western Cape Province, South Africa, close to the city of Stellenbosch on a fruit orchard located on the southern flank of the Simonsberg (Fig. 2.1) on a 30 % slope at an elevation of approximately 400 m above sea level. The region is dominated by a Mediterranean climate with hot, dry summers (Dec-Mar) and mild, moist winters (May-Sep) (Ndebele et al., 2020). Mean annual precipitation sum in Stellenbosch is 742 mm (Meadows, 2015). The regional wind system includes strong winds from the southeast that dominate the summer months.

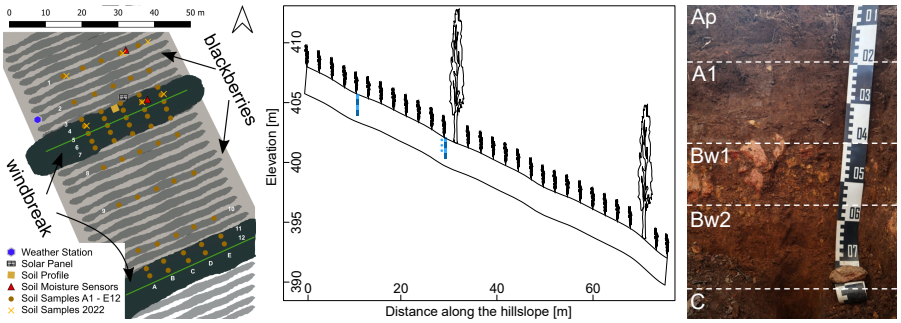

Figure 2.1: Left: Sketch of sampling design and location of the alder-blackberry AFS near Stellenbosch, South Africa. For illustrative purposes, the alder canopy is shown in green and the blackberry rows in grey shading. The triangles show the location of the soil water sensors for the monitoring, each point signifying four soil water content sensors and three matric potential at the point near the windbreak. Middle: Transect of the slope indicating the location of soil water content sensor stacks at different depths (blue rectangles) and matric potential sensors (blue circles). Right: Photograph of the soil profile with horizon delineations and characterisation as Cambic Mollic Umbrisol (loamic, humic).

The study site contains multiple single tree row windbreaks of Italian alder (*Alnus cordata* (Loisel.) Duby), a non-native deciduous tree species planted perpendicular to the prevailing wind direction. The 40 study trees are arranged in a linear form from east-northeast to west-southwest with regular between tree spacing, the studied windbreak has a length of 45 m (Fig. 2.1). The windbreak trees developed a particular oval crown shape due to the close row spacing of the windbreak

with exception of the last trees in the row, which developed a rounded crown on the row edge. The trees are approximately 15 to 20 years old and are pruned annually to limit encroachment on the first rows of the intercropping space. The study windbreaks were spaced approximately 40 m apart with blackberry (*Rubus fructicosus* L. 'Var. Waldo') canes arranged in parallel rows 2 m apart and perpendicular to the slope between each windbreak row. The 5- to 6-year-old blackberries usually start shooting in late spring (October) and are harvested from mid-January to mid-March. One month after fruiting, they are cut back to the base. In the summer months (late November to January), a drip system provided irrigation. Informally, approximately three times a week, each plant was irrigated with 2.3 L d^{-1}, distributed in cycles of 10 min. Once a year, before spring, a slow-release fertiliser was applied.

2.2.2 *Field measurements, sampling, monitoring and laboratory analyses*

A field campaign was conducted in September 2019 where the majority of the one-time sampling and on-site measurements were carried out. During this campaign, the long-term monitoring equipment for water fluxes was also installed, actively recording data between September 2019 and March 2020 (hereafter called the measurement period). An additional small-scale campaign took place in March 2022, when further undisturbed soil samples were taken.

Meteorological measurements

Meteorological data were recorded in 10 min intervals from mid-September 2019 until mid-March 2020 with an ATMOS 41 weather station (METER Group) in combination with a ZL6 Cloud90 data logger. Figure 2.1 shows the position of the weather station at the study site. The following variables were measured at a height of 2 m: solar radiation, precipitation, water vapour pressure, air temperature, barometric pressure, horizontal wind speed and wind direction.

Soil sampling and laboratory analyses

During the campaign in September 2019, a representative soil profile pit at the research site was prepared and described with field methods following the FAO guidelines for soil description (Jahn et al., 2006). A composite sample from each identified horizon was taken for soil texture and nutrient analyses in order to classify the soil according to the *World Reference Base for Soil Resources*, WRB (IUSS Working Group, 2014) (Fig. 2.1). Spatial topsoil (0-5 cm) sampling was carried out along five parallel downslope transects, crossing several blackberry and two alder rows (Fig. 2.1). Per transect, 12 samples of approximately 300 g were liberated with a hand shovel, yielding a total of 60 topsoil

samples. These samples were air-dried and passed through a 2 mm sieve, before transporting them to Germany for physical and chemical analyses.

From each soil sample, an aliquot was dried at 105 °C to determine residual water content. Subsequently, the samples were milled (Siebtechnik TEMA), dried again at 105 °C, and combusted at 1150 °C for total carbon (C) and nitrogen (N) concentrations (Vario EL cube, Elementar Analysesysteme GmbH, Langenselbold, Germany). For soil classification purposes, some laboratory analyses with air-dried soil samples were carried out. We determined pH in a 1:2 soil-solution ratio with ultrapure water and with a glass electrode (pH meter 704, METROHM GmbH, Filderstadt, Germany). Potential cation exchange capacity (CECpot) was determined using 1 M ammonium acetate at pH 7. Exchangeable cations (Ca, Mg, K and Na) were displaced with sodium acetate and measured through inductively coupled plasma optical emission (ICP-OE) spectroscopy (Spectro Ciros CCD ICP Side- on Plasma Optical Emission Spectrometer, Kleve, Germany). The soil texture analysis of the soil profile samples was conducted after removal of organic material with hydrogen peroxide (H_2O_2) and chemical dispersion with tetrasodium pyrophosphate ($Na_4P_2O_7$) according to the sieve and pipette method (ISO 11277:2002, 2002).

Additionally, we took three undisturbed soil samples in 250 mL cylinders from a selected soil profile pit, one at the surface and one each at depths of 0.3 and 0.5 m during the field campaign in September 2019, to determine soil hydraulic properties and some additional variables. Soil hydraulic conductivity of the undisturbed samples was measured with the Ksat apparatus (UMS GmbH, Munich). Soil water retention characteristics on drying samples were measured on the same samples in the HYPROP device (UMS GmbH, Munich, Germany). A small fraction of the sample (about 10 g) was then transferred to the WP4C potentiometer (Decagon Devices Inc., Pullman, WA, USA), and subsequent weighing, further drying and measuring contributed further reference points to the water retention curve. Soil texture was determined through wet sieving of ground soil, and smaller fractions were again separated with the sedimentation method after Köhn (ISO 11277:2002, 2002). Organic compounds were destroyed with the application of H_2O_2.

In the second campaign in March 2022, 12 additional undisturbed soil samples were taken and analysed in the same way as described above. We took the samples in the first (within the alder root zones) and eighth (as a reference without the windbreak influence) blackberry rows at three positions (east, mid and west). At each position, we sampled at two depths, as close as possible to the surface and at 20 cm depth.

Monitoring soil water dynamics

Eight time-domain reflectometry (TDR) probes (TRIME PICO IPH, IMKO GmbH, Ettlingen, Germany) were installed in two 4.2 cm diameter access tubes. Four sensors per tube were assembled and stacked directly on top of each other. The individual sensors have a length of about 0.18 m, integrating over this depth, so four sensors per tube covered a depth of approximately 0.8 m. Each sensor has a measurement volume of 1 dm^3. The sensors were installed at two locations (Fig. 2.1): (1) in the first blackberry row of the field, close to the windbreak, within the assumed rooting influence of the windbreak and (2) in the eighth blackberry row, as a control that is removed from the rooting influence of the windbreak. Two additional TDR probes (TRIME PICO 32, IMKO GmbH, Ettlingen, Germany) with a measurement support volume of approximately 0.25 L were installed at a depth of 0.1 m next to each tube to explicitly cover the topsoil water content. Furthermore, we inserted three dielectric water potential sensors (MPS-2, Decagon Devices, Inc., Pullman, WA, USA) in a profile adjacent to the windbreak tube at depths of 0.1, 0.3 and 0.4 m to measure matric potential. Data were recorded at 15 min intervals (TrueLog100, Truebner GmbH, Neustadt, Germany) between 21 September 2019 and 14 March 2020.

Terrestrial laser scanning and windbreak characteristics

The research site was scanned with a terrestrial lidar in September 2019 under negligible wind conditions. A RIEGL VZ 2000i (RIEGL Laser Measurement Systems GmbH, Horn, Austria) was employed with a multiple-scan-position approach to ensure a three-dimensional representation of the target vegetation and to reduce occlusion effects (Wilkes et al., 2017). As an amalgamated scanning target, the central windbreak was scanned from 32 scanning positions covering the alder trees: 14 positions were within 10 m distance from the windbreak and up to 10 m away from each other, and the remaining 18 positions were located at a distance of 15 to 25 m away, with wider scanning distances between scans. Trees were scanned under leaf-off conditions; however, a few trees had retained dried leaves within the inner crown from the previous vegetation season.

2.2.3 *Data analyses*

Meteorological data processing

The ultrasonic anemometer recorded unusually high values during heavy precipitation events. This error also occurred in some cases in the morning, likely attributable to water on the sensor affecting the transmission of the ultrasonic electromagnetic reflection. All events in question were referenced to the Stellenbosch airport climate station.

Wind and gust speed were considered outliers and replaced with "NA" if their values seemed unreasonable. The decision process was straightforward, as most of the outliers reached the maximum measurable wind speed of 30 m s^{-1} on low-wind days. The integrated cloud service was used to calculate PET by using the FAO Penman-Monteith method (Allen et al., 1998) based on the observations and yielded daily values. The aridity index (PET/P) was calculated after Budyko (1974) for (a) the whole observation period and (b) the same period but with an addition of 20 mm d^{-1} on three weekdays to account for irrigation inputs between December and March on days without precipitation. Precipitation events were identified by an automated detection routine, which defined a precipitation amount of $>$ 2 mm in less than 6 hours as a unique precipitation event and extracted start time and duration, precipitation amount and precipitation rate for each event. Precipitation events $<$ 2 mm in six hours did not result in significant changes in topsoil water content and were therefore not considered in further analyses.

Soil sample analyses

The nitrogen and carbon concentrations of the soil transect samples were considered replicates per row. Therefore, all five transect samples of one row were averaged to obtain a more robust estimate of the overall concentration distribution across the slope. The water retention curves of the profile soil samples were parameterised with the PDI model (Peters, 2014), which is a modified version of the work from Van Genuchten (1980) and Mualem (1976) and used to estimate plant-available water as the difference in volumetric water content between FC and PWP.

Evaluation of soil water dynamics from the monitoring data

The retrieved data were checked for obvious outliers, e.g. due to maintenance work and other technical disturbances. For most analyses, data were aggregated to averaged hourly data. After general inspection of the time series and comparison with one another, the volumetric water content time series were used to retrieve information on root water uptake (Guderle and Hildebrandt, 2015) and on changes in soil water storage during precipitation events. Daily root water uptake (RWU) is derived after Jackisch et al. (2020), including a nocturnal correction from stepwise diurnal changes in soil water content between 2 consecutive days assuming that RWU is the decrease in soil water content between two subsequent nights. If the hourly soil water content time series of a sensor did not show a stepwise decrease, RWU could not be calculated for that sensor on that day. The water limitation factor f_w (e.g. Ghausi et al., 2023) was calculated as the ratio between actual and potential transpiration with the assumption that AET is represented

by RWU.
We determined soil water storage changes by subtracting two successive soil water content values and by multiplying by the sensor depth increment of 0.18 m. This allows us to compare storage changes between windbreak-influenced and reference locations at the different depths and to optionally close the water balance during precipitation events.

Tree and windbreak characteristics

The point clouds derived from the TLS campaign were processed to obtain structural tree data, foliage data and windbreak characteristics. Co-registration of scan positions was carried out using the software RiSCAN PRO 2.11.3 (RIEGL Laser Measurement Systems GmbH, Horn, Austria), following a standard software protocol to generate project point clouds. In the single scans, points were removed if the distance was further than 60 m from the scanning position, the pulse deviation was greater than 10, or with calibrated reflectance lower than -10 dB and greater than 0 dB. Additionally, isolated scan points were removed as these were considered to be noise. Lastly, cubic down-sampling (25 mm voxel side) was applied to the final project point cloud. The point cloud model of the windbreak was extracted, and individual tree point clouds were manually segmented for 18 individuals in sequence, starting from one of the edges. The tree point clouds were used to model the tree structures and estimate tree parameters (e.g. diameter at breast height (1.3 m from ground), tree height and volume) with TreeQSM v2.3.2 (Calders et al., 2015; Raumonen et al., 2013; Raumonen and Åkerblom, 2022). An estimation of the uncertainty of the tree parameters derived from the quantitative structure models (QSMs) was carried out by categorising the tree point clouds into occlusion classes; the estimated precision of one randomly chosen tree was extended to all individuals in the group (Raumonen and Åkerblom, 2022). Wood volume was converted to woody biomass by assuming a wood density of 420 kg m^{-3}, considering an average value for *Alnus* sp. (after World Agroforestry, 2023). The belowground root biomass was estimated as 28.54 % of the aboveground woody biomass (Frouz et al., 2015).
The leaf creation algorithm by Bohn Reckziegel et al. (2022) was used to estimate foliage by restricting leaf classes to "small", "medium" and "large" categories with corrected ratios according to leaf sizes for *Alnus* sp. (San-Miguel-Ayanz et al., 2016). The leaf spacing definition was varied from 2.0 to 3.0 cm to estimate total leaf area on a tree basis and leaf dry mass, assuming the specific leaf mass of black alder (*Alnus glutinosa* (L.) Gaertn.) of 13.3 $\pm$ 0.3 m^2 kg^{-1} (Johansson, 1999). The calculated leaf area index (LAI) was used to approximate cumulated interception over the course of a rain event. An empirical estimation of a leaf area dependent interception storage value of 0.0001 m was

applied, as such a value has been used in many different modelling studies providing satisfactory estimates of the interception storage (e.g. Zehe et al., 2001). The leaf-area-dependent interception storage value is multiplied with the LAI to yield interception estimations.
The shadow model by Bohn Reckziegel et al. (2021) was utilised to estimate shading effects of the windbreak through the QSMs. This enabled an estimate of the shade cast under and surrounding the leafless windbreak. A nominal date representing the site conditions was chosen as 25 September as experienced in the field campaign. The initially acquired QSMs were simplified with two replacement iterations (Bohn Reckziegel et al., 2022). The tree structures were bound together in a data frame to expand the model capabilities from single to multiple trees in a simulation. After removing four trees closest to the windbreak edge, we mirrored the remaining trees for simulating a windbreak with a total of 29 trees. The shadow model was fed with 60 s solar irradiance data from 2019 (January to December), provided by Stellenbosch University (University of Stellenbosch, 2023) and derived from the Sonbesie meteorological station (33°55'42.84" S, 18°51'55.08" E, 119 m a.s.l.) less than 10 km from the research site. Shadow projections were simulated on a ground surface of 0.4 ha (100 m east-west, 40 m north-south) with a grid cell size of 10 cm x 10 cm, and centralised to the windbreak position for each time interval of 10 min; this was applied in order to simulate the shade cast specific to the windbreak in its defined position.

2.3 RESULTS

2.3.1 *Meteorological observations*

The measurement period fell within the South African summer months. The average measured air temperature was 19.5 °C with a minimum of 7.5 °C and a maximum of 35.7 °C. The precipitation sum during the measurement period totalled 245 mm; notably, 118 mm fell during one single storm event on 25 October 2019 (Fig. 2.2, upper part). The measured wind direction at the study site was predominantly westerly in spring or early summer and easterly in late summer or autumn with an average speed of 2.2 m s^{-1}. PET was estimated to average 5.2 mm d^{-1}, with a peak in late February of 11.2 mm d^{-1} (data not shown), and cumulative PET reached a total of 913 mm for this period.
The aridity index for the entire period gave a value of 3.7, clearly larger than 1 and fell into the water-limited arid region of the Budyko curve. When accounting for the irrigation in the summer, the aridity index dropped to 0.65, indicating a humid and energy-limited regime. We identified 13 rainfall events $>$ 2 mm, ranging in total precipitation from 2.5 mm to 117.6 mm and in measured maximum intensity from

4.1 to 82.6 mm h^{-1} (table 2.1). On average, the events had a low intensity of 1.6 mm h^{-1} and a duration of 11 h 41 min. The longest event lasted 37 h.

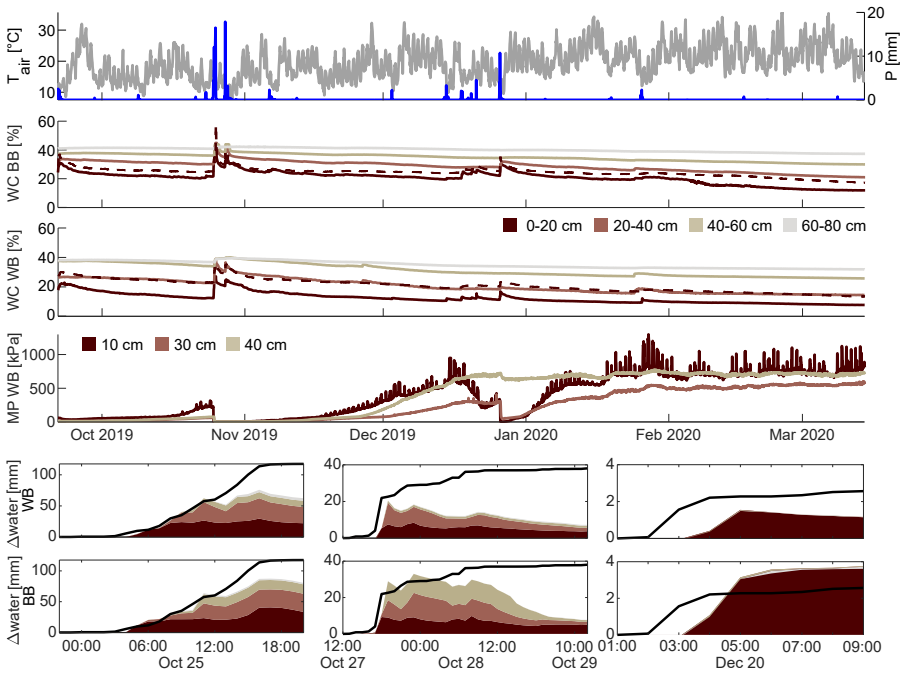

Figure 2.2: Meteorological observations (precipitation P, air temperature T) of the whole measurement period (upper panel). Soil water content (volumetric WC) and matric potential (MP) time series at both locations (middle panels; WB: windbreak, BB: blackberries). The dashed line represents the 10 cm soil water content sensor. The lower panels show cumulative precipitation (line) and cumulative soil water storage change of each sensor for selected precipitation events (see fig. A.1 for remaining events), for both the windbreak (upper row) and the blackberry (lower row) location. The different colours represent the different depths of the sensors.

2.3.2 *Soil sample analyses*

Soil profile and undisturbed samples

The soil profile (Fig. 2.1) was classified as Cambic Mollic Umbrisol (loamic, humic) based on the international soil classification system WRB. The texture isloamic across all horizons (table 2.1) of $>$ 50 % in the upper horizon, followed by low base saturation in all other horizons. The supplementary qualifier "humic" (IUSS Working Group, 2014) was added due to the high average carbon content within 50 cm from the mineral soil surface. The three undisturbed profile samples taken adjacent to the soil water equipment and the additional samples collected in 2022 were analysed for soil hydraulic properties (Fig. 2.3, Table A.1).

Table 2.1: Observed precipitation (P) events above 2 mm per 6 h.

Event	Start date	Duration	P. Amount	Max. P. Rate	Initial Soil Moist.
		[h]	[mm]	[$mm\ h^{-1}$]	[-]
1	21 Sep 2019 11:00:00	23.0	10.5	12.2	0.51
2	08 Oct 2019 20:00:00	2.0	2.5	7.1	0.51
3	23 Oct 2019 11:00:00	6.0	4.1	22.4	0.37
4	24 Oct 2019 23:00:00	21.0	117.6	65.3	0.37
5	27 Oct 2019 13:00:00	37.0	38.1	82.6	0.59
6	06 Nov 2019 07:00:00	14.0	5.5	17.3	0.57
7	02 Dec 2019 21:00:00	3.0	2.6	9.2	0.32
8	14 Dec 2019 17:00:00	2.0	4.3	5.1	0.26
9	17 Dec 2019 17:00:00	15.0	8.5	72.4	0.26
10	20 Dec 2019 02:00:00	7.0	2.6	4.1	0.28
11	21 Dec 2019 05:00:00	1.0	4.6	10.2	0.30
12	26 Dec 2019 06:00:00	10.0	23.1	45.9	0.32
13	25 Jan 2020 21:00:00	11.0	7.1	13.3	0.24

The lower soil was homogeneous between locations. The topsoil was denser at the windbreak than at the blackberry, and the overall moderate bulk density ranged from 1.01 to 1.25 g cm^{-3} with the exception of the soil profile sample at 0.5 m of 1.49 g cm^{-3}. Topsoil organic matter content was similar at both locations and decreased with depth (averages from 11.5 % in the shallow to 10.4 % in the deeper soil). The windbreak topsoil averages matched with the deeper soil averages for the following parameters (averages in parentheses): porosity (0.57, Fig. 2.3), water content at FC (0.359 m^3 m^{-3}, Fig. 2.3), PWP (0.171 m^3 m^{-3}) and PAW (0.187 m^3 m^{-3}). The blackberry topsoil had a greater porosity and the water contents at FC and PWP as well as the PAW were lower. Topsoil hydraulic conductivity was nearly 3 times greater at the blackberry crop than at the windbreak but only 20 % more in the lower soil depths (Fig. 2.3).

Table 2.2: Characteristics of the five horizons identified in the soil profile (Fig. 2.1).

Horizon	Depth	Texture	pH	CEC	Base saturation	C(org)	N
			(H_2O)	[$\frac{mmol_c}{kg^1}$]	[%]	[%]	[%]
Ah1	0-20 cm	Silty Clay Loam	6.9	221	74	2.89	0.17
Ah2	20-40 cm	Silty Clay Loam	5.8	175	28	2.37	0.13
Bw1	40-55 cm	Clay Loam	5.0	144	20	1.22	0.08
Bw2	55-75 cm	Clay Loam	4.9	127	24	0.89	0.06
C	$>$ 75 cm	Clay Loam	4.8	117	26	0.54	0.05

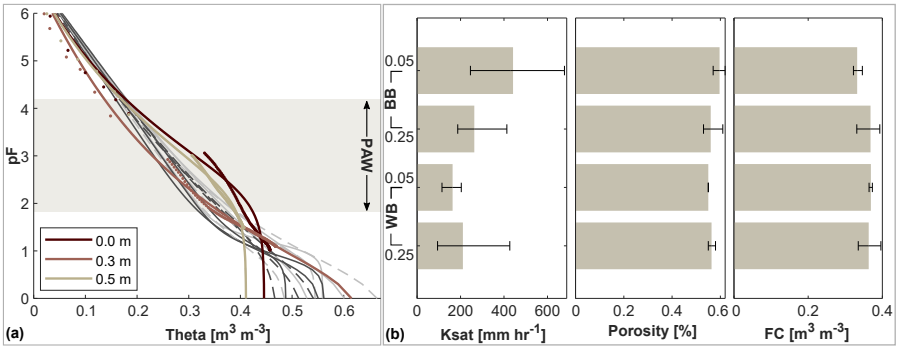

Figure 2.3: Various soil characteristics of the undisturbed samples. The left panel (a) shows soil water characteristic curves (vol. water content theta vs. soil suction pF) of undisturbed soil profile samples taken at different depths at the monitoring location within the windbreak rooting influence, adjacent to the soil water content sensors. The values (dots) were taken during the drying process of the sample under laboratory conditions and parameterised with the PDI model by Peters (2014) (lines). Lines in grey represent additional undisturbed soil samples (darker shade are the upper samples, dashed line represents the WB samples). The shaded boxes illustrates the area of the PAW (plant-available water storage). The right panel (b) displays averages (bars) and ranges (lines) of different properties of the additional soil samples from March 2022: Soil hydraulic conductivity (Ksat), porosity and water content at field capacity (FC).

The soil water retention curves (Fig. 2.3) of the top and bottom sample exhibit similar shapes but different porosities, whereas the middle sample curve is less steep and decreases more homogeneously, starting at a much higher saturated water content. The deepest sample has the lowest saturated water content and a porosity of 0.44, while the top sample has a porosity of 0.56 and the middle sample of 0.58. Overall, the soil physical properties reveal a higher PAW at the windbreak in comparison to the blackberry cropped area.

Topsoil transect samples

Both carbon and nitrogen contents decreased with increasing distance from the alder windbreaks. The highest values, reaching a carbon content of 9 % C and nitrogen content of 0.6 % N, were found within the windbreaks, whereas contents of 3 % C and 0.3 % N were measured farthest from the windbreaks (Fig. 2.4). The value range of the carbon-to-nitrogen (C:N) ratio is narrower in the vicinity of the alders compared to areas situated further from the tree line.

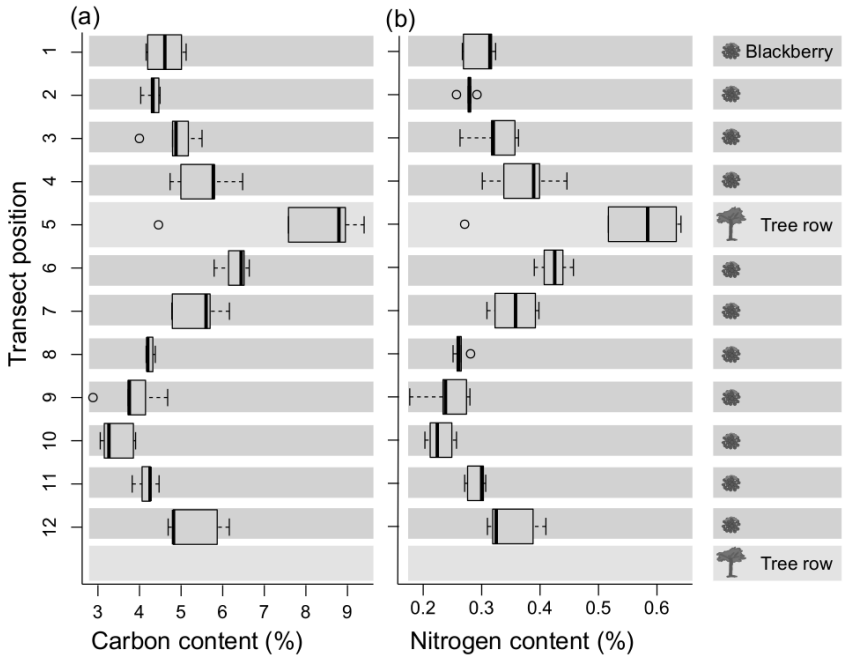

Figure 2.4: Carbon (a) and nitrogen (b) content of the five averaged transect topsoil (0-5 cm) samples.

2.3.3 *Soil water monitoring*

Volumetric water content and matric potential

All sensors captured the drying processes during the summer months, which dominated the soil water content and matric potential measurements (Fig. 2.2). The water content differed with depth and between the two measurement locations. At both locations (blackberries and windbreak), the upper soil water content was consistently lower than that at greater depths. In addition, the soil water content was generally higher at the blackberry location (31.1 %) compared to the measurements at the windbreak (24.9 %). Reactions to rain events were observable; however, the magnitude of the reactions differed between locations, events and sensors and is described in more detail below. Observed matric potential also followed the rainfall dynamics and grew substantially during the drying of the soil in the summer although not reaching the PWP (pF = 4.2 or -1500 kPa). Note that the matric potential time series of the top sensor was heavily influenced by daily fluctuations (Fig. 2.2), which become more pronounced when the soil reached drier conditions ($<$ -500 kPa). The two deeper sensors also displayed this signal, but it was more attenuated.

Root water uptake

The daily root water uptake (Fig. 2.5) calculation was not successful on many days, leading to missing values for 48 % of the observations (one value per sensor per day) at the windbreak and 56 % at the blackberry location. Missing days were spread over the entire measurement period, with only 4 d of RWU estimates available from all eight sensors. At the windbreak, gaps occurred most frequently in the topsoil (20-40 cm) whereas at the blackberry location it occurred more often for the sensors located at deeper depths (40-60, 60-80 cm). On days without missing values (21 d at the windbreak, 14 d at the blackberry location), 44 % of the estimated RWU primarily occurred within 20-40 cm, followed by 28 % in the top 0-20 cm at the windbreak. In the blackberries 70 % was abstracted from the top 0-20 cm. Note that on the 4 d with complete sensor data, the RWU was consistently greater at the blackberry compared to the windbreak location (12 October: 0.56 mm d^{-1} < 0.82 mm d^{-1}, 13 October: 0.72 mm d^{-1} < 0.85 mm d^{-1}, 18 October 0.66 mm d^{-1} < 1.22 mm d^{-1}, 21 November: 0.4 mm d^{-1} < 1.17 mm d^{-1}).

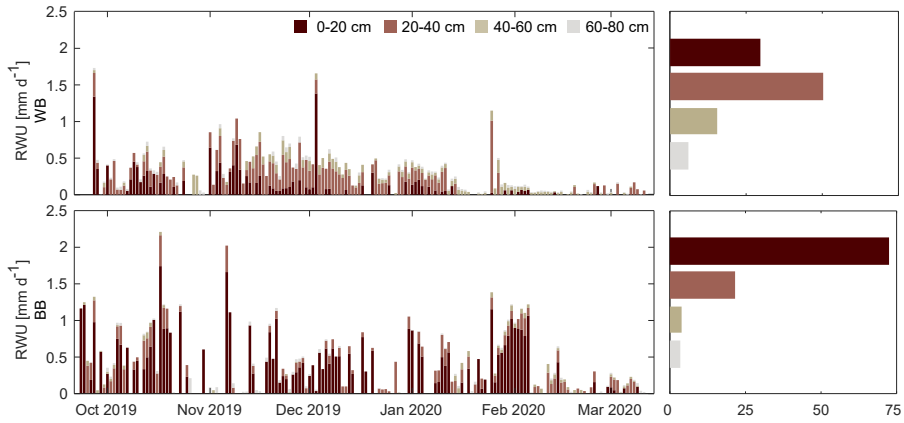

Figure 2.5: Stacked daily root water uptake (RWU) at the windbreak (WB) and blackberry (BB) location estimated from water content measurements at respective depth integrals. Panels on the right show how much each depth interval contributes to overall RWU [%].

Neglecting water storage in the trunk, RWU provides a rough transpiration estimate and allows - together with the estimated PET - the calculation of the water limitation factor. Doing so for the days where RWU was available for at least all four sensors at one location (29 instances) yielded in a mean value of 0.098 (range: 0.058–0.223) at the windbreak and of 0.128 (0.034-0.230) at the berries. This indicates that transpiration is strongly water-limited.

Event-based analyses

When defining a rain event as a minimum accumulated precipitation of 2 mm and continuous rainfall periods of less than 6 h, we identified

13 distinct events during the monitoring period (Fig. 2.2, table 2.1, Fig. A.1). The most precipitation during one event accumulated a total of 118 mm of rainfall within a 21 h period and occurred on 25 October 2019. Two days later, another storm delivered 38 mm of rainfall over 37 h, making it the second-largest event. Two more events with precipitation exceeding 10 mm were recorded, while the smallest event captured 2.5 mm of rainfall on 8 October 2019. Across all events, soil water content reactions are rather immediate throughout the different sensors. Figure 2.2 presents a combination of accumulated precipitation and changes in cumulative soil water content storage for selected events: the largest two (24 and 27 October 2019, fourth and fifth events) and one smaller event (20 December 2019, the 10th event). Note that accumulated total storage increase was for all events greater in the blackberries than in the windbreak. During the smaller event in Fig. 2.2 it even increased local rainfall supply, probably due to lateral flow processes. The two largest events ($>$ 30 mm) lead to an increasing soil water content until the sensors at the depth of 40-60 cm. Accumulated total storage change was during the last storm at both sites, clearly smaller than the rainfall supply, while during the fifth event (Fig. 2.2, bottom middle panel) the increase came close to the total rainfall at the blackberries. There was furthermore a clear difference in the sequence how the sensors responded. On 24 October 2019, there was a gradual downward percolation of water as reflected in the sequential storage response, whereas on 27 October 2019 all three upper sensors showed a simultaneous increase in soil water content, particularly at the blackberry location. Moreover, during the latter event, the soil did not retain the water; instead, soil water content rapidly declined once the precipitation ceased, which differed from the behaviour in response of the first event.

2.3.4 *Windbreak characterisation*

The windbreak consists of 40 aligned trees spaced evenly without gaps. Table 2.3 provides information on the tree structure and QSM-derived attributes. A large degree of heterogeneity of the windbreak's tree structure is demonstrated by DBH measurements (diameter at breast height, standard measurement at 1.3 m above ground) ranging from 7.7 to 33.3 cm and tree height variations between 4.3 and 13.3 m. The QSM optimisation provided precise estimates of tree heights (CV % ca. 1 %). Tree point clouds classified with high occlusion had higher uncertainties in QSM-derived tree parameters. The estimated LAI-dependent interception storage capacity yielded 0.664 mm on the alder leaves if assuming a LAI value of 6.64 m^2 m^{-2} based on a leaf spacing of 2.5 cm for trees within the windbreak row (Table 2.3).
Excluding the edge trees exhibiting a more open grown form, the total wood volume was found to be 0.6 m^3 m^{-1} (i. e. per linear metre of

windbreak), including 0.4 m^3 m^{-1} of branch wood. The estimated dry total biomass (trunk, branch, coarse roots) amounted to 259.3 kg m^{-1}. The variation of biomass stocks above and below the ground are noted in Table 2.3.
The shadow model suggested a substantially reduced solar insolation at the soil surface due to shading effects of the trees (up to 75 % of incoming solar radiation intercepted). This shading effect spread up to 4 m towards the north (uphill) and up to 9 m towards the south (downhill). Along the east-west axis, the shading effects were greater in size but less intense than in the north-south axis. Specific zones of minimum radiation (≈5 MJ m^{-2}) occurred within the windbreak, mainly towards the southern side.

Table 2.3: Windbreak properties derived from tree data (QSM based) and additional point cloud methods.

Group	Property	Unit	Values	Description
Structure	Orientation	-	ENE-WSW	Windbreak cardinal direction
	Tree Count	count	40	Number of trees in the windbreak
	Tree Spacing	m	1	Planting spacing (trunk-to-trunk)
	Width	m	9.46	Measured windbreak width
	Length ttt	m	39	Measured trunk-to-trunk windbreak length
	Length ctc	m	48	Measured crown-to-crown windbreak length
	Plant Coverage	-	0.819	Ratio of the min. binding box and the alpha-hull of leaf points
Volume	Trunk	m^3 m^{-1}	0.1	Trunk volume per linear metre of windbreak
	Branch	m^3 m^{-1}	0.4	Branch volume per linear metre of windbreak
	Root	m^3 m^{-1}	0.1	Root volume per linear metre of windbreak
	Total	m^3 m^{-1}	0.6	Total volume (trunk, branch, coarse roots) per linear metre of windbreak
Biomass	Aboveground	kg m^{-1}	201.7	Aboveground biomass (trunk, branch) per linear metre of windbreak
	Belowground	kg m^{-1}	57.6	Belowground biomass (coarse roots) per linear metre of windbreak
	Total	kg m^{-1}	259.3	Total biomass per linear metre of windbreak (without leaves)
Foliage	Leaf Mass	kg m^{-1}	3.46; 4.12; 5.12	Leaf dry mass per metre of windbreak (leaf spacing 3, 2.5 and 2 cm)
	Leaf Area	m^2 m^{-1}	45.00; 53.69; 66.64	Leaf area per metre of windbreak (leaf spacing 3, 2.5 and 2 cm)
	LAI	m^2 m^{-2}	5.56; 6.64; 8.24	Leaf area index (with leaf spacing 3, 2.5 and 2 cm)

2.4 DISCUSSION

2.4.1 *Windbreaks influence dominant processes of the water balance*

In the following, we discuss the various processes of the water cycle occurring at the soil-atmosphere boundary on a plot scale and how they are influenced by the windbreak. Tracking water input, we investigate water movement into and within the soil, water redistribution and its pathway out of the study area.

Windbreaks alter microclimatic precipitation patterns

The measurement period occurs in the South African summer months, including January, which is historically the driest month of the year with, on average, 16 mm (in our study 9.1 mm) of precipitation. Total precipitation sum was 245 mm (30-year average for the same period is 206.5 mm) and partially covered the annual average of 787 mm for the region (Meadows, 2015; Veste et al., 2020; Climate-Data.org, 2024). Accurate irrigation volumes and frequencies were not available. Assuming that irrigation volumes were consistent throughout the seasons, the trickle irrigation system may have provided a weekly water input of up to 60 mm. In comparison to the precipitation, this accrued to a total of 240 mm per month, which can be considered to significantly contribute to the overall water balance, exceeding the long-term average of 132 mm of the wettest month.
By intercepting rainfall and storing part of it on leaves and branches, trees reduce the amount and kinetic energy of rainfall reaching the surface and, hence, its availability to vegetation below the crowns of the windbreak trees. The capacity of trees to store precipitation depends on specific characteristics, such as crown density and leaf surface area, the size and dynamics of the rainfall event itself and the prevailing climatic conditions (Baptista et al., 2018; Schumacher and Christiansen, 2020). We found that the tree branch volume was approximately 3 times higher than the log volume; consequently, the total wood surface area was high. This indicates a strong branching of the windbreak structure and, therefore, dense vegetation (i.e. low porosity). Our assumption considers that interception storage capacity is directly proportional to LAI, making this variable valuable for analysing different forest types and tree species, even under varying growth conditions (Schumacher and Christiansen, 2020). A LAI storage capacity of 0.664 mm per event results in a total interception of 8.5 mm for all events during the measurement period, accounting for 3.5 % of the total precipitation for the measurement period. It is important to acknowledge that our value may underestimate the total interception, as events smaller than 2 mm are not considered. Including all events (32 events with precipitation > 0.1 mm) would yield an interception of 21.2 mm or 8.6 % of rainfall. Interception is

generally influenced by two factors: (1) vegetation characteristics such as density, age, and height and (2) precipitation properties such as intensity, duration, and frequency. The literature gives interception values of, for example, 22 % of yearly rainfall for temperate deciduous broadleaf forests, which would lead in our case to 53.9 mm for the measurement period or 173 mm for a whole year (Dingman, 2015). Interception in windbreaks is likely to be lower than in closed-canopy forests as branches are all the way down the canopy exposed to wind movement, thereby shedding additional water from the canopy. Lower branches in closed canopies are likely to experience less movement and can therefore hold water on canopy surfaces until it is evaporated. The LAI values were higher than those typically found in shrublands (approximately 2.0) and similar to those found in temperate and tropical forests as well as tree plantations (Bréda, 2008). Overall, we observed a higher proportion of rainwater stored in the soil at the blackberry location in contrast to the windbreak location, where on average 63 % and 54 % of the rainfall reached the soil column, respectively. This can potentially be attributed to interception differences between the two locations. The difference between the two locations is 26.5 mm for the entire period, which aligns with the interception amount of 40 mm yr^{-1} stipulated in the literature for alder species (Muthuri et al., 2004). However, the alternated wind field due to the obstacle in the flow path might also cause a change in the precipitation pattern at and around the windbreak. Häckel (1999) states an increase of up to 15 % in precipitation behind the obstacle (until up to 10 times plant height) and a reduction of 10 % directly at the windbreak.

Windbreaks carry potential to buffer surface runoff thereby reducing erosion

Water movement processes, such as infiltration, surface runoff and lateral subsurface flow, can be observed during and after precipitation events, but soil physical properties can equally indicate hydrological behaviour. Infiltration determines the splitting of rainfall into surface runoff and soil water fractions. Observed Ksat values (302.3 mm h^{-1} $\pm$ 191.3 mm h^{-1}) varied in the range of silty soils. Great heterogeneity of topsoil Ksat is expected due to the difference between the soil in the berry rows (lightly packed soil, flattened) and between the rows (compacted, rock fragments, steeper parts) and was confirmed by a nearly threefold average at the blackberry location compared to the windbreak. Ksat values exceeded maximum precipitation intensities (max 82.6 mm h^{-1}) at both locations, providing favourable conditions for water infiltration into the soil. The porous soil inhibited a particularly high air capacity compared to common fine-pored soils. Both indicate that 21 % of infiltrated water was not held against gravity, i.e. not stored in the topsoil, and therefore drained a substantial part into deeper soil layers. The water percolated quickly downward in the topsoil (about 16 cm h^{-1} for Ksat near the windbreak and 44 cm h^{-1}

for the blackberry crop).
Nevertheless, we did observe instances (event numbers 1, 5, 9, 10, 11; see also Table 2.1) where soil water storage changes exceeded the precipitation input as illustrated in Fig. 2.2. This can be attributed to either surface runoff or lateral soil water redistribution. In the first case, the soil reached saturation or infiltration excess and, therefore, water did not percolate into the soil, leading to its accumulation and downslope movement on the soil surface. The matric potential surpassed the FC threshold during the late October and December events (event numbers 4, 5 and 7-12), confirming the occurrence of surface runoff. Either the water moved on the surface until it was lost to the study site or it infiltrated at a different location into the cropped area. Due to the aforementioned heterogeneous surface between the rows, it is likely that surface water formed on the compacted and steeper parts of the slope and infiltrated in the flattened area around the blackberry plants or was buffered by the windbreak. In general, for most events, the cumulative soil water storage at both locations did not align with the recorded precipitation amount, supporting the occurrence of lateral redistribution at the soil surface or subsurface. In the case of lateral subsurface flow, i.e. soil water redistribution, water moved horizontally instead of percolating downwards when reaching a less permeable soil layer. This was evidenced by a substantially decreasing Ksat with depth (at 0.5 m Ksat = 3.2 mm h^{-1}) and might benefit the windbreak.
The often-observed delayed responses of soil water content changes after the onset of a precipitation event can be an indicator for both infiltration after surface runoff and lateral redistribution. Additionally, the simultaneous reaction of the deeper sensors with the shallower ones is evidence for preferential flow through, e.g. macropore input (fifth event in Table 2.1, bottom middle panel in Fig. 2.2).
The distribution of nitrogen and carbon concentrations (Fig. 2.4) supported the occurrence of lateral redistribution, as the enrichment around the windbreak was likely a result of a combination of erosion from downslope surface runoff and the accumulation from the trees themselves (see section 2.4.2). We observed very high precipitation intensities (max observed 82.6 mm h^{-1}), which probably produced surface runoff with high kinetic energy and, therefore, had the potential to produce splash or sheet erosion even in cohesive soils. Possibly, the windbreak may not be apparent in the soil water content changes but downslope erosion of fine soil could explain the unexpected observed lower Ksat values near the windbreak, which is underpinned by larger bulk density and lower porosity at the windbreak. We did not find considerable texture differences between the two locations, but fine particles could be masked through the formation of aggregates (Jackisch et al., 2017). Carbon addition may also increase and stabilise aggregates in fine-grained soils.

Windbreaks reduce crop evapotranspiration

Root water uptake calculations did not work for approximately 50 % of the data points due to the absence of a decrease in the soil water content time series during the day, which results in a typical step-shaped curve that is necessary for RWU estimation (Jackisch et al., 2020). The influence of the irrigation on these estimations is unclear, although it should be consistent at both locations, thus allowing relative interlocal comparison. Nevertheless, we are cautious about the achieved RWU estimates at this site due to missing data.

The RWU pattern differed between the two locations (Fig. 2.5) with a higher proportion occurring in the topsoil at the blackberry location and a more evenly distributed uptake around the 20-40 cm depth within the windbreak. This indicates that the alder trees draw water from a broader range of soil horizons than the blackberry crop. The perennial blackberry plants have a main root, which can extend vertically to a maximum depth of 1.5 m (depending on soil type) and have numerous secondary roots, growing horizontally for 30-60 cm before descending vertically (Bruzzese, 1998). Alder trees are water-demanding species with high evapotranspiration rates due to the absence of a mechanism to control stomatal regulation (Herbst et al., 1999). It is unclear whether the studied *A. cordata* exhibits deep rooting on the thin and rocky soils of the steep slope at our study site (80 cm soil depth at our exemplary soil profile). However, it is reasonable to assume that the species can reach the deeper soil layers due to its rooting potential. If the trees tap water sources below 80 cm, it would not have been captured with the installed measurement devices which in turn would explain why we observed much less water uptake at the windbreak when compared to the blackberries. Without additional information, it is difficult to determine whether the observed differences in RWU patterns are due to different rooting depths between the two species. The RWU cannot be used to estimate evapotranspiration of the windbreak. However, the water limitation factor was estimated for days with complete sensor data and gives an idea of how much of the available radiation energy is used for RWU and, therefore, transpiration and plant growth. For the days under consideration, less RWU (f_w: 9.8 %) occurred at the windbreak in contrast to the blackberry location (f_w: 12.6 %), which could be caused by (a) a lack of RWU estimates due to unsuitable soil water content time series or (b) the sensors not being installed in a suitable location (adjacent to root or deep enough) and therefore not sufficiently capturing the RWU.

Interestingly, the Budyko aridity index indicated a shift from a water-limited system to an energy-limited system when considering the additional irrigation input (changing from 3.7 without irrigation to 0.65 with irrigation). This is confirmed by the matric potential sensors, which showed that the plant did not reach the PWP (Fig. 2.2), i.e. the

point at which water fluxes are nearly immobile. Water becomes a limiting resource for many plants already at lower absolute matric potential values. The water supplied to the system by irrigation was the dominant component of the water budget, and as a consequence, the AET was closer to the PET. Consequently, estimations of wind and sun shading effects can provide an idea of the AET at the field site. A simulation demonstrated the windbreak's potential reduction of solar radiation on the ground, which can be up to 75 % in the immediate vicinity of the windbreak on a sunny day, as observed on 25 September 2019. The PET was estimated at 10.8 mm for the entire day from the meteorological data without shading; however, some areas of the blackberry crop did experience the shading effect of the windbreak. For instance, on the southern side of the windbreak, on a part of the field where the solar energy is reduced by 50 % for approximately 6 h, the daily PET decreased from 10.8 to 6.9 mm d^{-1}. On the northern side of the windbreak, where the blackberries and soil were protected from the southerly winds occurring that day (depending on the distance up to a 30 % reduction in PET), assuming a 15 % reduction, in PET due to wind speed reduction the PET reduced from 10.8 to 9.2 mm d^{-1}. If both effects were to occur on the same side, the cumulative impact could lead to a reduction to 5.8 mm d^{-1}, resulting in an AET that is 54 % of the PET.
While this example calculation is based solely on theoretical values and lacks actual data for validation, it underscores the importance of the windbreak in a water-scarce region. A 30 % reduction in water demand can be crucial for the sustainability of natural and agricultural ecosystems. In a nearby vineyard, Veste et al. (2020) measured a 20 % reduction in wind speed and evapotranspiration due to tree shelterbelts. For the sake of completeness, it should be noted that sunlight is essential for the growth of the blackberry crop, and excessive shading may adversely affect growth and thus the yield of the field; hence, a detailed assessment of shading effects is crucial. Shading is predominately a factor of height, volume and porosity of windbreak crowns; other structures in the landscape; and aspect and slope.

2.4.2 *Windbreaks induce benefits for water availability and nutrient distribution*

Windbreaks potentially improve soil water storage capacities

One way to estimate plant-available water is through the inspection of the water retention curve and different storage capacities quantified by soil hydraulic properties (Fig. 2.3). As previously mentioned, we observed high porosity and high air capacity (21 %) in the soil, determining that a large fraction of the shallow soil drained instead of storing the water. It was also quite striking that Ksat is substantially

larger in the blackberry soil, even though an estimation based on the very similar texture and porosity values would also result in similar Ksat estimates. This clearly indicates that structural effects in the soil with a high fraction of fine pores holding water, but also a fraction of well drainable pores, are allowing water to percolate.

Interestingly, the three different volumetric pore compartments of the soil (1) air capacity or drainable volume, (2) effective field capacity PAW and (3) wilting moisture PWP are nearly the same (approx. 20 %). This could be beneficial to the ecosystem. By percolating further into the soil, water is protected from evaporation. A less permeable layer deeper in the soil profile can collect the percolated water, plants that are able to root down to such a depth can benefit from this source. The fraction that is beyond the wilting point inhibits the same size as the fraction that percolates down and is available for plants at greater depths. Usually, the drainable fraction is much smaller in fine pore soils.

Bogie et al. (2018) found significant differences in water retention at the PWP alongside changes in surface properties brought about by higher CEC of organic matter in coarse soils. This is in contrast to our samples, which had higher topsoil organic matter concentration but similar PWP. The retention curves differed mainly in the wet range and were rather similar in the dry range. The spread in the wet range was greater for the lower samples, while the upper samples varied less and had slightly steeper curve shapes. In the topsoil, PAW was greater at the windbreak (19.7 %) than in the blackberry crop (16.4 %), generally resulting in a higher potential to retain water in the soil near the windbreak. The deeper samples displayed very similar values for PAW (19.3 % and 19.2 %). As shown in the previous section, overall less water reached the soil at the windbreak even though the potential to store it based on texture is greater.

Both the volumetric water content (at both locations) and matric potential (measurements at the windbreak only) observations consistently show that the topsoil is drier than the soil at greater depths (Fig. 2.2). The drier surface is due to evaporation of soil water combined with water withdrawal by plants from the topsoil, whereas the deep layers are not affected by evaporation and only to some extent by root water uptake. The former can be seen in the observations of the matric potential, which exhibited pronounced daily fluctuations. The matric potential sensors did not reach the PWP of -1500 kPa during the measurement period. The uppermost sensor reached values below -1000 kPa for 53 of the 4200 data points, all occurred between January and March mostly around midday (range from 11:00 to 17:00 LT, with an average at noon). This coincides with the times of the day when the field site is irrigated (informally for a few hours every 2 to 3 d during the summer). Both the time series of matric potential and supplemental irrigation indicated that sufficient water was available

throughout the period and that the plants did not experience any severe water stress.
The soil water content time series recorded at any location frequently reached the PWP (estimated from retention curves: the top sensor at windbreak location for 86 % and top sensor at the blackberry location for 20 % of 4200 hourly data points, respectively). The main difference between the locations is that at the blackberry location the PWP was reached only towards the end of summer (after 8 February), whereas at the windbreak this limit was reached several times throughout the observation period. We were more likely to trust the absolute values of the matric potential in this context (among other reasons), because the volumetric water content sensors were used with the calibration provided by the manufacturer and not a field-site-specific setting and, therefore, susceptible to offset errors.

Nutrients accumulate around windbreaks and windbreaks enhance carbon sequestration potential

Possible reasons for the considerably higher nitrogen and carbon concentrations in the windbreak row are (a) the relocation or erosion of soil material following surface runoff in the upper and steeper parts of the slope to the flatter slope at the windbreak and (b) the continuous addition of N-rich alder biomass in form of litter fall, root exudation and root biomass, leading to higher microbial activity. Italian alder is a N-fixing tree and is able to capture atmospheric nitrogen in symbiotic root nodules (Claessens et al., 2010). There are a number of N-fixing species that seem to retard the decomposition of native soil carbon. Thus, this fact combined with their own root carbon productions causes the increase in soil carbon normally observed among N-fixing species. The bulk of the increase in soil organic carbon could result from dead roots arising from the trees. So, erosion is probably less important than root turnover when it comes to carbon input.
An additional potential not discussed in much detail in this study is the carbon sequestration of the windbreaks in the landscape. From the terrestrial laser scans, we estimated total dry biomass of 259 kg m^{-1} of windbreak. Under the rough assumption that water/woody biomass is a 50/50 split and carbon constitutes 50 % of dry biomass (Thomas and Martin, 2012); as well as according to the molecular weight of CO_2, we can suggest that 238 kg CO_2 equivalent (Guest et al., 2013) is sequestered in the biomass of the study alder trees. Sheppard et al. (2024), for example, showed that a poplar windbreak in South Africa of similar dimensions could store nearly 200 t of CO_2 equivalent per kilometre of windbreak in the aboveground portion alone. In comparison with forested land this may not be much, but as an additional carbon sink on farmland it presents a large additional potential for short- to mid-term carbon storage.

2.5 CONCLUSIONS

Windbreaks play a significant role in shaping the water dynamics of their surroundings, yielding various benefits when implemented and managed effectively, particularly in regions with limited water resources. Our investigation into their impact on the water balance utilised a range of methodologies, including analyses of sensor data and soil sampling.

The windbreaks not only altered local precipitation levels but also influenced its distribution. Proximal to the windbreak, precipitation input was reduced by approximately 3.5 % due to interception, while on the leeward side the effects can lead to up to a 15 % increase in precipitation levels due to disruptions to the wind field. These effects could explain the observed higher proportion of water being retained in crop compared to windbreak soils. However, a more precise understanding of interception storage and the water usage of trees, through sap flow measurements or improved root water uptake estimates, is needed to refine the water balance assessment. Discrepancies in soil water content may also stem from variations in hydraulic conductivity, which determine infiltration rates. Observations indicated lower hydraulic conductivity at the study windbreak compared to the blackberry location, possibly due to soil erosion during high-intensity precipitation events. Nonetheless, topsoil conditions generally favoured infiltration, with a significant portion of water draining the topsoil and reaching deeper layers. Since the water at greater depths was protected from evaporation, plants might benefit by tapping water from this source. By reducing wind speeds, windbreaks reduced crop evapotranspiration, while irrigation shifted the system from water-limited to energy-limited conditions, leading to increased actual transpiration. This is corroborated by soil water measurements, indicating no water stress in plants. Furthermore, windbreaks contributed to soil health by accumulating nutrients and enhancing carbon sequestration potential in contrast to monoculture farmland, i.e. traditional crop framing without trees.

This interdisciplinary work explored numerous aspects of AFSs and acquired different perspectives, confirming hypotheses through cross-method analyses (e.g. surface runoff detection in event-based sensor data combined with nutrient distribution analysis). The combination of additional monitoring data and repetition of campaign-based measurements with modelling studies would help with closing the water balance and might be able to fill remaining gaps and shed light on open questions regarding water fluxes in AFSs.

Part III

CARBON INPUT ON SOIL PHYSICAL AND HYDROLOGICAL PROPERTIES

This study is a manuscript prepared for publication in a scientific journal. It has been submitted as:

Hoffmeister, S., Hassler, S. K., Lang, F., Maier, R., Nyoka, I., Zehe, E. "Coupling of soil carbon and water cycles in two agro-forestry systems in Malawi." https://doi.org/10.5194/egusphere-2025-1719.

3

INFLUENCE OF CARBON INPUT ON SOIL PHYSICAL AND HYDROLOGICAL PROPERTIES IN TWO AGROFORESTRY SYSTEMS IN MALAWI

ABSTRACT

Consequences of climate change are likely to pose severe challenges on agriculture in Southern Africa. Agroforestry systems (AFSs) can potentially alleviate some of the adverse affects and offer management solutions to a sustainable use of the landscape. Positive effects of AFSs which have been shown frequently include soil carbon (C) and nitrogen input, sustaining favourable nutrient cycling and protection against erosion. The influence of the AFS tree component on the water cycling of the crops, however, is still relatively unknown.

In this study we assessed the influence of Gliricidia-maize-intercropping on carbon cycling and water fluxes compared to maize as a sole crop at two well-established long-term experiments in central and southern Malawi, run by the World Agroforestry Centre ICRAF. The controlled setup and different durations of the experiments ($>$ 10 and $>$30 years) at the two sites allowed comparisons of the maize control and Gliricidia treatment, the two sites with comparable climate but different soil characteristics, and also potentially the different experiment ages. We examined soil C contents and stability in different density fractions, soil physical characteristics and aggregation as well as soil hydrological characteristics. We also monitored soil moisture and matric potential in different depths, determined retention curves on samples in the lab and from field data and analysed soil moisture responses to rainfall events to assess the influence of the AFS on water fluxes.

Our results show a clear increase in C contents and stability as a result of the Gliricidia impact compared to the control, especially pronounced at the site with the generally lower baseline C contents. The treatment effect is also visible in soil physical characteristics such as porosity and bulk density, which is mirrored by a greater saturated hydraulic conductivity. These treatment effects were, however, not directly translatable into soil water dynamics as the latter were influenced by several additional factors such as soil texture and interception. The Gliricidia plots showed greater soil water storage capacities and retained overall more water, while generally both treatments were not under sever water stress during the observation period. We also noticed a protective effect against soil drying below the topsoil facilitated by the Gliricidia. Furthermore, infiltration shifted towards

more immediate/macropore infiltration under Gliricidia.
We conclude that the AFS treatment of adding Gliricidia into maize cultivation has a considerable effect on nutrient and water cycling in the crop, while the effect on water fluxes is not straightforward. While the differences in soil moisture and matric potential never lead to a shortage of water for the crops, a detailed examination of water fluxes require respective measurement in the field as they cannot be deduced from soil physical characteristics directly. AFS can thus not only support carbon accumulation and stabilization, but a sensible combination of trees and crops can also be beneficial for a more sustainable use of the available water in climate change induced shifts in precipitation.

3.1 INTRODUCTION

Agriculture in Southern Africa faces increasing challenges as a consequence of climate change (Fauchereau et al., 2003), such as nutrient depletion (Mbow et al., 2019), soil erosion (Montanarella et al., 2016; Olsson et al., 2019) and shifts in water availability (Trisos et al., 2022). This affects both food security (e.g. Tumushabe, 2018; World Food Programme, 2019) and ecosystem resilience (Jose, 2009; Sheppard et al., 2020a), hence adapted land use systems are required to respond to these challenges.

Agroforestry systems (AFSs) – combinations of crops and/or livestock with a woody perennial species – have been shown to offer promising management options in the light of these challenges. Depending on the species combination and the respective climatic and landuse setting, introducing a woody component into agricultural systems can provide a variety of benefits (Sheppard et al., 2020a). As shelterbelts or windbreaks, they can protect soils from erosion and crops from damages as well as excessive evapotranspiration (Cleugh, 1998; Littmann and Veste, 2008; Makate et al., 2019). The trees within AFSs also affect the nutrient cycling of the crops in various ways. While possible competition for nutrients might be a fear of many farmers when first implementing AFS, many beneficial short- and long-term interactions are well documented.

The trees in AFS provide additional carbon (C) input and increased soil organic matter (SOM) contents (Jose, 2009; Kuyah et al., 2019), augmenting soil fertility. The input can occur in various ways, e.g. via active incorporation of biomass into the soil, around the crops or simply the decomposition of plant materials and roots directly around the trees (Shi et al., 2018). Nitrogen (N) deficiency is a major problem in tropical cropping systems and often the most limiting nutrient (Ikerra et al., 1999). The integration of legume species can therefore increase plant-available N in the soil and lead to a fertilisation effect, thus reducing the need for artificial addition of fertiliser. Gliricidia sepium (Gliricidia) is a well approved intercrop legume tree species for nutrient demanding maize cultivation. Numerous studies have demonstrated its beneficial impact on carbon sequestration and nutrient supply when intercropped with maize (Akinnifesi et al., 2010) while increasing yields (Akinnifesi et al., 2006; Beedy et al., 2010; De Schutter, 2012; Ribeiro-Barros et al., 2017).

However, long-term sustainable improvement of SOM contents requires not only input but also stabilization of organic matter at mineral soil surfaces and within aggregates. This stabilization process is dependent on soil texture (Schweizer et al., 2021) and other physiochemical parameters like pH value, calcium (Ca) and magnesium (Mg) and the presence of sesquioxides (Rasmussen et al., 2018). Iron (Fe-) and aluminium (Al-) containing sesquioxides are known to be important

for aggregate formation and organic matter stabilization. This is especially true in soils with low activity clays (Barthès et al., 2008), where a relatively high ratio of pedogenic Fe to Al clay has been shown to support organic carbon stability against oxidation, allowing persistence in the soil (Kirsten et al., 2021). Depending on how stable C is bound within the soil, it can be grouped into different fractions: free light fraction (fLF), in aggregates occluded light fraction (oLF) and heavy fraction (HF), where C is bound to soil minerals (Golchin et al., 1997). The amount and stability of C in soils is strongly linked to soil structure (Bronick and Lal, 2005), and intercropping AFS with legume trees has been shown to increase aggregation (Blair et al., 2006) and aggregate stability (Chaplot and Cooper, 2015). Changes in soil structure in turn influence soil physical and hydrological characteristics, e.g. pore size distribution or water retention, affecting soil water at the macro scale (Williams et al., 1983; Nimmo and Akstin, 1988; Pachepsky and Rawls, 2003). Consequently, also the link between C inputs and soil hydrology has been examined.

Adding organic C in the form of manure can enhance soil structuring and lead to increased total porosity and water retention of the soil (Bodner et al., 2015). This effect seems to be stronger in soils with lower initial C content (Rawls et al., 2004), pointing to the interplay of mineral surfaces binding organic substances and subsequent aggregate formation. In a modelling study, Feifel et al. (2024) also found improved water retention and higher storage capacity of soils with increasing soil organic carbon (SOC) contents, however, the effect was dependent on soil texture and stronger in sandy soils. The texture-dependency of the SOC effect on water retention was also documented as part of a recent carbon-sensitive pedotransfer function approach (Bagnall et al., 2022) which also found a marked increase (about double) in plant-available water as a response to SOC input.

For AFS, the influence of C input on soil structure and water fluxes has also been studied, reporting that increasing C contents as a consequence of intercropping with legume trees lowered bulk density (García-Orenes et al., 2005) and improved water retention (Rawls et al., 2003). Farmers might be concerned to implement AFS due to a potential negative impact of the tree component on the crops, such as increased soil evaporation (Feifel et al., 2024) or competition for water in the root zone. This balance is very much depending on the climatic conditions and the combination of the species in the AFS. A more detailed discussion of the varied benefits and concerns in implementing AFS can be found in the review by Sheppard et al. (2020a). For instance, the different leaf stages and rooting depths together with a seasonality in rainfall did not lead to any competition for water in intercropping systems of coppiced Gliricidia and maize in a very common AFS in southern Malawi (Chirwa et al., 2007). However, there is still a lack of knowledge to which extent C-induced short- and long-

term changes in soil structure affect water fluxes in these systems.
Effects of land-use change only become evident after several years and are needed to be observed over multidecadal time spans (Dearing et al., 2010). Hence, long-term monitoring sites or experiments are essential to evaluate the effect of C-input strategies. The World Agroforestry Centre ICRAF in Malawi has been running experimental trials of combining maize crops with Gliricidia plants at two sites for more than 30 and more than 10 years, respectively. The sites are located in the same climatic zone and have large overlap in the intercropping treatments included in the experiments. Additionally, management conditions are similar (same pruning frequency, seeds, weeding activities) and also spacing between maize and Gliricidia are the same. They are therefore ideal to study the effect of Gliricidia on various processes and characteristics.
Gliricidia is well suited for the Southern African region due to its high leaf-N content, high biomass production and drought resistance (Kerr, 2012). The Gliricidia/maize intercrop has been shown to induce positive effects on soil fertility (Beedy et al., 2010), maize yields (Chirwa et al., 2003) and with the addition of inorganic fertiliser leads to higher maize productivity (Akinnifesi et al., 2007). Maize may take advantage of the nutrients from the Gliricidia prunings and Gliricidia's capabilities of retrieving nutrient from deeper soil layers (Makumba et al., 2009). Further, a combination of Gliricidia and maize could sequester more soil C than a maize monoculture (Makumba et al., 2007).
The influence of the long-term SOM stabilized aggregates and other soil structure characteristics on hydrological properties of these soils has not been studied in great detail yet. Hence, we use the unique setup of two of ICRAF's long-term experimental trials of Gliricidia and maize to analyze the changes in SOM and nutrient status as well as soil hydrological properties, time series of hydrological fluxes and rainfall events. We address the following research questions:

1. Does the AFS treatment increases C contents of the soils?
2. Do changes in SOM contents and stabilization affect soil structure and hence hydraulic characteristics?
3. How do these changes in hydraulic characteristics manifest in soil water fluxes and state variables?

3.2 METHODS

3.2.1 *Site description and management*

The study was conducted at two field sites in Malawi, at Chitedze Agricultural Research station close to Lilongwe in central Malawi and Makoka Agricultural Research Station close to Zomba in the south of the country (Fig. 3.1). Both sites offer controlled agroforestry

experiments run by the World Agroforestry Centre (CIFOR-ICRAF), among them trials of intercropping *Gliricidia sepium* (Jacq.) Walp. trees with maize (*Zea mays* L. hybrid variety MH41) (Akinnifesi et al., 2007; Chirwa et al., 2007), but differ in the duration of the experiment and in some soil and climatic conditions.

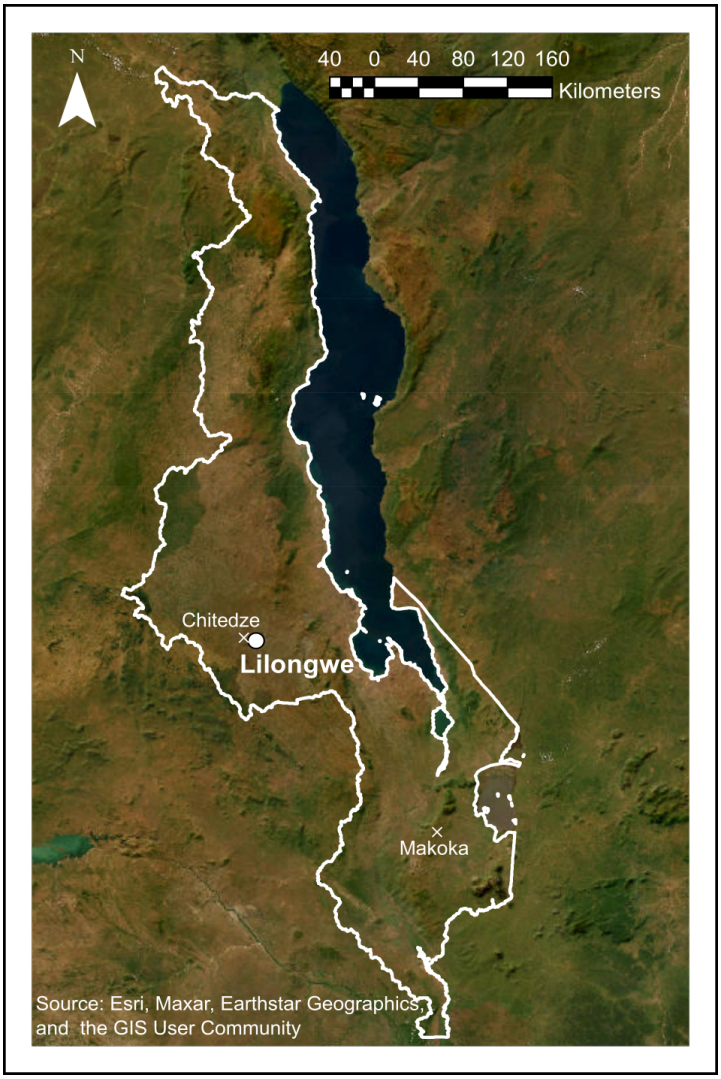

Figure 3.1: Map of the study sites Chitzedze and Makoka Research station in Malawi.

The Chitedze site (13°59'S and 33°38'E, 1146 m a.s.l.) is located in the Lilongwe plain and has a mean annual temperature of 20 °C and annual rainfall amounts to 800-900 mm with 85 % of these rains occurring between November and April (Malunga et al., 2017). Soils at the site are chromic Luvisols (IUSS Working Group WRB, 2022; Malunga et al., 2017), providing high cation exchange capacity and high agricultural potential for annual crops (Brown and Young, 1965). The experiment in Chitedze was established in 2009 in a split-plot design as an agroforestry demonstration site. The two parts within a

plot include two different cropping practices for the maize, the plots themselves represent different combinations of maize, tree component and fertiliser application. For our experiments, only the Gliricidia-maize intercropping and the control treatments were of importance.
The Makoka site (15°30'S and 35°15'E, 1029 m a.s.l.) is located in the southern region of Malawi and receives a mean daily temperature between 16 and 24 °C (Chirwa et al., 2003) and mean annual rainfall of 1024 mm, unimodally occuring mainly between November and April (Ikerra et al., 2001; Malunga et al., 2017). The soils were classified as Ferric Lixisols (Ikerra et al., 1999; IUSS Working Group WRB, 2022). The experiment in Makoka was established in 1992 in a randomised complete block design with three replicates per treatment, treatments varying in combinations of tree component and different crops as well as fertiliser applications (Ikerra et al., 1999). This study focused on the comparison of maize-only control plots and the AFS plots of Gliricidia with maize (Akinnifesi et al., 2007).
The management of these plots follows common practice of planting the maize in ridges each year before the rainy season starts. In the agroforestry treatments, Gliricidia was planted on alternate ridges with a spacing of 1.50 m between ridges and 0.90 m within the ridge, resulting in a planting density of 7,400 trees per hectare, as outlined in a previous study by Makumba et al. (2006). The Gliricidia trees are cut three times a year to a height of 30 cm, in October, December, and February and tree pruning was incorporated into the soil ridges. Therefore, the soil in the ridges cannot be considered as undisturbed as it is strongly mixed between the different depths.
The size of the maize plants was recorded exemplarily around the locations where we took the soil samples for measuring hydrological characteristics (big cylinders), at both sites and in both control and Gliricidia plots. In Chitedze, we measured only 5 plants due to time constraints (2 in the control, 3 in the Gliricidia treatment), in Makoka we measured 22 plants (10 in the control, 12 in the Gliricidia plot). Hence, this can only give a rough estimate on plant sizes. We also took photographs for visual comparison.
Pedological and hydrological characteristics were sampled and monitored at both sites in a field campaign in February/March 2022 but also including some analyses of previous campaigns in 2019 at the site Chitedze and in 2021 at the site Makoka.

3.2.2 *Soil sampling and analyses for texture, nutrients and soil physical characteristics*

On each of the plots we took undisturbed soil samples with the help of small cylinders (4 cm height and a volume of 100 cm^3) to examine bulk density and soil physical characteristics and disturbed soil samples for the analysis of nutrients, pedogenic oxides, texture and

soil texture. In Chitedze the sampling was undertaken in June 2019 as part of different study at the site. Ten sampling points were chosen per plot within the maize ridges at a spacing of approximately 3.5 m. At each point, two undisturbed samples in cylinders were extracted from depths between 0-10 and 10-20 cm, in the following named 5 and 15 cm depth. As the main campaign for the comparison of the two sites occurred in February/March 2022, we repeated the sampling at the same points with a hand shovel in 0-10 cm and 10-20 cm depth to be able to assess the current nutrient levels for the comparisons.
At the Makoka site, sampling was done in the campaign in February/-March 2022, with only five sampling points per plot. Samples were taken within the maize ridges, similar to the sampling in Chitedze, at approximately 5 and 15 cm depth. Due to time and budget constraints, not all analyses could be done for the small-cylinder samples in Makoka. Soil physical characteristics were carried out. For the nutrient analyses, the pooled samples of the upper and lower depth based on the 2021 sampling campaign were analysed.
The samples were transported to Germany and analysed in the laboratory of the Chair of Soil Ecology at the University of Freiburg. We analysed texture by sieving and sedimentation after the destruction of the organic matter according to DIN ISO 11277:2002, 2002. The amount of water dispersible clay (WDC) was determined for the samples from the site Makoka, by using only distilled water as dispersant. We estimated total exchangeable Ca-, Mg- and K-cations according to the standard method (Anderson and Ingram, 1990) and pedogenic oxides (Fe, Al and Mn) using the dithionite extraction method (Mehra and Jackson, 1958).
Analyses of total carbon and nitrogen were done in an elemental analyser (Vario EL cube, Elementar, Langeselbold, Germany) after standard preparation techniques. In order to determine the stability of the C input by the Gliricidia biomass, we also determined the relative proportions of C in different density fractions, the free light faction (fLF), the occulded light fraction (oLF) and heavy fraction (HF) according to the method of Golchin et al. (1997) and the process described in Graf-Rosenfellner et al. (2016). Bulk density was determined by drying the samples at 105°C and weighing, then relating the dry mass to the cylinder volume.

3.2.3 *Soil sampling and analyses for hydrological characteristics*

At both sites we took samples in the control and intercropping plot using large cylinders (4 cm radius, 5 cm height, 250 cm^3 volume) to assess a range of characteristics such as bulk density, saturated hydraulic conductivity (Ksat) and water retention curves. Samples were taken at three locations distributed in the plot, within the maize ridges and at two depths, 5 cm and 25 cm. The cylinders were transported to

Germany and analysed in the laboratory of the chair of hydrology at the Karlsruhe Institute of Technology (KIT).
Bulk density was determined after drying the samples at 105 °C and referring dry weight to the cylinder volume. The saturated hydraulic conductivity of the samples was determined with the Ksat apparatus (UMS GmbH, Munich) which uses a Darcy approach with a falling head. We measured water retention characteristics of the samples with the HYPROP apparatus (UMS GmbH, Munich, Germany) which uses tensiometers in two depths to record water potential while measuring the weight of the sample during evaporative drying. The apparatus is limited by the air entry point of the tensiometers to an approximate minimum of -800 hPa, therefore we combined the method with the WP4C PotentiaMeter (Decagon Devices Inc., Pullman, WA, USA), where lower potentials can be reached using a chilled mirror approach. With the help of the in-build HYPROP software, water retention curves were parameterised using the van Genuchten equation (Van Genuchten, 1980):

$$\theta(\psi) = \theta_r + \frac{\theta_s - \theta_r}{[1 + (\alpha|\psi|)^n]^{1-1/n}} \tag{3.1}$$

where θ_r is the residual water content in $m^3\ m^{-3}$, the saturated water content is θ_s in $m^3\ m^{-3}$, the scaling parameter is α, the absolute matric potential ψ and the dimensionless shape parameter is n.

From the retention curves we also derived porosity (water content at pF = 0) and plant-available water as the difference between water contents at pF = 4.2 and pF = 1.8. Soil hydrolological characterics were also determined on the small cylinder samples which were used for the nutrient and texture analyses. To measure total porosity, vacuum pycnometry at field moisture state was used. Saturated hydraulic conductivity was determined using the falling-head method (Hartge and Horn, 2009).

3.2.4 *Monitoring of meteorological and hydrological variables*

At both the Chitedze and the Makoka sites we installed a small meteorological measurement station in the control plot to record variables such as air temperature, relative humidity and precipitation. The temperature measurements seemed a bit spurious, possibly due to a malfunctioning sensor and some issues with the shielding. We, therefore, did not use these measurements. The precipitation was recorded with rain gauges (Chitedze: ECRN-100 Rain Gauge, Pullman, WA , USA; Makoka: Rain Collector, Davis Instruments, Hayward, CA, USA). The recorded tipping counts were translated to mm rainfall by multiplying with a factor of 0.2 as suggested by both manufacturers.
We assessed the influence of the site conditions and the agroforestry

treatment onto the water fluxes in the soil by monitoring soil moisture and matric potential in different depths at the two sites and on both control and Gliricidia plots. During the field campaign in 2022 we installed soil moisture sensors (TDR-310H, Acclima, Meridian, USA) in the rooting zone of the maize close to the ridges in depths of 10, 15, 25 and 60 cm. The top sensors were at 10 cm in Makoka and 7 cm in Chitedze as these were the shallowest possible depths to take an undisturbed sample for comparison. Unfortunately, there was some sensor failure in the maize plot in Chitedze and we only have the time series for the top sensor. In the same profiles where the soil moisture sensors were installed, we also inserted two matric potential sensors (MPS-2, Decagon Devices, Pullman, USA) at 10 and 25 cm depth. The sensors were connected to a data logger (YDOC ML417, YDOC, Ede, The Netherlands) and the fluxes were monitored from March to May 2022.

From the time series of soil moisture and matric potential responses to rainfall events were determined and water content changes calculated. We define a rainfall event as a segment of time during which more than 2 mm of rain were recorded, framed by periods without precipitation of minimum 6 h. Precipitation events with less than 2 mm did not lead to significant changes in topsoil water content and were therefore not included in the analyses. These events were classified according to their amplitude, time to soil moisture response after the rainfall and depth until soil water storage changes were visible. The soil water storage changes were calculated based on the difference of two successive soil water content measurements. The difference was then multiplied by the sensor depth increment of 0.18 m to acquire the change in storage. Additionally, we used the time series of field-measured soil moisture and matric potential to derive field retention curves in a similar way as for the values gained from the samples in the laboratory.

3.3 RESULTS

The aim of all analyses was to compare the AFS treatment with the corresponding monocropping version but also the differences between the sites and with depth.

3.3.1 *Soil characteristics and maize heights at the sites*

The texture classification at both sites showed differences between sites but also between treatments. At both sites, the sand fraction was the largest, followed by clay and lastly silt fractions (table 3.1). Chitedze had less sand than Makoka and therefore qualified as clay loam and Makoka with a higher sand fraction as sandy clay loam (according to IUSS Working Group WRB, 2022). In Chitedze the sand and silt

fractions of the control were larger than those of the AFS and vice versa for the clay fraction. Differences between depths were minor and negligible in Chitedze compared to the difference due to treatment or site. In Makoka, differences in the treatments were reversed: the AFS sand and silt fractions exceeded the ones of the control and vice versa for the clay fraction.

Table 3.1: Different soil characteristics such as texture, pedogenic oxides and nutrients for both sites, separated according to site, treatment and depth. Abbreviations are: WDC – water-dispersible clay; Fed/Ald/Mnd – dithionite-extractable Fe/Al/Mn; CEC – cation exchange capacity; C – organic carbon; N – nitrogen. The values in parentheses are standard errors of the mean. For texture in Chitedze, we also show the calculated averages of the two depths for easier comparison with the Makoka data. The numbers behind the site indicate: y – sampling year and n – sample size.

Site	Chitedze (y = 2019, n = 10)				Makoka (y = 2021, n=5)	
Treatment	Control		Gliricidia		Control	Gliricidia
Depth [cm]	5	15	5	15	0-20	0-20
Clay [g kg^{-1}]	283 (4)		315 (4)		310 (9)	293 (5)
	282 (5)	283 (5)	316 (6)	313 (6)		
Silt [g kg^{-1}]	285 (4)		258 (2)		163 (7)	191 (5)
	285 (6)	285 (6)	257 (3)	258 (3)		
Sand [g kg^{-1}]	433 (4)		428 (4)		527 (15)	570 (10)
	433 (5)	432 (5)	427 (5)	428 (5)		
WDC [g kg^{-1}]					96.1 (4.5)	70.4 (2.2)
Fe_d [g kg^{-1}]	43.05 (0.69)		44.12 (1.08)		32.21 (0.86)	28.27 (0.52)
	40.64 (0.49)	45.45 (0.68)	40.01 (0.84)	48.23 (0.65)		
Al_d [g kg^{-1}]	6.66 (0.11)		7.04 (0.26)		3.66 (0.15)	3.03 (0.04)
	6.43 (0.18)	6.89 (0.09)	5.94 (0.11)	8.14 (0.09)		
Fe_d/Al_d	6.46		6.27		8.80	9.33
CEC [$\frac{mmol_c}{kg^1}$]	99.9 (2.5)	93.9 (2.6)	97.3 (1.7)	88.1 (0.9)	51 (2.2)	90 (5.7)
C [g kg^{-1}]	27.3 (0.5)	30.1 (0.6)	28.9 (0.5)	31.4 (0.3)	7.2 (0.3)	16.4 (1.7)
N [g kg^{-1}]	1.7 (0.04)	1.9 (0.04)	1.9 (0.03)	2.0 (0.02)	0.7 (0.0)	1.4 (0.1)
C:N [ ]	15.7 (0.1)	16.0 (0.1)	15.0 (0.1)	15.6 (0.1)	9.9 (0.2)	11.3 (0.3)

The analysis of pedogenic oxides yielded higher values of both dithionite-extractable Fe (Fe_d) and Al (Al_d) in Chitedze compared to Makoka (see table 3.1), with an average of 43.0 g kg^{-1} and 44.1 g kg^{-1} Fe_d in the top 0-20 cm in Chitedze in control and Gliricidia treatment, respectively. In Makoka the values were 32.2 g kg^{-1} in the maize-only plot and 28.3 g kg^{-1} in the plot with Gliricidia. Al_d values averaged 6.7 g kg^{-1} for the control and 7.0 g kg^{-1} for the Gliricidia plot in Chitedze and 3.7 g kg^{-1} and 3.0 g kg^{-1} for control and Gliricidia in Makoka, respectively. Both sites have high levels of Fe_d and Al_d. The ratio of Fe_d/Al_d was higher in Chitedze (6.5 for the control, 6.3 including Gliricidia) compared to Makoka (8.8 for the control, 9.3 including

Gliricidia). The difference between treatments is only significant for Chitedze's topsoil (significance level of 0.05).
The carbon-to-nitrogen (C:N) ratio and its relationship with SOM fractionation also provided valuable insights into the degradability and stability of organic materials in the soil. The C:N ratio reflects the amount of carbon in organic material relative to nitrogen, serving as an indicator of SOM degradability and its susceptibility to microbial decomposition. The C:N ratio (table 3.1) was on average considerably wider at the C-rich Chitedze site (15.6, averaged across depths and treatments) than in Makoka (10.6). The treatment effect was minimal in Chitedze, the maize monocrop having an average C:N ratio of 15.9, whereas the Gliricidia had 15.3, with slightly higher values in the subsoil compared to the topsoil. In Makoka, the intercrop showed a wider C:N ratio of 15.4 than the maize control with a ratio of 9.9.
The maize plants in plots including Gliricidia were larger than in the control plots. The visual impression of the sites confirmed this (see Fig. 3.2).

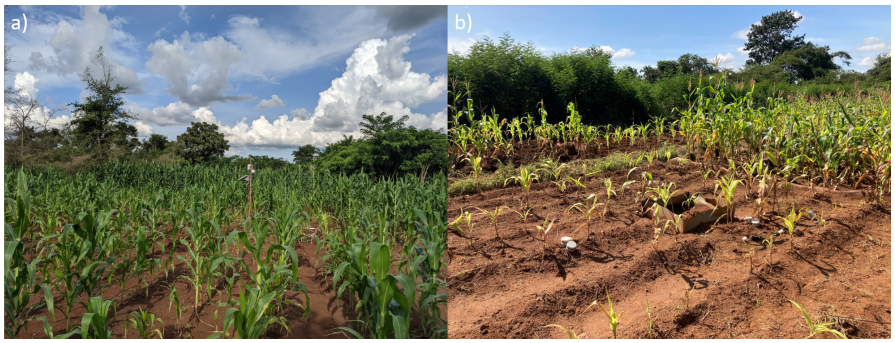

Figure 3.2: Photograph of the maize plants in maize-only control plots compared to the plots including Gliricidia. a) Chitedze site: in the foreground is the control plot, in the background behind the meteo station is the Gliricidia plot. b) Makoka site: In the foreground/to the left the control, to the right is the Gliricidia plot.

Our exemplary measurements of the maize plants indicate possible confirmation of this visual impression. The maize plants in Chitedze in the control plot were on average 92.5 cm high (n = 2, 100 cm and 85 cm of height), in the plot including Gliricidia the plants reached 101.7 cm (n = 3, sd = 27.2 cm). In Makoka, the maize-only plants were 65.7 cm high (n = 10, sd = 37.5 cm), the plants in the plots with Gliricidia reached an average height of 132.8 cm (n = 12, sd = 36.5 cm).

3.3.2 *Carbon content and stability of organic matter*

Makoka is the agroforestry site which has been established for a much longer time, with 30 years experiment duration. Hence, it might make sense to consider C contents of the same treatment age as in Chitedze (approx. 10 years). Makumba et al. (2006) reported for Makoka 8.8

g C kg^{-1} in the topsoil at the initiation of the project and 6.6 g C kg^{-1} for the control and 10.9 g C kg^{-1} for the Gliricidia treatment nine years after initiation (table 3.2). The treatment difference after approximately ten years was therefore with 4.4 g C kg^{-1} substantially larger at Makoka than the above mentioned treatment difference of 1.5 g C kg^{-1} in Chitedze.

Table 3.2: Comparison of C content in topsoil samples (0 – 20 cm) in Makoka and Chitedze at different periods after initiation of the AFSs.

Location - Year (AFS age)	Control C content [g C kg^{-1}]	Gliricidia C content [g C kg^{-1}]	Difference C content [g C kg^{-1}]
Makoka - 1992 (0) [a]	8.8		
Makoka - 2001 (9) [a]	6.6	10.9	4.3
Makoka - 2020 (28) [b]	7.0	17.3	10.3
Makoka - 2022 (30)	7.2	16.4	9.2
Chitedze - 2022 (10)	28.7	30.2	1.8

[a] Makumba et al. 2006 (data from 1992, 2001)

[b] Maier et al. 2023 (data from 2020)

If we look closer into our data, we see that the comparison between sites showed substantially higher overall C content at Chitedze compared to Makoka (Fig. 3.3 a). The differences between control and Gliricidia were minimal at the Chitedze site, with 28.7 g kg^{-1} C in the control across both depths and 30.2 g kg^{-1} C in the Gliricidia treatment. In Makoka, the site with generally lower C contents, the treatment effect was very pronounced with considerably higher C contents in the Gliricidia plot (16.4 g kg^{-1} C) compared to the control plot (7.2 g kg^{-1} C).

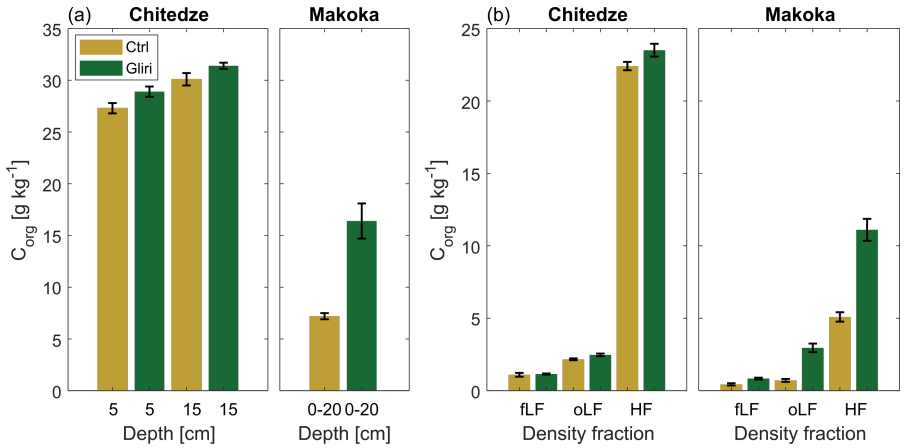

Figure 3.3: C content (a) and density fractionation of organic C (b) in the control (Ctrl = yellow) and the Gliricidia treatment (Gliri = green) at the sites Chitedze and Makoka.

Considering the C contents in the three different density fractions, we see that 10 years of agroforestry treatment at the Chitedze site did not

lead to higher C content in any specific fraction (Fig. 3.3 b). In Makoka, the strong increase in C contents after 29 years of agroforestry mainly occur in the aggregate-protected oLF (4-fold increase) and in the HF (2-fold increase) (Fig. 3.3 b).
A comparison of the C contents in the oLF fraction with the water-dispersible clay amounts in the 10 samples in Makoka (table 3.1) showed a negative relation (Fig. 3.4).

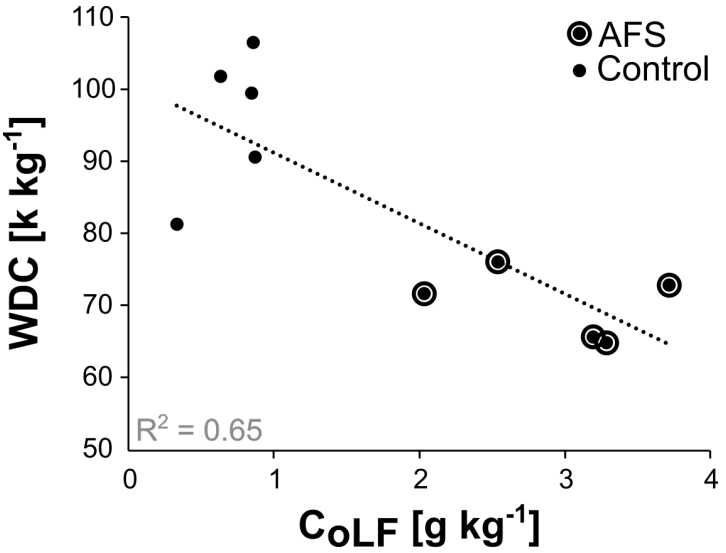

Figure 3.4: Relationship between the aggregate-protected C fraction (oLF-C) and water-dispersable clay (WDC) contents at the site Makoka.

Analysis of the soil density fractions revealed distinct variations in carbon and total nitrogen accumulation across fractions (table A.3). In both treatments, the occluded light fraction (oLF) displayed the widest C:N ratio, followed by the free light fraction (fLF), with the heavy fraction (HF) showing the narrowest ratio.

3.3.3 *Soil physical and hydrological characteristics*

Bulk density was determined at both sites as part of the soil characterisation in the small cylinders and as well as part of the hydrological characterisation in the large cylinders. The soils in Chitedze had generally lower bulk density compared to Makoka, however the variability in the data due to the small sample size is very high (Fig. 3.5). At both sites, bulk density clearly increased with depth. The treatment effect was more ambiguous. In Chitedze, there was no apparent difference between treatments, whereas in Makoka values of bulk density seemed to be slightly lower in the Gliricidia treatment compared to the control. However, the variability again masked the difference.
Porosity was slightly higher at the Chitedze site compared to Makoka (Fig. 3.5). Differences with depth were mainly apparent as decreases in porosity from topsoil to subsoil. The treatment effect was not clearly

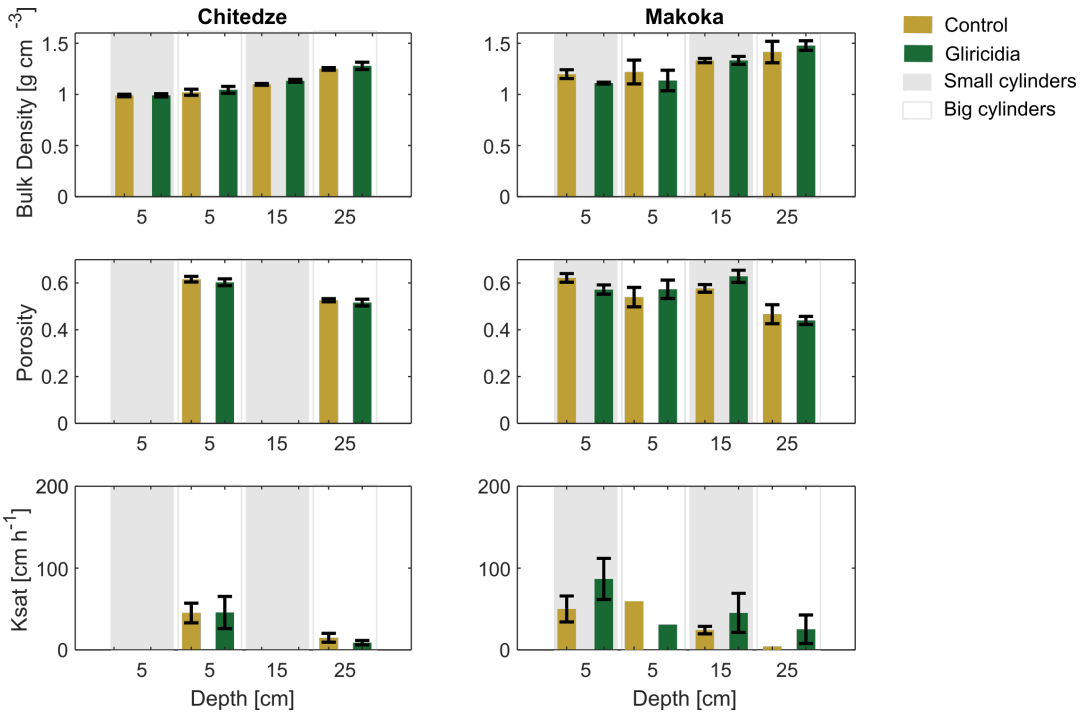

Figure 3.5: Bulk density, porosity and Ksat in 5 and 15 cm (small cylinders) and 5 and 25 cm (big cylinders) depth. For Chitedze n=10 and Makoka n=6 per treatment and depths. Detailed numbers can be found in the appendix (Table A.2).

visible in the comparisons. In Chitedze values between the Gliricidia plots and the controls were similar. In Makoka the shifts were also not distinguishable from the error margin, with the possible exception of a slight increase in the subsoil porosity from control to Gliricidia (Fig. 3.5).
Saturated hydraulic conductivity in the topsoil matches as expected with regard to the differences in C content and porosity, showing no difference between the control and Gliricidia treatment in Chitedze. For Makoka we found higher Ksat values in the Gliricidia treatment compared to the control, as we would have expected due to also higher C contents and porosities. The subsoil painted a similar picture for both, Chitedze and Makoka. However, difference in Ksat between the treatments were within the error bars. In all cases Ksat decreased with depth.

3.3.4 *Water retention curves*

Figure 3.6 compares the laboratory water retention curves obtained from the big soil samples to retention curves derived from the soil moisture and matric potential monitoring in the field.
There is a clearly distinguishable difference between laboratory topsoil and subsoil water retention curves (Fig. 3.6, a and b). The top-

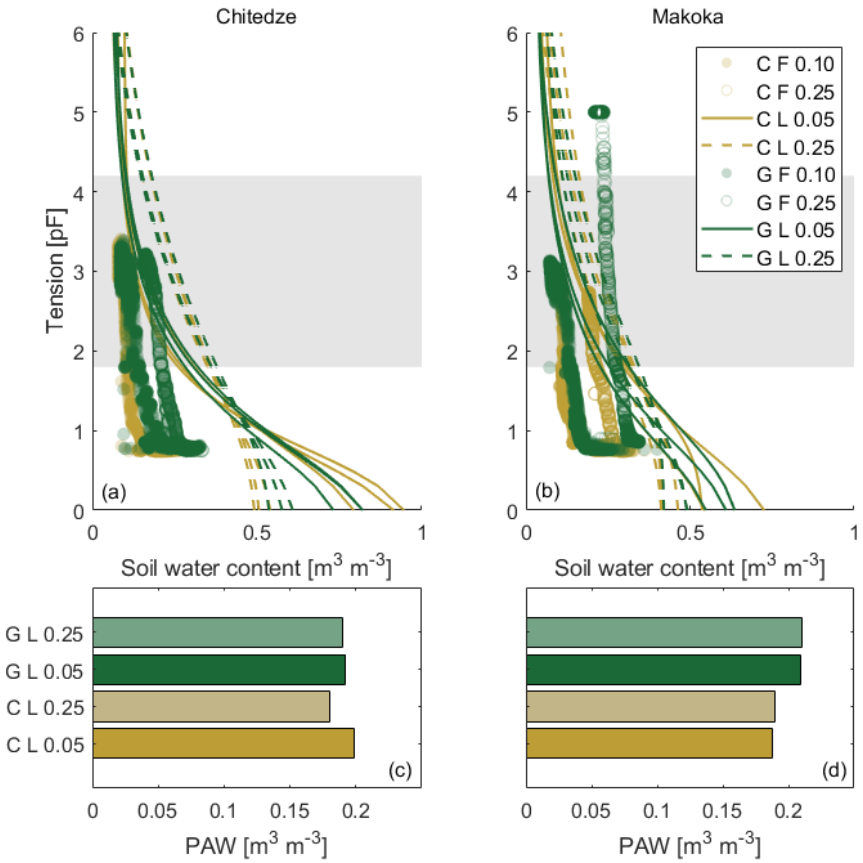

Figure 3.6: Soil water retention curves at Chitedze (left) and Makoka (right). Each line curve is derived from a sample analysed in the laboratory (L) and dotted curves from field measurements (F). The solid lines represent topsoil (5 cm depth) samples (numbers in legend stand for the depth) and dashed lines for samples at 25 cm depth. The colours indicate the treatment with yellow being the control (C) and green the Gliricidia (G). The grey box highlights the range of plant-available water (PAW), i.e. from pF = 1.8 (field capacity) to pF = 4.2 (permanent wilting point). The bottom panels show the calculated PAW for the different treatments and depths for the two sites.

soil samples have always greater porosity and flatter curves in the more humid range. This is more pronounced in Chitedze than in Makoka. Porosity values contained a similarly clear pattern: Porosities in Chitedze were overall higher than in Makoka (see section 3.3.3 and Fig. 3.5). The differences between treatments need to be considered separately for the two locations. In Chitedze, the control SWRCs were flatter in the topsoil and slightly steeper in the subsoil. Additionally, porosities were about 10 % higher in the Gliricidia treatment compared to the control. In Makoka, however, there were no distinguishable differences between in the treatments.

The comparison of laboratory (Fig. 3.6, a, b, lines) and field (Fig. 3.6, a, b, dots) retention curves, yielded an apparent "offset" around

pF 0.8 – 1 at the wet end of the field retention curves. There was generally a clear difference between laboratory and field data, and the SWRC barely overlapped. The field SWRC were overall steeper and of rather similar shapes. The distance between the field SWRC was, however, stronger than for the laboratory SWRC. The largest contrast was between the curves of the different depths, SWRC of different treatments were rather overlapping. Both laboratory and field SWRC were steeper in the subsoil compared to the topsoil.
Plant-available water (PAW) is indicated by the grey box in figure 3.6 (c and d) and two interesting patterns can be observed in the laboratory data. In Chitedze, PAW in the control had slightly higher values compared to the AFS treatment, however, generally the differences are not very pronounced. Makoka's PAW differed between treatments with higher values in the Gliricidia.
In the field data, it is harder to identify clear patterns as the soils did not dry out until the wilting point. Nevertheless, due to the steep slopes, it can be assumed that PAW is much smaller than the ranges observed in the laboratory.

3.3.5 *Monitoring of soil moisture and matric potential*

At both sites, water content and matric potential were monitored. We first consider the time series of water content.

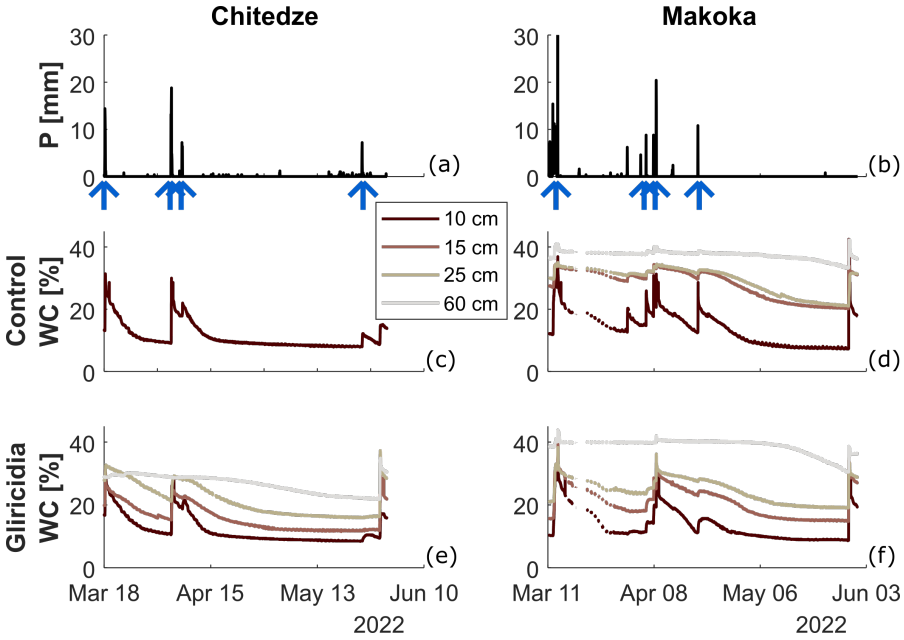

Figure 3.7: 15-min volumetric water content observations at both locations for both treatments respectively; colour code indicates measurement depth. Missing time series for the Chitedze maize treatment.

First of all, it must be mentioned that in the control plot in Chitedze only one of the four sensors operated (Fig. 3.7 c). Therefore, only data

from the topsoil sensor are available. In general, soil water content time series showed behaviour as expected. The water content showed increases during rainfall events and continuous drying afterwards until the next rain event occurred. Topsoil sensors recorded driest values and the deepest sensor the wettest values.
At a first glance, there was no clear difference in overall water content between neither the locations nor the treatments. However, the available topsoil sensors in Chitedze as well as Makoka's soil water content measurements showed dampened, smoothed and slower responses after rainfall in the Gliricidia throughout all depths compared to the control. The drying process after a rain event seemed stronger in the Gliricidia compared to the control. Additionally, the drying was more pronounced i.e. steeper in Makoka compared to Chitedze.
Further, we investigated the matric potential time series monitored at two depths in both locations and both treatments.

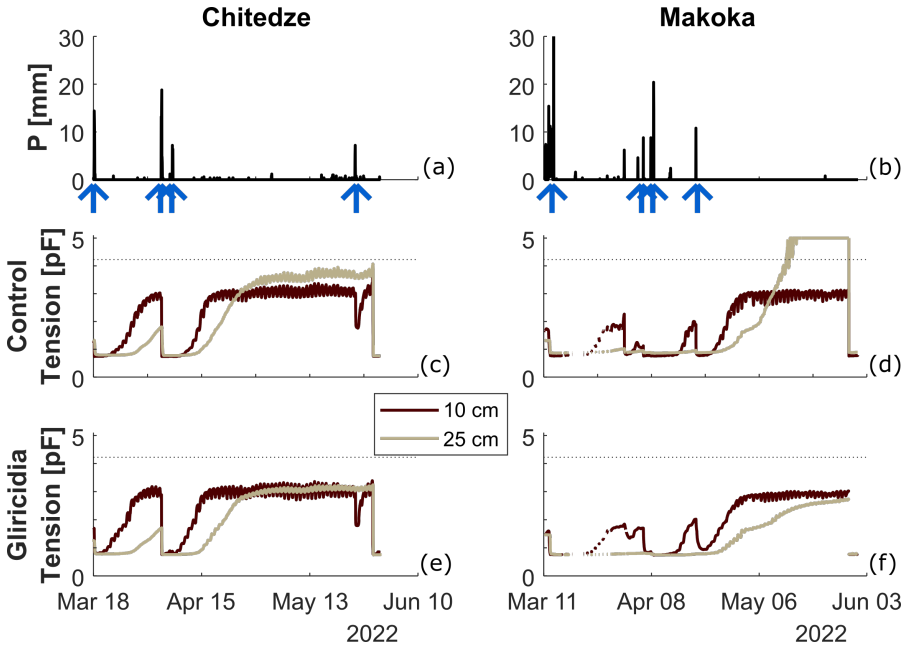

Figure 3.8: 15-min matric potential observations at both locations for both treatments, colour code indicates measurement depth. Dashed line indicates the PWP at pF = 4.2.

In a similar manner as the soil water content, the matric potential time series followed the precipitation patterns (Fig. 3.8). The lower sensors at Chitedze responded almost concurrently with the top sensors at the onset of a rain event, but clearly lagged behind in the drying process. The lower sensor in the Makoka control plot (Fig. 3.8 d) reported during the last month some erroneous looking data potentially reaching a maximum measurement value after already being quite a bit out of its accurate measurement range.
Nevertheless, one clear pattern observed in the treatments is that the subsoil sensors dried out stronger throughout the observation period

compared to the topsoil sensors, and the control's subsoil drying exceed the one of the Gliricidia. Overall, it appeared that more water remained available in the Gliricidia treatments (pF 2-3) compared to the control (pF 3-4). Only the sensor in the Makoka control plot (Fig. 3.8 d) reached the PWP.

3.3.6 *Analysis of rain events*

Analysis of rain events, specifically, the soil's response can be insightful to understand water dynamics. In total, we identified four rain events (> 2 mm and 6 h of inter-event period) in Chitedze and ten events in Makoka.
Rainfall events in Chitedze ranged from 3 mm to 69.4 mm, lasting between 7 h to 11 h. The Makoka events ranged from 3.8 mm to 146.4 mm and their durations from 1 h to 44 h. To explore the soil's response to the rain events we calculated the soil water storage changes during and after an event.

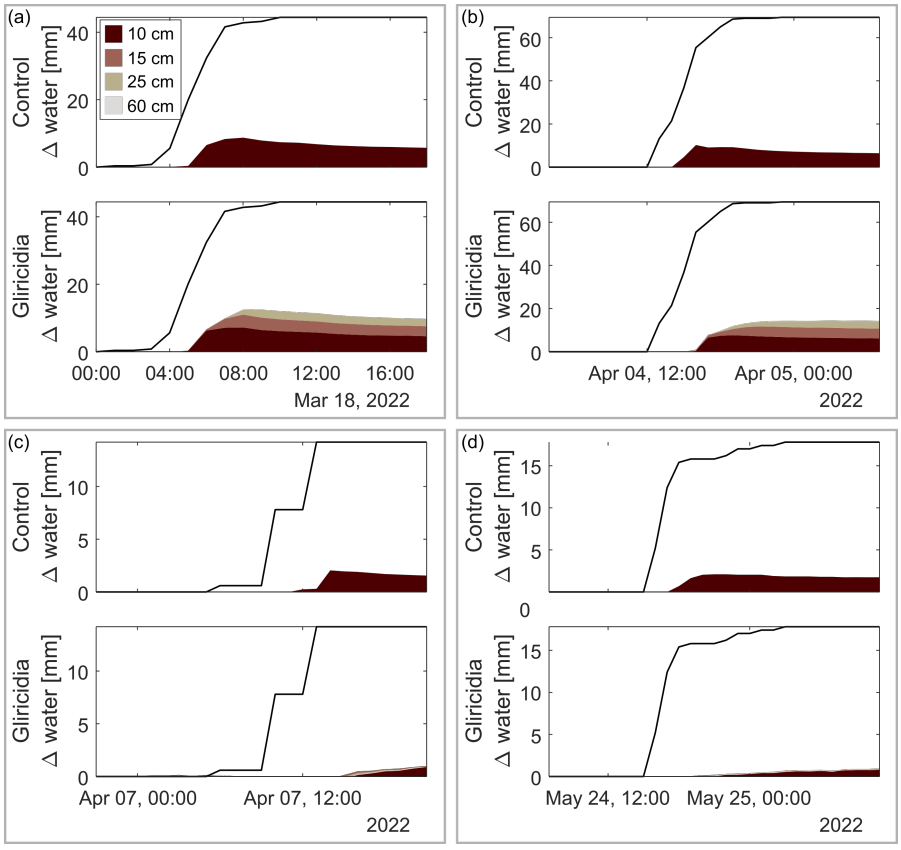

Figure 3.9: Cumulative precipitation (line) of four different precipitation events (E1-E4 from Fig. 3.7, blue arrows) and the responses in soil water storage at different depths estimated from the soil moisture sensors and separated by treatment in Chitedze.

We show four (of five, the missing one showed only minor response in the soil water content) observed events for Chitedze in figure 3.9 and point out the limitation that only the top sensor in the maize control functioned properly. In the smaller rainfall events, the topsoil sensor in the control appeared to have responded faster and sometimes also stronger compared to the sensor in Gliricidia (Fig. 3.9, c and d), where the response was delayed or less intense. In the events with more precipitation (Fig. 3.9 a and b), the water slowly percolated downwards in the Gliricidia plot as demonstrated by the sequential storage increases with increasing depth. Naturally, the amplitudes slightly decreased with depth, reflecting partial storage of infiltration in the layers above. It appears that in both events (a) and (b), the top sensors reached field capacity, however, not full saturation (Fig. 3.8 a).

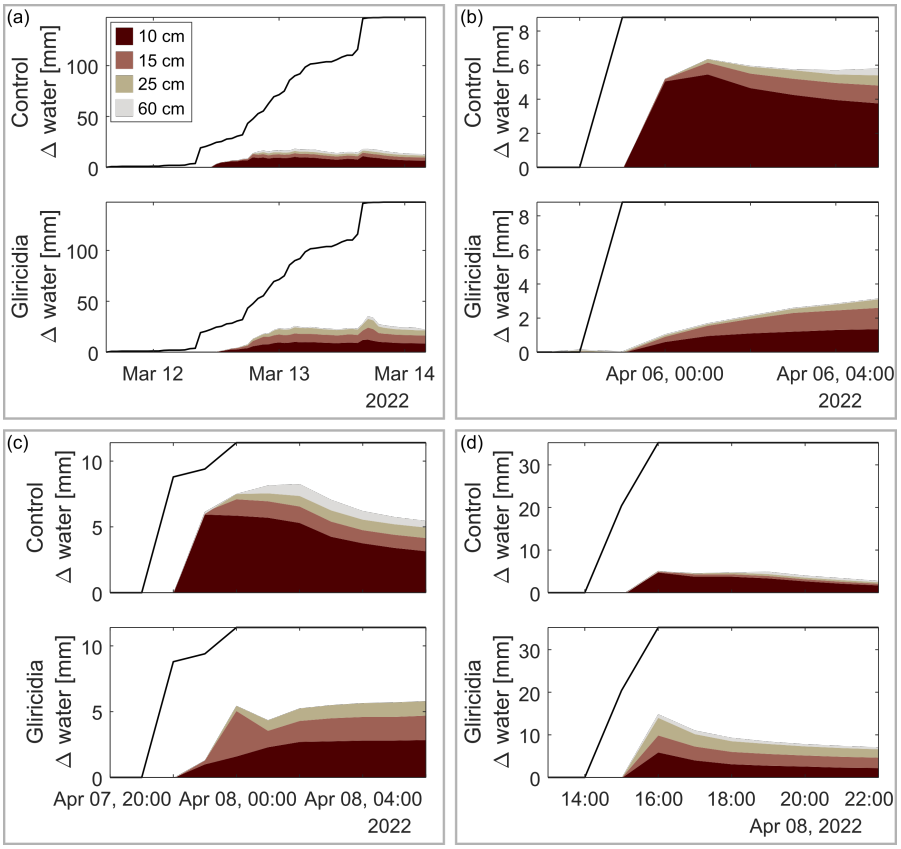

Figure 3.10: Cumulative precipitation (line) of four different precipitation events (E5-E8 in Fig. 3.7, blue arrows) and the responses in soil water storage at different depths estimated from the soil moisture sensors and separated by treatment in Makoka.

In Makoka (Fig. 3.10), fortunately, all eight sensors were functioning. Therefore, we could assess soil water storage changes in both treatments for the whole 80 cm. The largest event in the measurement period had a cumulative precipitation of 146 mm (Fig. 3.10 a). For this event only a small fraction of the precipitation percolated into the soil. The largest difference appeared to be the response of the deepest

sensor in the Gliricidia, which was quite strong and lasted over 24 h. During the other events, which were comparable in size to the ones in Chitedze, we also observed differences between treatments. The sensors in the Gliricidia plots at greater depths reacted simultaneously to the topsoil sensor. Further, the deeper Gliricidia sensors showed stronger reactions than the ones in the control plot. At the control plots, the topsoil sensor showed strongest reaction and also stronger than in the Gliricidia plots. The sensors in the control again responded with a stronger delay, which increased with depth. The lowest sensor reacted only very seldomly to a precipitation event in both treatments.

3.4 DISCUSSION

3.4.1 *Agroforestry treatment increases C contents, relative effect is stronger in soils with generally lower C content*

Two main C content patterns were observed in this study: 1) Overall the C content was higher in Chitedze (topsoil average: 29.45 g C kg^{-1}) compared to Makoka (topsoil average: 11.8 g C kg^{-1}) and 2) C content differences due to treatment effects were larger in Makoka (topsoil: 9.2 g C kg^{-1}) than in Chitedze (topsoil: 1.5 g C kg^{-1}) (table 3.2). The latter providing some more evidence that AFS can increase soil C, supporting already existing literature (Nabuurs et al., 2007; Ramachandran Nair et al., 2009; Nabuurs et al., 2022).
The treatment difference was after ten years substantially larger at Makoka than in Chitedze, which indicates that soils with low C content store additional C more effectively as they tend to be farther from reaching their theoretical C saturation point. On the contrary, soils with already high C saturation, as it is the case at Chitedze, are less efficient at storing extra C and are therefore less responsive to C-input measures (Stewart et al., 2008). Also, Iwasaki et al. (2017) found a negative relationship between initial soil organic C content and the rate of soil organic C differences in Japan. Hanegraaf et al. (2009) observed highest organic C accumulation in Dutch grasslands and maize fields with lowest initial soil organic matter content. However, they also pointed out initial soil organic matter content alone cannot explain the diverse SOM trends generally observed in their study. In soils and soil horizons with varying textures and mineral compositions, different stabilization mechanisms are dominant (Lützow et al., 2006).

3.4.2 *Carbon content and pedogenic oxides affect hydraulic characteristics*

Stability and aggregate formation

The soil structure plays a critical role in agricultural productivity by influencing various soil functions. One of the primary indicators of

soil structure status is aggregate stability (Six et al., 2002). For Alfisols, which correspond to Luvisols and Lixisols in the US soil taxonomy, soil organic matter is the dominant factor influencing aggregation (Bronick and Lal, 2005). This finding aligns with the results of Atsivor et al. (2001), who reported that increases in soil C content can enhance soil stability through improved aggregation, particularly under sustainable agricultural practices compared to conventional farming. The stability of aggregates depends not only on the amount of soil C but also on how C is bound within the soil matrix. WDC is an important parameter, often used as an indicator of both soil aggregate stability and erodibility (Paradelo et al., 2013).

Our results at the Makoka site indicate that the Gliricidia treatment was associated with lower WDC, which suggests the formation of more stable aggregates compared to maize monocropping. Gliricidia intercropping enhanced C storage, particularly in the more stable oLF- and HF-fractions indicating free mineral surfaces left to bind and stabilize biomass C (Castellano et al., 2015). The fLF-fraction, representing less stable C pools, remained relatively constant across treatments reflecting generally high C mineralization and C-turnover rates of rapidly decomposing N-rich legume biomass in tropical climate. The high and very high levels of pedogenic oxides (Al, Fe) at Makoka and Chitedze respectively also likely contribute to soil stabilization (Barthès et al., 2008), adding to the to the potential structural benefits typically attributed to increased SOM in AFS treatments.

Previous studies, such as Maier et al. (2023), observed a significant increase of more stable C fractions where C is bound to minerals and stabilized within soil aggregates. This suggests that Gliricidia derived C is incorporated into soil aggregates, thereby contributing to a more stable soil structure. This structural enhancement could theoretically impact bulk density and Ksat by increasing porosity within the soil matrix. Literature supports this relationship between soil organic carbon and soil structure, indicating that soil organic carbon plays a pivotal role in promoting aggregation, stability and influencing pore size distribution, which in turn affects water retention and water movement (Williams et al., 1983; Nimmo and Akstin, 1988; Bronick and Lal, 2005; Pachauri, 2012; Bagnall et al., 2022).

The potential effects of treatments on bulk density and Ksat, both of which are closely related to soil porosity, will be evaluated in the upcoming section. Soil structure is intricately linked to the distribution of pore sizes, which, in turn, affects water movement and retention (e.g. Nimmo and Akstin, 1988). The potential changes in BD and Ksat could, therefore, provide further insight into the mechanistic links between C sequestration, soil structure, and water dynamics under different management practices.

Comparison of soil physical characteristics and soil water dynamics

Differences in porosity, bulk density and Ksat were not directly relatable to C content in a straight forward manner. On the one hand, the expected differences in porosity were not observed, as the variations fell within the error margins. In Chitedze, a slightly higher porosity than in Makoka corresponded to overall lower bulk density. This aligns with the general understanding that OM and pedogenic oxides contribute to soil structure and hence affect porosity and bulk density. However, no treatment-related variations were observed. In contrast, Makoka showed measurable differences in both soil C and WDC with the treatments, which were accompanied by corresponding variations in bulk density and also Ksat.

The literature provides contradicting evidence regarding the relationship between organic matter and Ksat. Lado et al. (2004) showed that Ksat can increase in high-OM soils due to improved aggregate stability and reduced slaking. Similarly, Fu et al. (2015) reported that high SOC content is often accompanied by increased Ksat, especially in soils with high biological activity and porosity. In Makoka, where differences in OM and soil structure were more pronounced between treatments, variations in Ksat were observed, suggesting that soil texture and composition modulated the effect of OM on hydraulic conductivity.

In contrast, Nemes et al. (2005) found indications of a negative correlation between OM and Ksat. They suggest that while OM can increase porosity, it also retains water, thereby reducing the amount of water available for free flow. This results in a complex interaction where OM enhances hydraulic conductivity by improving soil structure but simultaneously restricts water movement by retaining moisture. Our findings align with this complex relationship, as higher C content in Chitedze's soils did not result in significant Ksat changes despite higher porosity compared to Makoka.

The absence of significant Ksat changes in Chitedze could be attributed to the specific interaction between soil texture and OM quality, highlighting the need for more detailed studies on how different OM types and soil conditions affect hydraulic properties.

Water retention curves from our study showed that topsoil samples had greater porosity and flatter retention curves in the more humid range. The treatment differences appeared smaller than differences in depth, as the former curves overlap more than the latter. The porosities of the field retention curves exceed the porosity values measured in the laboratory. The sensors were not calibrated to the field site-specific soils, which could be one of the reasons for the difference between field and laboratory retention curves. On average, both sites demonstrated more plant-available water (PAW) in the top 25 cm in the AFS treatment; however, a treatment difference was barely noticeable in Chitedze. Interestingly, the clear treatment differences in Makoka's soil C were reflected in the PAW, but the generally high soil C level in

Chitedze did not result in higher PAW compared to Makoka. The literature shows varied connections between these variables. For instance, Rawls et al. (2003) reported that the relationship between soil water retention and organic carbon content is strongly influenced by soil texture. Their work suggests that in sandy soils, an increase in OM content leads to an increase in water retention, while in fine-textured soils, the effect is less pronounced or even reversed at lower organic carbon levels. High soil C as e.g. in Chitedze's topsoil may be contributing to improved PAW, as highlighted by studies that report SOC's ability to enhance water-holding capacity (Lal, 2020; Feifel et al., 2024). However, the PAW in the Makoka AFS treatment exceeded Chitedze's PAW, potentially because it contained more sand than Chitedze and therefore the effect of stronger water retention took place. The matric potential time series also confirmed that in Makoka's Gliricidia, where we had more sand compared to the control, more water was available throughout the measurement period. The vertical distribution of soil C also plays a critical role in the soil water balance, as indicated by Feifel et al. (2024), who found that shallow C-rich soil layers increase evaporation, while deeper incorporation improves water availability for crops. The contrasting findings between Chitedze and Makoka emphasize the importance of site-specific factors in determining soil hydraulic properties. While OM generally improves porosity and water retention, its effect on Ksat and PAW is highly dependent on the interaction with soil texture, structure, and C distribution.

3.4.3 *Changes in hydraulic characteristics are visible in water dynamics*

The interesting question is, if these small differences are also visible in the time series measurements of soil water content, matric potential, and more specifically in their response to and after precipitation events. Based on the observed soil hydraulic properties, i.e. similar Ksat values, we expected similar infiltration responses to rainfall events at both locations. We also expected to see faster and more infiltration visible in stronger AFS sensor responses as a consequence of the treatment differences. However, we observed both, differences between sites and between treatments. Yet, comparisons were not straightforward though; between treatments in Chitedze because only the top sensor was available for the control plot, and between the sites because the events differed in intensity and rainfall amount. Two events were relatively similar at both sites with precipitations of 12-15 and 35-40 mm. It appeared that in Chitedze the sensors reacted later after the onset of precipitation than in Makoka, where reactions happened rather immediate. Treatment differences were easier to observe. In Chitedze, the amounts of water reaching the soil differed with stronger reactions in the control plot. Especially during smaller events, the sensors in the Gliricidia plots did not show a strong reaction. In addition, the

sensors in Makoka's control plot measured greater changes in water content, except for the biggest event with over 100 mm of rainfall. One possible explanation is interception. Depending on the season, maize and Gliricidia leaves cover more ground in the AFS plot. Additionally, the maize crop was larger in the Gliricidia compared to the control. Larger interception capacities in the Gliricidia plot potentially prevented rainfall to reach the soil and to be detected by the sensors. This could also be a reason for the different reaction times between the two sites. The maize plants were generally larger and healthier in Chitedze than in Makoka. Another treatment difference observed in Chitedze's AFS plot was that the deeper sensors reacted with more delay to the rainfall than the top one, indicating "slow" percolation rather than macropore infiltration. This delayed response can be attributed to the fact that the Gliricidia plot in Chitedze contained more clay and less sand than the control plot, which tends to reduce the speed of water movement. The lower Ksat further indicated slower water movement through the soil. In contrast, Makoka's Gliricidia plot displayed an almost immediate response in the deeper sensors, which reacted nearly simultaneously with the onset of rainfall. This rapid response suggests faster infiltration. The Gliricidia plot in Makoka contained more sand, which increases soil drainage and promotes rapid water movement, and less clay, reducing water retention and allowing quicker infiltration. The soil had a higher Ksat value than the control (difference on average 123 mm h^{-1}) permitting water to move quickly through the soil profile. Additionally, the higher carbon content and greater PAW allowed more water to be stored. Similarly, Chirwa et al. (2003) found higher infiltration rates in their AFS treatment as compared to monocropping. The rapid sensor response in the Makoka AFS might be facilitated by macropores, possibly from root structures or more biological activity in the AFS treatment compared to the control. Graham and Lin (2011) classified flow regimes based on the sequence of soil moisture sensors responses across a soil profile. Preferential or macropore flow referred to the events where deeper sensors reacted faster than shallower sensors. The deeper sensors in Makoka's control plot showed a delayed response compared to the top sensors. This delay may be due to the absence of macropores and was potentially enhanced by the control's higher clay content relative to the Gliricidia, which slowed down water infiltration and percolation. Furthermore, the lower Ksat in the top layer restricted water flow, causing moisture to move more gradually through the soil profile. One aspect to be mentioned regarding the soil water potential is the flattening of the curve during a precipitation event. The wetting does not continue until matric potential is nearly zero, but rather flattens around approximately pF=1. One reason could be that the soil has a lower (drier) air-entry potential and therefore limits water fluxes into the ceramic disk of the sensor, whose air-entry potential is at -5 kPa.

Another reason for not closing the water balance, in particular during the strong precipitation events, is that the water infiltrates at the same rate as it is redistributed into the deeper soil, hence, storage change remains stable. The high rainfall intensity of up to 30 mm during a 15 min measurement interval (120 mm h^{-1}), does not exceed Ksat but reach close to unsaturated conductivity values (Fig. A.2). The soil reaches an infiltration saturation state, therefore water remains ponding at the surface due to the absence of topographic gradients. The ponding water continues infiltrating at the rate of redistribution. The soil water measurements do not reach saturation, however, the relatively slow drying when rainfall ceased supports this. Furthermore, the water tables may slowly rises upwards along the flanks of the ridges (Fig. 3.2) increasing the surface area where infiltration can occur.
After rainfall events, we expected slightly slower soil drying and less water loss in Makoka due to smaller porosity and greater PAW, especially in the Gliricidia plot, and smaller maize plants leading to less ET. In both locations, the drying effect was stronger in the Gliricidia compared to the control plots, with site Makoka experiencing overall the strongest drying. This difference can likely be attributed to the higher sand content in the Gliricidia plot (particularly in Makoka) enhancing drainage and accelerating the drying process. Interestingly, in both sites, the deeper soil layers in the control dried out faster and more intensely than in the Gliricidia plots. This could indicate that root water uptake from maize plants was greater at depth in the control plots, possibly due to the plants accessing water reserves more effectively in response to limited surface moisture. Additionally, the plants were less protected or could grow different root structures without competition to the Gliricidia roots. Matric potential measurements also indicated that more water remained available in the Gliricidia treatments compared to the control plots. This suggests that the Gliricidia, potentially due to higher C content, retained more water overall. It implies a generally greater storage capacity for water in the Gliricidia plots, enabling them to hold moisture more effectively than the control plots. These findings are in line with reports by Chirwa et al. (2007) in AFS of Gliricidia and pigeon pea in southern Malawi. They also found that there was enough water stored in the soil so that both plants had sufficient water available.

3.4.4 *Implications of introducing AFS for nutrient and water availability*

In the following, we point out further aspects of introducing trees into monoculture crop fields regarding nutrients and water availability.
In terms of maize growth, the height of maize plants serves as an important measure of both yield potential and canopy interception, with taller plants indicating better growth conditions. Maize plants

were generally taller and healthier in Chitedze than in Makoka, and more vital in the Gliricidia compared to the control treatment. The improved growth in Chitedze may be attributed to more favourable conditions and a higher nitrogen availability in the Gliricidia treatment as observed in both the results and supporting literature on rooting depth and nutrient cycling.

Since CEC is mainly found in clay minerals and soil organic matter, it is an important factor for soil fertility and can potentially be linked to soil texture and organic matter (Beedy et al., 2010). Gaiser et al. (2012) showed that legume-derived organo-mineral compounds enhance soil CEC in a tropical Acrisol. Corresponding with consistent C contents at Chitedze, also CEC had no response on Gliricidia residue input. At Makoka though we found significantly higher CEC in the Gliricidia treatment corresponding to Beedy et al. (2010), who found a significant increase in soil CEC associated with Gliricidia, suggesting a key role of these trees in maintaining CEC in agricultural fields. This would furthermore explain our strong differences in maize plant size and vitality in the legume intercropping treatment compared to sole maize in Makoka.

Furthermore, we did not find any indications for severe water competition between the maize plants and the Gliricidia, which was also confirmed by Makumba et al. (2009) for a Gliricidia-maize intercropping system. The matric potential remained below the critical PWP at both sites under Gliricidia treatment, indicating no occurrence of water stress for the plants. Chirwa et al. (2007) found in Makoka that soil water content was generally lower in the Gliricidia system at the beginning of the cropping season (end of dry season), indicating that the trees depleted soil water during the dry period. However, they also point out that rainfall exceeded potential evaporation during cropping season. If the Gliricidia is coppiced during crop growth, they fall into a dormant phase and do not compete for resources with the crop.

3.5 CONCLUSIONS

Introducing trees into agricultural systems in the form of AFSs influences nutrient, energy and water cycling in the crops. In our example of a long-term experiment of maize and Gliricidia we saw a clear treatment effect on nutrient contents on soil C and stabilising effects on soil structure.

The link between soil structure in the form of bulk density and porosity and hydrologically relevant characteristics such as hydraulic conductivity and retention properties was not directly apparent. While there was an influence of C contents and stability on Ksat, the differences between sites and treatments did not consistently reflect differences in bulk density and porosity. Consequently, this means that it is not straightforward to deduce changes in water fluxes from soil physical

characteristics alone; the respective soil moisture and matric potential dynamics need to be measured as well for a reliable analysis of e.g. potential water availability to the crops.
In the context of climate change, we saw that some of the envisioned challenges for agriculture in Southern Africa can be alleviated with the help of AFSs. In the system we studied, a more stable soil structure as a consequence of the introduced organic matter would potentially be less susceptible to soil erosion, and the better nutrient availability could sustain higher and more stable yields. A sensible combination of trees and crops, such as in the studied Gliricidia with distinctly different growing seasons, minimised competition for water. At the same time, the input of organic matter and changes in soil structure can buffer dry spells by protecting against fast soil desiccation and supporting the rewetting as a consequence of the next rainfall. With climate change induced shifts in precipitation patterns this can lead to a more sustainable use of the available water and add to the benefits of AFSs.

Part IV

WATER RETENTION AND PERMANENT WILTING POINT IN PROCESS-BASED MODELLING OF AGROFORESTRY DYNAMICS

This study is a manuscript prepared for publication in a scientific journal. It has been submitted as:

Hoffmeister, S., Wienhöfer, J. and Zehe, E. "The role of water retention and permanent wilting point parametrization in process-based modelling of soil water dynamics."
http://dx.doi.org/10.2139/ssrn.5175785.

4

THE ROLE OF WATER RETENTION AND PERMANENT WILTING POINT PARAMETRIZATION IN PROCESS-BASED MODELLING OF SOIL WATER DYNAMICS

ABSTRACT

This study examines the response of a process-based model to changes in soil water retention parametrisation and variation of the permanent wilting point (PWP). Both, water retention and the PWP are especially critical in water-limit regions/periods, when they substantially determine water fluxes. Despite the important role of water retention parametrisation in soil hydrological modelling, its influence on modelling results is rarely questioned. Accordingly, the little evidence of one universal PWP is lacking a thorough debate of its validity. Therefore, we want to quantify how these two items influence soil hydrological modelling.

We used a physically-based hydrological model to simulate soil water dynamics at a windbreak agroforestry site near Stellenbosch, South Africa, where irrigated blackberry rows were intercropped with Italian alder trees. Model parameters were initialized based on field measurements and laboratory analyses, and various numerical experiments were performed to evaluate the model's sensitivities and the impact of management strategies on soil moisture dynamics in the time and frequency domain using complete empirical mode decomposition, a frequency analysis tool. The results clearly demonstrated the strong influence of the soil water retention parametrisation on water balance components, partially even exceeding the impact of management strategies. The Peters-Durner-Iden model showed overall greater alignment with observed dynamics and stability than the Van Genuchten/Mualem model, which greatest weakness showed in the water-limited period. As the key component differentiating between latent and sensible heat flux, the PWP played a pivot role in hydrological modelling by determining the onset of plant wilting while simultaneously impeding further plant transpiration. This led to substantial effects on soil moisture dynamics.

This study also underscores the importance of dynamic model evaluation in hydrological assessments as it has the potential to offer more insights into the model's strengths and limits of representing observations, particularly on shorter timescales such as daily or subdaily. We identified limitations in current hydrological models regarding water retention parametrisation and constant PWP assumptions, advocating

for future research to explore these impacts and develop comprehensive frameworks for evaluating multiple ecosystem services in agroforestry systems.

4.1 INTRODUCTION

Process-based hydrological models are crucial for investigating the water balance of terrestrial systems and their sensitivities to management practices and climate changes. To begin with, a straightforward approach for using such a model is to show that it closely portrays the behaviour of the often extensively monitored system of interest. Afterwards, we can use the verified model to perform virtual experiments, e.g. exploring the role of soil characteristic and bedrock topography on runoff generation (Hopp et al., 2009; Wienhöfer and Zehe, 2014; Loritz et al., 2017) or infiltration and solute transport (Klaus and Zehe, 2010; Klaus and Zehe, 2011). The credibility of these virtual experiments is based on the fact that these models are grounded in conservation laws and rely on spatial patterns of parameters that can be directly measured in the field (Zehe et al., 2014).
Nevertheless, we also acknowledge the longstanding controversy about the short-comings of the Darcy-Richards equation, for example to cope with preferential flow (Beven and Germann, 2013; Zehe and Jackisch, 2016; Sternagel et al., 2019). Especially the question about the appropriate choice of the soil hydraulic model is rarely addressed, despite the importance of soil water characteristics (Novick et al., 2022). In this study, we explore the significance of the soil hydraulic model for process-based modelling of soil hydrology. To this end, we compare the widely used van Genuchten/Mualem (VGM) model (Van Genuchten, 1980; Mualem, 1976) to the Peters-Durner-Iden (PDI) soil hydraulic model (Peters et al., 2024). The PDI model is similar to the VGM model but distinguishes between capillary and non-capillary water, which is expected to provide more reliable matric potential values in dry conditions. Differences between the two models can be substantial, as illustrated in Fig. 4.1. For instance, at the permanent wilting point (PWP) of pF = 4.2, the water content can vary by up to 6 %. This variation is significant because the PWP is a key parameter that determines the water limit for plant transpiration.
While textbooks generally define the PWP as the water content at a soil water potential of $\Psi = 10^{-4.2}$ cm, or 4.2 pF, this value was established empirically for sunflowers (e. g. Scheffer and Schachtschabel, 1992). The Earth is, fortunately, not exclusively covered by sunflowers and, moreover, as Richards et al. (1950) suggested, the PWP might even for sunflowers vary from 3.8 to 4.6 (pF). Thus, we question the universal validity of a PWP value of 4.2 pF and test the influence on water balance and soil moisture dynamics by varying the PWP value (Fig. 4.1). In recent years, several experimental studies were conducted to test the validity of the PWP at $\Psi = 10^{-4.2}$ or 1500 kPa, of which most found a great variability in soil matric potential at plant wilting depending on soil texture and the plant species (Garg et al., 2020; Chagas Torres et al., 2021). For instance, Freitas et al. (2023) found a

range of -180 kPa to -2266 kPa for the PWP of *Physalis peruviana* in sandy soils, whereas it ranged from -665 to -1611 kPa in a sandy clay loam. Similarly, Wiecheteck et al. (2020) found for the PWP of wheat and barley with different soil textures varying from -1637 to -2417 kPa.

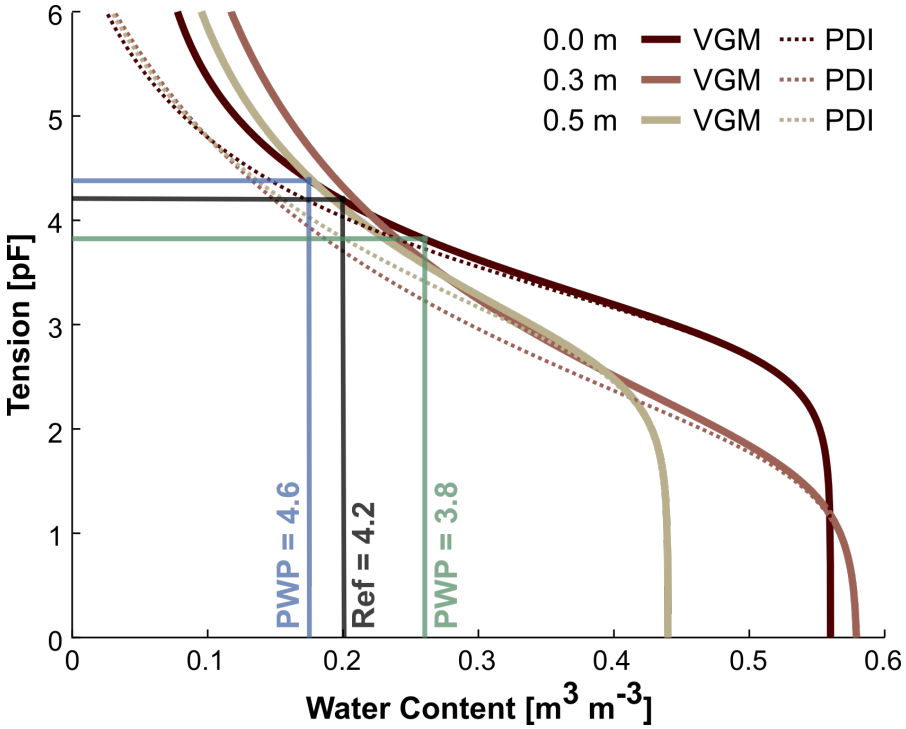

Figure 4.1: Soil water retention curve of three samples taken from a soil profile pit at an agroforestry site near Stellenbosch. The solid lines present parametrisation with the van Genuchten/Mualem model, whereas the dotted lines used the Peters-Durner-Iden model. Black, green and blue lines indicate how differences in two models influence e.g. the water content at wilting point and additionally how different pF-values of thereof in turn also alter the soil water content at the respective suction.

A comprehensive understanding of the water balance is essential for a wide range of applications in agriculture and forestry. Here, we study agroforestry systems (AFSs), which are often located in semi-arid regions or ones that regularly experience dry periods and are highly vulnerable to climate change impacts (Sheppard et al., 2020a; Douville et al., 2021). These systems combine woody perennials with agricultural crops and/or livestock, which can be arranged in in various configurations (e.g. alley cropping, hedgerows, boundary planning). Unsurprisingly, the use of validated models to inform effective management is also common practice in the agroforestry community, for instance, to shed light on the short- and long-term results of different agroforestry designs, including their effects on yields,

financial outcomes, and broader environmental impacts (Burgess and Rosati, 2018). A significant strength of such models lies in their ability to represent a continuum from pure forestry through various AFS to rotational and monoculture agriculture (Burgess et al., 2019). Successful models include YIELD-SAFE for growth and yield (Werf et al., 2007), Hydro-SVAT for eco-physiological and basin-reservoir dynamics (Gómez-Delgado et al., 2011), a spatially explicit landscape-scale model for evaluating ecosystem services (Kay et al., 2018), and the WaNulCAS model for water, nutrient and light capture (Van Noordwijk and Lusiana, 1998). AFS models are useful for exploring specific ecosystem services, but they often lack the ability to provide accurate and reliable estimations for a comprehensive range of ecosystem services.

Particularly systems in the global south are often monitored on a campaign basis and lack long-term and spatial high-resolution datasets (Hassler et al., 2024a). This data scarcity poses a significant challenge for both process-based hydrological and AFS models, which ideally require extensive data on key soil and plant characteristics, as well as time series of states and fluxes for model testing and verification. In line with Loritz et al. (2017), we explore the value of diverse and distributed information sources, including topography, soils, and vegetation patterns to constrain the spatially model setup as meaningful representation of the target hillslope in a data-scarce system and explore options for a model evaluation based on rather short target time series.

In dry regions, where runoff data may be scarce, soil moisture observations serve primarily, such as in our case, as modelling target. It is well-known that the footprint of Time Domain Reflectometry (TDR) observations is much smaller than the representative elementary volume of soil water storage (Zehe et al., 2010). Due to large soil heterogeneity, TDR observations exhibit substantial small-scale variability, with the spread of soil moisture observations at the 10-meter scale potentially being as large as the spread across an entire catchment (Zehe et al., 2010; Mälicke et al., 2020). Despite this variability, distributed soil moisture observations are rank-stable at both small and large scales. This means that while individual observations may not represent water storage at larger scales, they accurately reflect temporal changes in storage (Mälicke et al., 2020). Therefore, calibrating the model to a single soil moisture observation is not meaningful. Instead, we focus on calibrating the model based on dynamic changes in water content and matric potential, which are more representative at larger scales. Specifically, we evaluate the model in the spectral domain (Schaefli and Zehe, 2009) using empirical model decomposition (Torres et al., 2011). Spectral methods are well suited to analyse temporal model performance in different frequency bands, while being rather insensitive to differences in the mean.

In summary, we examine the impact of different soil hydraulic models and parameterizations on process-based simulations of the water balance in a data-scarce AFS. Specifically, we address three main research questions:

1. How does the choice of the soil hydraulic model constrain a behavioural model setup?
2. How do meaningful changes in the PWP affect the simulated water balance?
3. What is the advantage of using spectral methods to evaluate the model and the simulated delta changes, while avoiding overfitting to short and non-representative time series of soil water content and soil water potentials?

By addressing these research questions, this study aims to advance the understanding and modelling of soil water dynamics, particularly in the context of the water balance of agroforestry systems and the impact of different management practices. The manuscript structure follows these questions in the discussion after thoroughly presenting the site, the model and the modelling experiments, and the results from the latter.

4.2 MATERIALS AND METHODS

4.2.1 *Agroforestry site and data*

The agroforestry site studied is a windbreak system consisting of blackberry rows (*Rubus fruticosus* L. Var. "Waldo") intercropped by rows of Alder trees (*Alnus cordata* (Loisel.) Duby) serving as a wind block, which was characterised during measurement campaigns and deployment of monitoring equipment (Hoffmeister et al., 2024; Hassler et al., 2024b). The southward facing slope is located just outside Stellenbosch, South Africa, and exposed to strong south-easterly winds during hot and dry summer months, resulting in high evapotranspiration rates (Meadows, 2015; Hassler et al., 2024b). The field site is located at an elevation of approximately 400 m above sea level, with a slope incline of about 15 %. It is part of an operational fruit farm, and the specific field under study is currently cultivated with blackberry. Linear windbreaks composed of Italian alder segment the field of blackberry canes arranged in parallel rows, spaced 2.5 m apart. During the summer months (November to January), the plants are irrigated using a drip system, typically three times a week for 1.5 h at a rate of 2.3 L h^{-1}.
A weather station installed in the field measured air temperature, precipitation, solar radiation, relative humidity, wind speed and direction for a period of roughly six months (mid-September 2019 to mid-March

2020) at a 15-minute interval. These were complemented by matric potential measurements (MPS2, Meter, Germany) in a profile at 0, 0.3 and 0.5 m depth next to the windbreak and soil water content measurements (TDR profile, IMKO, Germany) adjacent to the latter installed within a PVC tube at 0-0.2, 0.2-0.4, 0.4-0.6 and 0.6-0.8 m depth. A second soil water content profile station was set up in the eighth berry row, which is not influenced by the roots of the windbreak.
Additionally, several soil samples were taken to characterise the soil texture and properties such as bulk density, soil water retention and saturated hydraulic conductivity (all data and details in Hassler et al., 2024a). The parameters of the water retention curve were derived from 250 ml cylindrical soil samples analysed in the laboratory. The water retention curve was measured with the simplified evaporation and dew point method and evaluated using the HYPROP-FIT software (Pertassek et al., 2015). The values for the different soil types (depth layers) are summarised in table 4.1 (soil type 1-3).

4.2.2 *Model and model setup*

Process-based model Catflow

The physically-based hydrological process model CATFLOW simulates soil water dynamics based on the two dimensional Darcy-Richards equation using curvilinear orthogonal coordinates (Maurer, 1997; Zehe et al., 2001). Surface runoff is simulated via Saint-Venant Equations in combination with Mannings law. The hillslope module is designed to simulate infiltration excess runoff, saturation excess runoff, re-infiltration of surface runoff, lateral water flow in the subsurface, return flow and solute transport. It separately calculates three components of the evapotranspiration flux with a surface energy balance approach using the Penman-Monteith equation namely (1) direct evaporation of canopy interception, (2) transpiration from canopy leaves, and (3) soil water evaporation. For each component, soil, canopy, and canopy interception conductance are parametrized differently with a set of empirical equations derived in the Weiherbach project (Plate and Zehe, 2008). Stomata conductance is calculated following the model of Jarvis (1976). The model has been successfully used to explore controls on flash flood runoff generation (Villinger et al., 2022; Manoj J et al., 2024), the water balance of forested systems (Loritz et al., 2017; Loritz et al., 2021), the sensitivity of simulated transpiration to the choice of the stomata conductance models (Loritz et al., 2022), the role of preferential flow paths for generation of subsurface stormflow (Wienhöfer and Zehe, 2014) and for pesticide leaching (Klaus and Zehe, 2011).

Model initialisation and parametrization

The model domain represents the in-depth investigated part of the AFS and consists of a 76 m long slope of 1 m width and 2.26 m depth using a grid size of 0.067 m in the vertical and 0.52 m in the downslope direction. This is sufficiently fine to assure that the spacing in between the windbreak and blackberry rows is well resolved. We assigned the corresponding land-use characteristics to the respective nodes (Fig. 4.2). Initial values of land-use parameters (e.g. leaf area index, plant height) were partially based on estimations from laser scans of the windbreak (Hassler et al., 2024b) and partially based on literature values (table 4.2). These values were adapted during the calibration process to match modelled and measured soil moisture and matric potential observations.

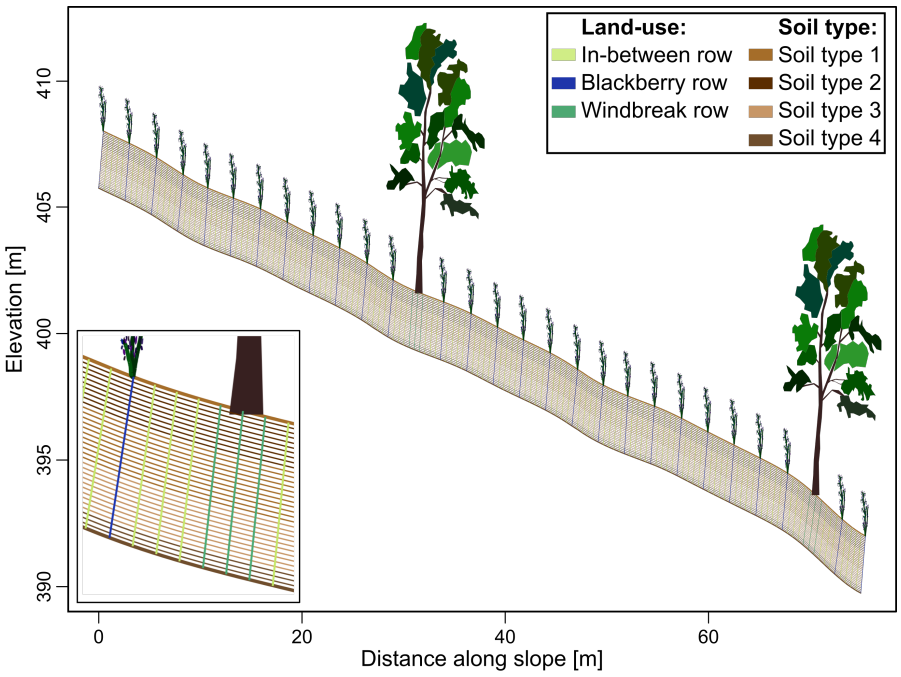

Figure 4.2: Cross-section of the hillslope indicating its discretization as model input and associated land-use parameters (table 4.2) and soil types (table 4.1). The trees indicate the location of the windbreaks and the bushes the blackberry crop rows. The zoom window displays a close up of the soil horizons (vertical lines indicate surface land-use nodes and horizontal lines the soil horizon the horizontal nodes are associated to).

The soil was characterised based on three soil horizons of the sampled soil profile during the field campaign in 2019 (Hassler et al., 2024b), followed by a fourth horizon lowering the outflow at the lower soil depth end (which is a mix of soil types 1, 3 and low saturated hydraulic conductivity). The lowest horizon was not sampled, because the soil was too hard and compact, but therefore allowed the reason-

able assumption of a rather impeding layer below approx. 70-80 cm depth. The laboratory measurements of soil water retention, saturated hydraulic conductivity and bulk density were used to parametrise the soil types (table 4.1). To represent the observed variability in soil properties we added uncorrelated noise to the saturated hydraulic conductivities using multipliers ranging from 0.8 to 1.2.

Table 4.1: Parameters of different soil types associated to the horizontal nodes as displayed in figure 4.2. The following values were used for the VGM and PDI parametrization: Saturated soil moisture θ_s, residual soil moisture θ_r, reciprocal air entry point α, quantity characterising the pore size distribution n, weighing factor for capillary and film flow ω, empirical tortuosity τ (ω and τ used in PDI only). Ksat represents the saturated hydraulic conductivity.

Soil type	Ksat	θ_s	θ_r	α	n	ω	τ	Bulk dens.
	[m s^{-1}]	[-]	[-]	[m^{-1}]	[-]	[-]	[-]	[kg m^{-3}]
1	$7.3e^{-5}$	0.56	0.05	0.13	1.406	0.0102	-4.30	1167.75
2	$1.5e^{-5}$	0.58	0.05	2.13	1.207	0.0017	-3.30	1110.28
3	$8.9e^{-7}$	0.44	0.05	0.235	1.277	0.0021	0.21	1492.26
4	$8.9e^{-8}$	0.44	0.05	0.235	1.277	0.0102	-4.30	1492.26

The model was initialized with matric potential observations (MPS2 measurements next to the windbreak in a profile at 0, 0.3 and 0.5 m depth). At the left boundary, which corresponds to the hillcrest we use a no flux boundary, while at the right downslope boundary we used a seepage condition, allowing optional subsurface flow to leave the system. The lower boundary was set to gravity flow.
The model was driven with atmospheric boundary conditions at the top boundary, representing hourly precipitation, solar radiation, relative humidity, air temperature and wind speed coming from our own installed weather station for a period of six months. The irrigation was accounted for by modifying the precipitation time series, creating a second one representing the irrigation. The latter was exclusively assigned to the land-use nodes of the blackberry rows. Irrigation was simulated on three working days (Mo, Wed, and Fri) for two consecutive hours with 10 mm h^{-1} (20 mm per day, 60 mm per week). No irrigation happened during days with precipitation.

Table 4.2: Parameters associated with the three different small-scale land-use types that were associated to each surface grid point. If the values changed throughout the course of the season, the range of values is given. Only one value is given, if the parameter was constant.

Land-use	Leaf area index	Land cover fraction	Rooting depth	Plant height
		[%]	[m]	[m]
In-between rows	0 – 4.0	0.05 – 1.0	0.2	0.06 – 0.3
Blackberry	1.25 – 2.25	0.2 – 1.0	0.5	1.4 – 1.8
Windbreak	5.0 – 10.0	0.7 – 1.0	2.0	11.0

4.2.3 *Model evaluation*

The model output was assessed using different performance metrics in both the time and frequency domain and was also evaluated for the meaningfulness of the results.

Time domain

The strong non-linearity of hydraulic conductivity and water capacity can cause significant errors in the overall mass balance when solving the 2D-Richards equation in the potential based form, even when using a Picard iteration (Celia et al., 1990). Hence, it is advisable to verify the coherence of the different mass balance components, which is quantified by the cumulative mass balance error (MBE).
Since absolute values of the soil moisture observations may not be fully representative, we assessed the state of the soil water through the matric potential. Therefore, in terms of model performance the primary focus was on the dynamics of soil moisture and on fitting the order of magnitude of the matric potential. Consequently, indices that could capture these aspects were deemed most relevant. The matching between estimated and observed state variables was assessed using the Nash-Sutcliffe Efficiency (NSE). The NSE is defined as a normalized statistic that determines the relative magnitude of the residual variance compared to the measured data variance, thereby indicating how well the plot of observed versus simulated data fits the 1:1 line (Nash and Sutcliffe, 1970). A negative NSE indicates that the model performs worse than the average of the data.

Frequency domain

Complete ensemble empirical mode composition (cEEMD) allows inspection of time series in the frequency domain by dividing the input signal (e.g. measured air temperature) into its spectral components (Torres et al., 2011). It is based on the decomposition of a signal into intrinsic mode functions after adding Gaussian white noise to the signal to avoid mode mixing problems. To illustrate the method, we compare two signals with the same frequency but a phase difference (Fig. 4.3), one presenting the model, the other observations. In such a case, the NSE in the time domain suggests a poor model performance, yet both signals are largely identical (Ehret and Zehe, 2011; Seibert et al., 2016).
The separation of the signal Fig. 4.3, top plot "Signal"), whether from observations (blue line) or simulations (orange line), into fast and slow oscillations is achieved through a sifting process, which involves subtracting the signal's moving average from the signal itself. This procedure generates various modes (Fig. 4.3, IMFs 1-8, left column) and their corresponding periodograms (right column), enabling the

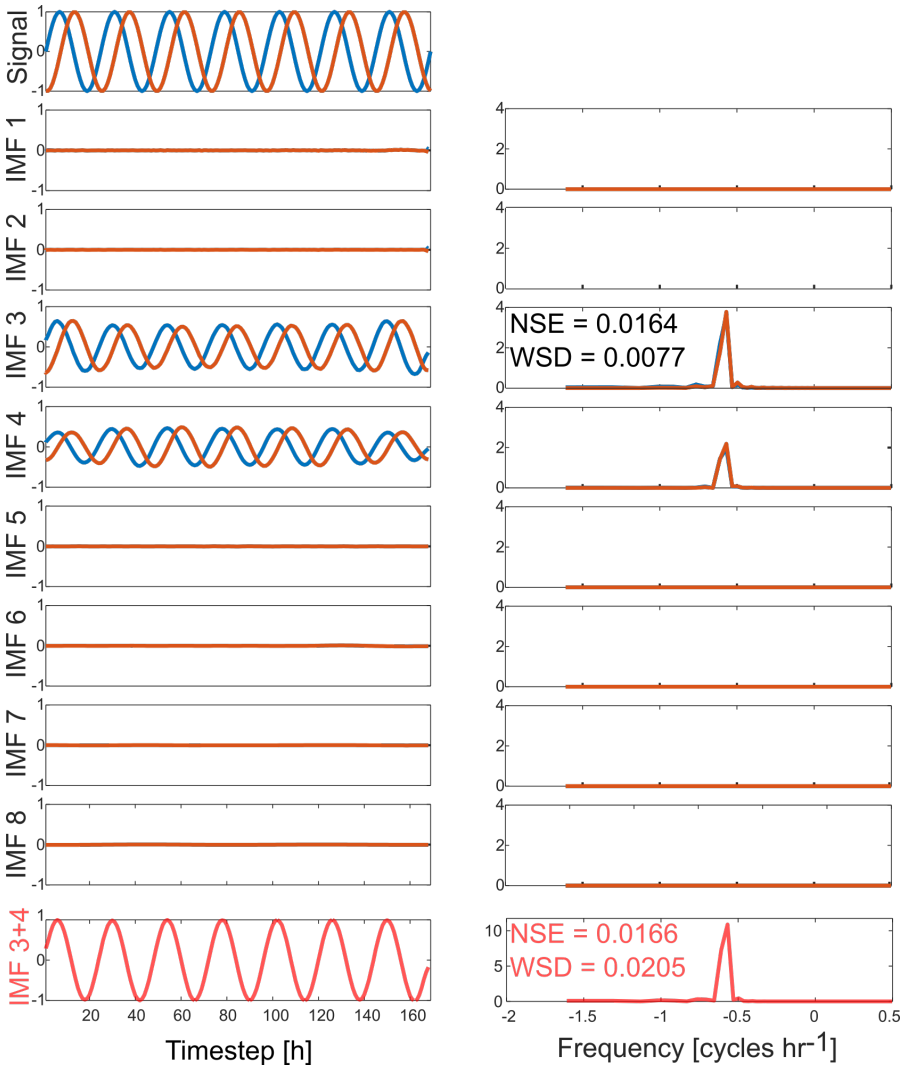

Figure 4.3: Example illustrating the complete Ensemble Empirical Mode Decomposition (cEEMD) method applied to a simple sine function (blue) and respective indices used in this study (NSE for the modes and WSD for their periodograms). The left column shows at the top the time domain representation of the original signal (blue) and a similar signal slightly shifted (orange), followed below by their respective decomposition into time series of intrinsic mode functions (IMFs). The right column presents the frequency spectrum for each IMF, highlighting the dominant frequencies. For each pair of IMFs (blue and orange), the frequency spectra were compared and quantified with the NSE and WSD as illustrated here only for IMF 3 and 3+4. IMF 1 and 2 represent high-frequency components, which contribute minimally to the overall signal. IMF 3 and 4 capture the main oscillatory modes of the original sinusoidal signal. IMF 5 to 8 contain lower frequency and residual modes, illustrating a trend or non-oscillatory patterns within the data. The lowest plot "IMF 3+4" illustrates how IMFs can be combined into one IMF.

comparison of different aspects of the signals. Here, we categorized the IMFs based on their main frequency into the bands: hourly/sub-

daily (e.g. max. frequency between 0.3927 and 3.6652 h^{-1} with an Eigen-frequency of 1.5708 h^{-1} assuming a period of 4 hours), daily, weekly, monthly and trend (everything of a lower frequency than the monthly such as seasonal, yearly etc.). The components of a similar main frequency were added together (such as in Fig. 4.3, lowest plot "IMF 3+4"). In fact, we only considered the subdaily, daily and trend components in our analyses, as subdaily frequencies were too noisy and the measurement period too short to explore monthly or seasonal frequencies. The coherence of two signals in time was determined by calculating the NSE between their respective IMFs in the three frequency bands.
The agreement of amplitudes, and thus of the partial variance in the different modes, was quantified by calculating the Wasserstein distance (WSD, Kantorovich, 1960) between the periodograms (Fig. 4.3, right column). The WSD determines the amount of work needed to transform one spectrum/distribution into another, ranging from zero to infinity.

4.3 MODELLING EXPERIMENTS

To explore the role of the soil hydraulic model and the PWP, we conducted numerical experiments with different settings and compared the results with observations as explained in the previous section. We combined these experiments with different water input/irrigation scenarios to further explore the model's sensitivities under different conditions by comparing the resulting simulations with a reference simulation. In general, all experiments were analysed in the time and frequency domain. Details of each experiment are described in the following.

Reference models with two soil-hydraulic models (Ref_VGM and Ref_PDI)

At first, we compared our two defined references models (Ref_VGM and Ref_PDI). Both reference models ran with the same settings except for using differing soil hydrological models (VGM and PDI). The soil hydraulic shape parameters, except for two additional parameters for the PDI model (tortuosity τ and weighing factor for capillary and film flow ω) remained the same (table 4.1: θ_r, θ_s, α, n and λ), only the underlying equations change. All following experiments were conducted with both the VGM and the PDI model.

Permanent wilting point (P38 and P46)

The model's sensitivity to variations in the PWP was tested in these experiments. Therefore, we ran the model two more times with exactly the same settings as the reference one and changed each time only the PWP (from 4.2 to 3.8 and 4.6, respectively).

No and doubled irrigation (NI and DI)

During the hot summer months, the orchard is daily supplied with water through drip irrigation in the blackberry rows (approx. 60 mm per week). To investigate how the soil water would evolve without this supply, we applied no irrigation (NI) to the blackberry rows. The measured precipitation (in total 242 mm) was the sole source of water input into the model. In the following exercise (DI), the irrigation input was doubled to approximately 120 mm per week by prolonging the irrigation window from two to four hours on irrigation days to see what would happen to the system if more water was added. This set of modelling experiments was exclusively compared to the outputs of the corresponding reference models.

4.4 RESULTS

The combination of visual and quantified comparison of the model outputs in the time and frequency domain facilitated a thorough evaluation of the controls on water balance and dynamics.

4.4.1 *Visual comparison of simulated and observed time series of water content and matric potential*

In Figure 4.4, we directly compare field observations at both sites (blackberry BB_Obs, wind break WB_Obs) with the simulated soil moisture time series (a, c, e, g) and matric potential (b, d, f) using the reference setups with either VGM (blue) or the PDI (brown) soil parametrisation.
A considerable offset between soil water content observations and simulations was observed. While the overall dynamics between observations and simulations were similar, the models struggled to accurately capture the summer drying period. Notably, the observations indicated consistently higher water content at the BB compared to the WB, a pattern not reflected in the simulations. Predominantly, soil moisture values from the VGM model were higher than those from the PDI model.
The agreement between matric potential observations and simulations was generally strong (Fig. 4.4). Both models demonstrated a similar order of magnitude in the topsoil (10 cm depth) and the subsoil (50 cm depth). However, significant difference emerged at the intermediate depth (30 cm), where the VGM-modelled time series reached the PWP and remained there, a behaviour not confirmed by the observations. This inconsistency occurred even earlier at the blackberry site than at the windbreak. At 50 cm depth, the PDI model showed closer alignment with observations. In the topsoil, the PDI model presented fewer fluctuations compared to the VGM model and smaller differences

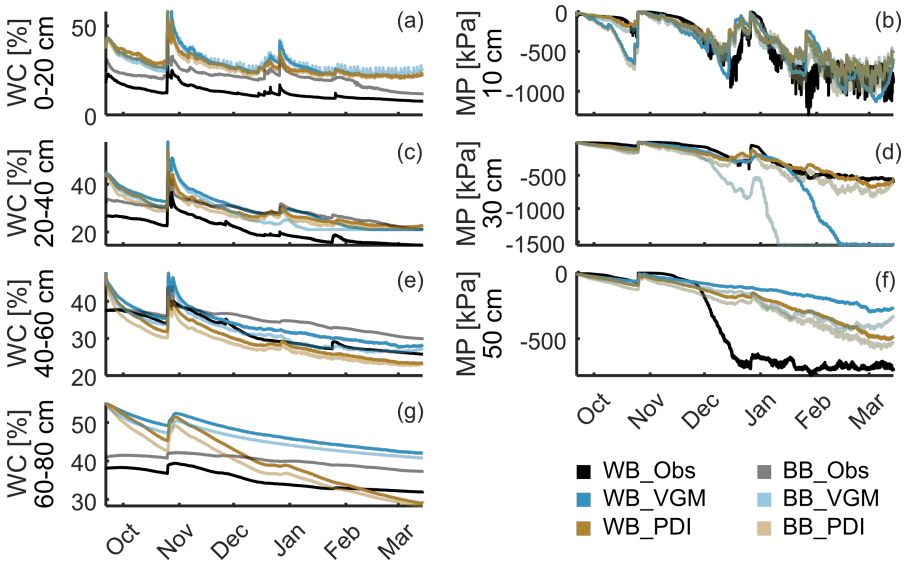

Figure 4.4: Time series of soil water content (WC, left column) and matric potential (MP, right colum) at different depths (10 cm, 30 cm 50 cm, 70 cm (only water content)). Observations (black) and simulations of the reference models at the windbreak (WB, solid) and in the blackberries (BB, opague) with the Van Genuchten-Mualem (Ref_VGM, green) and Peter-Durner-Iden (Ref_PDI, blue) soil hydraulic models. The y-axes are not equally scaled to allow for better visibility of the differences between the locations.

between the two locations.
Matric potential was selected as primary variable for model evaluation, given its role in driving soil water fluxes through potential gradients. Variations of the PWP revealed strong sensitivities in simulated matric potentials (Fig. 4.5).
The VGM model showed generally the largest deviations between the reference and scenario simulations with a PWP of pF 4.6 (P46_VGM), particularly at a depth of 30 cm (Fig. 4.5 c), where the model reached and remained at the PWP across all three cases. Notably, the PWP was reached earlier for P38 and P46 compared to the reference. While simulations using the PDI model also demonstrated sensitivity to variations of the PWP, the effects were markedly smaller than those observed with the VGM model.

4.4.2 *Metrics for model evaluation in the time and frequency domain*

In this section, we evaluate the model performance in terms of numerical accuracy as well as against observations in the time and frequency domains based on the Nash-Sutcliffe Efficiency (NSE) and Wasserstein Distance (WSD).

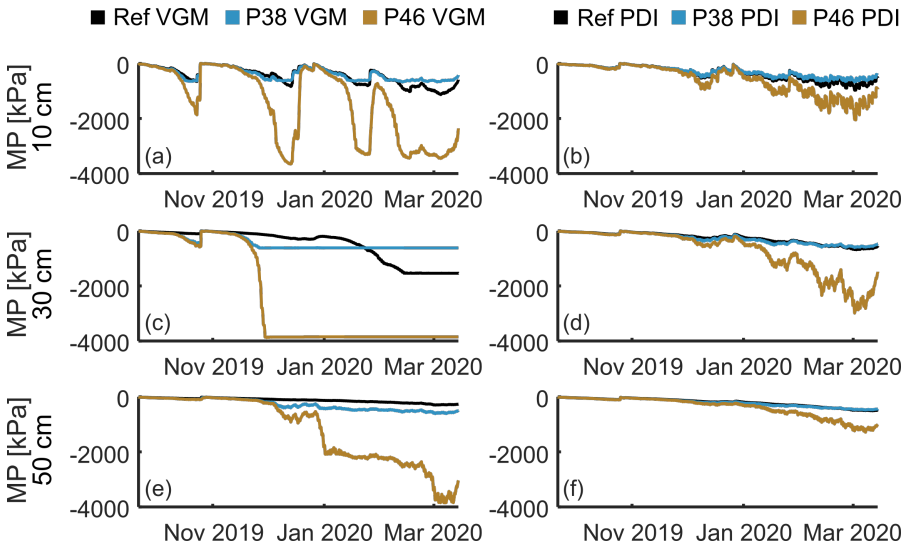

Figure 4.5: Comparison of matric potential simulations at three different depths (top to bottom: 10, 30 and 50 cm) at the windbreak for the two soil hydraulic models VGM (left) and PDI (right) and the different PWPs (3.8 and 4.6).

Numerical accuracy of the models

An important benchmark for the numerical accuracy and thus credibility of model simulations is given by the numerical mass balance error (MBE, table 4.3). It expresses how well the numerical scheme conserves the mass when balancing differences in fluxes against storage changes.

Table 4.3: Mass balance errors (MBEs) of the different modelling exercises for both soil hydraulic models.

Exercise	MBE VGM [mm]	MBE VGM [%]	MBE PDI [mm]	MBE PDI [%]
Ref	0.69	0.15	- 4.65	1.04
NI	8.04	3.40	- 5.80	2.46
DI	0.26	0.04	- 4.79	0.73
P38	1.34	0.30	- 4.67	1.04
P46	0.33	0.07	- 4.82	1.09

We decided a relative MBE of 5 % of the water input as acceptable threshold for our experiments, which corresponds to a range of 12 mm to 128 mm depending on the water input scenario. Since all obtained MBEs fell below this threshold, the simulations were deemed sufficiently accurate to consider associated differences as physically meaningful. In general, the MBE VGM covered a wider range and was consistently positive. In contrast, the MBE for the PDI model was always negative, slightly larger for most experiments, and exhibited greater stability across the experiments.

Model performances in the time domain

The simulated outputs were initially compared to observations, and their similarity quantified with the NSE in the time domain. Table 4.4 lists NSE values for VGM_Ref and PDI_Ref, while the NSEs of the other experiments are included in the supplementary material (Fig. A.3 and A.4). Among the water content time series, the windbreak simulations achieved the highest NSE values. Overall, the PDI demonstrated slightly better NSE performance (0.83) compared to the VGM model (0.81), especially in the matric potential.

Table 4.4: NSEs of the reference runs VGM_Ref and PDI_Ref. For the water content the depth indicates the middle of a 20 cm depth profile, where water content was averaged. Abbreviations are BB = blackberry and WB = windbreak. MP was not measured at 70 cm depth.

Location	Water content BB		Water content WB		Matric potential WB	
Depth	VGM	PDI	VGM	PDI	VGM	PDI
10	0.667	0.646	0.92	0.956	0.597	0.752
30	0.767	0.792	0.946	0.899	0.835	0.906
50	0.812	0.79	0.921	0.907	0.741	0.727
70	0.815	0.849	0.94	0.95	-	-

Model performances in the frequency domain

The cEEMD empirical method provides a much more detailed view on model performance. Along the lines shown in Fig. 4.2, Fig. 4.6 and 4.7 compare simulations and observations using the modes and the spectra. This method provides insights into how well the model aligns with observations, helping to discriminate phase shifts from biases and amplitude errors across different frequency bands. Phase shifts between model and observations may result, for instance, from discrepancies in the propagation of the wetting/drying signal to larger depths, informing corresponding mismatches in speed and thus hydraulic properties. Similarly, amplitude differences reveal a mismatch between signal dampening between model and the real system, informing about mismatches in storage changes and the underlying controls.

For water content, no substantial phase shifts between simulations and observations were observed across all frequency bands. However, minor shifts were noted in matric potential, particularly at the shallower depth, where trend simulations preceded the trend observations. The phase shift was more pronounced when using the VGM soil hydraulic model. The different NSEs computed for the individual modes revealed that overall hydrological model performance was dominated by the low frequent trend in the signal, which is in fact half of the annual cycle. This holds true for both soil hydraulic models

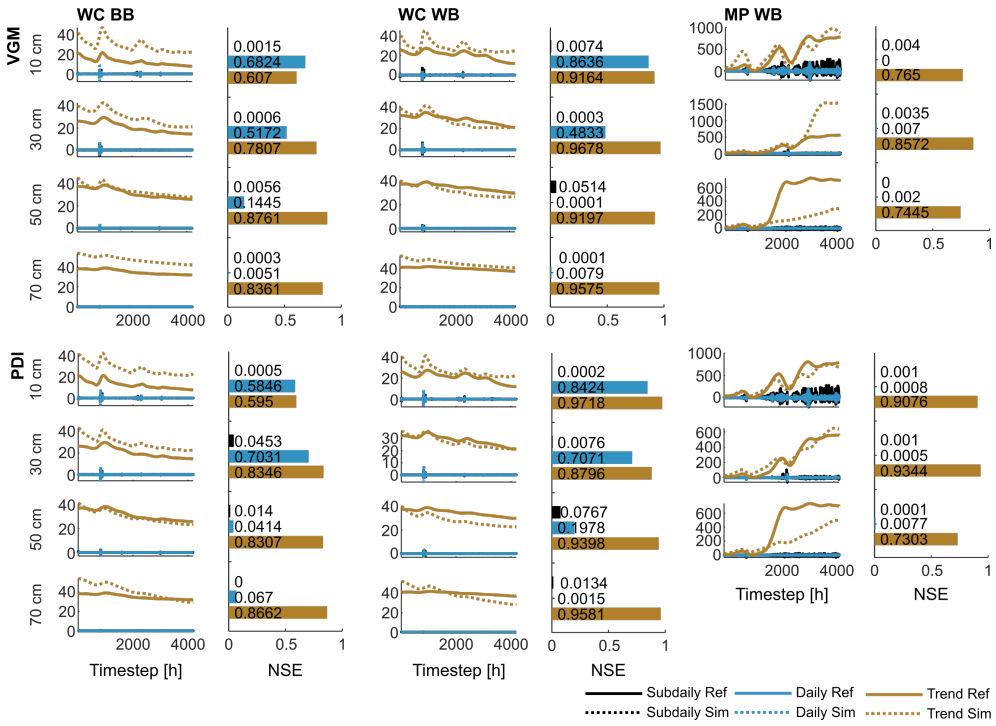

Figure 4.6: Intrinsic mode functions (IMFs) and Nash-Sutcliff-Efficiency (NSE) after decomposing the signal into empirical modes and adding them up into frequency categories (subdaily: black, daily: blue and trend: brown) for the VGM (upper) and PDI (lower) at the different locations (windbreak WB and blackberry BB) and measurement type (water content WC and matric potential MP). Displayed is only the reference run.

and data types. In case of the water content, the daily frequency was also well matched at 10 and 30 cm depth, but generally worse than the trend. The matching of subdaily modes, representing event scales, was consistently poor.

When comparing the soil hydraulic models, we generally find an offset between measured and simulated water content, especially at shallower depths. This offset was stronger in the VGM than the PDI model. Conversely, the PDI model simulated a stronger drying, which was obvious when comparing simulated and observed trend modes. The simulated matric potentials aligned better to observations when using the PDI model than those with the VGM, particularly at 50 and 70 cm depths. The "land-use" comparison revealed that the water content offset between trend simulations and observations was smaller at the windbreak across all depths compared to the black berries. For the PDI model, this offset was only evident at 30 cm depth. The comparison of the spectra (Fig. 4.7) offers insights into the model's ability to replicate the distribution of partial variances across the different frequencies relative to the original signal. The squared amplitudes of the different frequencies sum up to the total variance of the signal, providing a measure of model performance. Simulated

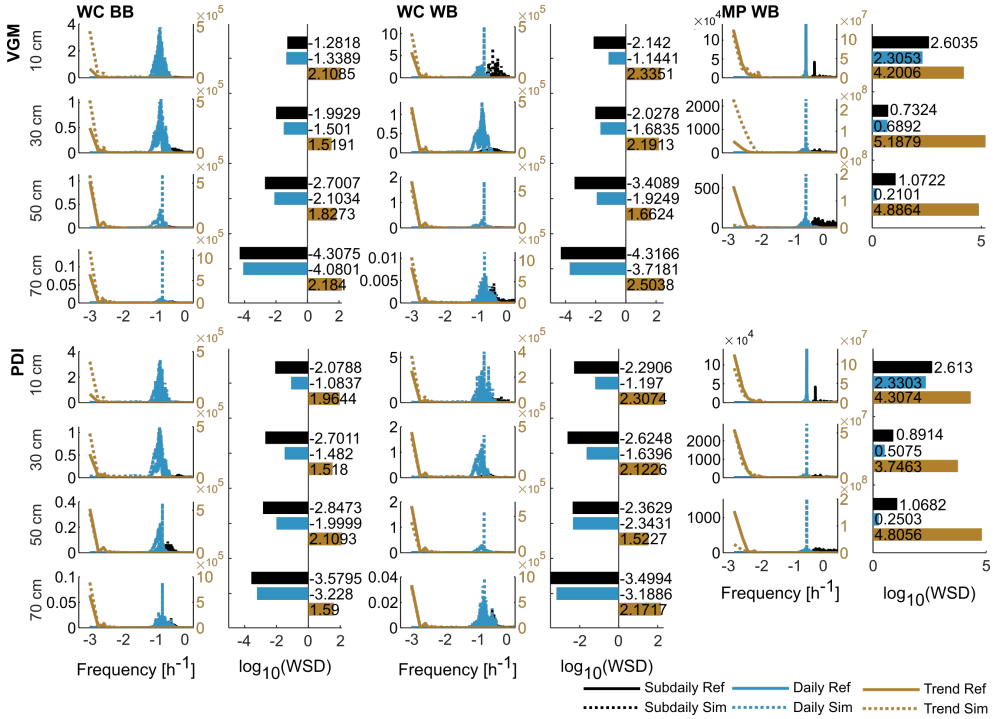

Figure 4.7: Periodograms and Wasserstein Distance (WSD, on log-scale) after decomposing the signal into empirical modes and adding them up into frequency categories (subdaily: black, daily: blue and trend: brown) for the VGM (upper) and PDI (lower) at the different locations (windbreak WB and blackberry BB) and measurement type (water content WC and matric potential MP). Displayed is only the reference run. The second y-axes in the periodograms belong to the trend.

amplitudes in the trend mode were consistently higher than those of the observations for both soil hydraulic models. While the PDI model yielded more accurate simulations of matric potential, the VGM model performed poorly at 30 cm depth. The overestimation was also evident in the daily simulations, but was less pronounced when using the PDI model compared to the VGM. Overall, the logarithmic WSDs for daily and subdaily water content signals were always below one, while those for the trend mode were above one. Furthermore, the spectral decomposition of matric potentials showed clearly localised, sharper peaks compared to the much wider, less structured spectra of water content. Additionally, we observed smaller variances and WSDs between simulated and observed trends in soil water content at the windbreak compared to the blackberry location.

The following section will compare and summarise the indices of variation in the PWP and irrigation experiments, highlighting key differences (the corresponding figures are provided in the supplementary material).
In the P38_VGM experiments, changes in NSEs were inconsistent,

whereas in P38_PDI NSEs were generally lower. There was no distinct pattern in the WSD, except for slightly greater values in PDI MP. Overall, the NSEs obtained with PDI exceeded those obtained with VGM, and the WSD for water content was lower in PDI simulations compared to VGM. In experiment P46, the VGM simulations produced somewhat better NSE values than the reference model at both sites, while PDI simulations were slightly worse. For both, the VGM and PDI model, the WSD for the water content spectra remained almost unchanged, whereas it increased for matric potential.
In case of no irrigation (NI_VGM and NI_PDI), NSE values for water content were very good when simulated with the VGM model (all > 0.92 except for 30 cm depth in the WB with 0.84), while the PDI performed a slightly worse. WSD values were rather similar and generally smaller for PDI than for VGM. Doubling the irrigation (DI) changed the picture: PDI simulations achieved higher NSE values than VGM simulations and these NSEs were generally larger than for the no-irrigation case. The NSEs of the individual modes were comparable to those of the reference experiments. WSD values of the VGM model remained similar or a bit lower for water content and for the matric potential higher. For PDI, water content WSD values were consistently higher.

4.4.3 *Water balance components for the model experiments*

We analysed the simulated water balance components and examined their sensitivities to changes in soil hydraulic models and the PWP. The general pattern across all experiments (Fig. 4.8) was as follows: infiltration and storage change were consistently larger than the lateral subsurface flux/interflow ("Subsurf") and groundwater recharge ("GW", Fig. 4.8 c and d). Transpiration and soil evaporation exceeded the total infiltration of water supply by rainfall and irrigation (Fig. 4.8 a and b). Consequently, the scenarios exhibited consistent negative storage changes ("SC)" (Fig. 4.8 c and d), indicating that the systems lost more water than they received.
For the reference setups, simulated infiltration was generally larger with the VGM model compared to the PDI model (Ref_PDI). At the same time, losses due to lateral interflow were greater for VGM, whereas groundwater recharge was consistently smaller compared to PDI. This suggests that the VGM model allowed for greater water infiltration and belowground flow. Notably, the drop in total storage was much larger in the PDI model compared to VGM, consistent with its higher simulated transpiration. This implies that simulated water availability to plant transpiration was larger, when using the PDI soil hydraulic model due to its lower absolute value of the soil water potential at a given soil water content compared to the VGM model (see Fig. 4.1). Overall, differences in simulated transpiration, storage

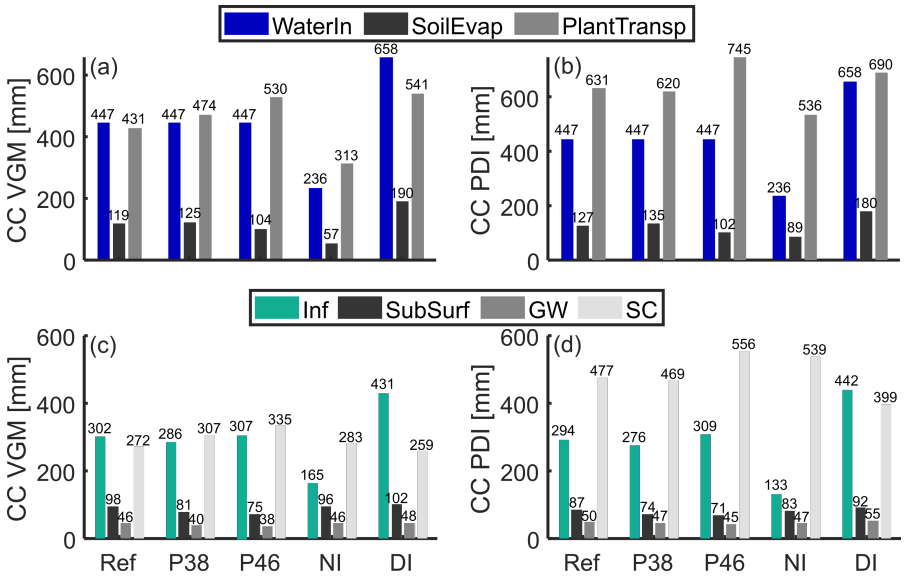

Figure 4.8: Absolute values of cumulated components (CC) of the mass balance at the end of the six months simulation period for VGM (left column, a and c) and PDI (right column, b and d) for the different model setups and modelling exercises. Abbreviations are as follows for a and b: "WaterIn" = water input, "SoilEvap" = soil evaporation, "PlantTransp" = plant transpiration; and for c and d: "Inf" = infiltration, "SubSurf" = subsurface flow at the lower boundary, "GW" = groundwater recharge, "SC" = storage change. The storage change is overall negative, i.e., soils are drying.

change and subsurface runoff were more pronounced between the soil hydraulic models than among the different modeling experiments, whereas the variations in the other two components were of similar magnitude. Additionally, the PDI model demonstrated generally a greater sensitivity to the irrigation experiments, such as infiltration response compared to the VGM model.

As expected, the highest infiltration occurred when most water was available, hence under the condition of additional irrigation (DI), while the lowest infiltration was simulated under the no-irrigation (NI) experiments. This variation in infiltration directly contributed to substantial differences in storage change, as subsurface runoff and groundwater recharge remained relatively consistent across the different irrigation scenarios.

Groundwater recharge varied in the range of 10 mm across the experiments using the VGM model and 5 mm using the PDI. It was highest when additional irrigation was applied, independently of the soil hydraulic model (DI_VGM and DI_PDI).

Variation to the PWP significantly influenced various hydrological components, though not always as expected. For instance, in the VGM model, storage change became more negative compared to the reference for both PWP cases, a pattern not mirrored in the PDI model. Across PWP experiments, storage change generally increased, while

subsurface fluxes and groundwater recharge became less negative. The main difference between the VGM and PDI models in this context was the variation in storage change.
Plant transpiration ("PlantTransp") emerged as the dominant component of the water balance, with its magnitude notably influenced by differences in water availability, which in turn depended on the choice of soil hydraulic model (Fig. 4.8 a and b). Transpiration simulated by the PDI model was substantially higher than that by the VGM model (on average: 12.3 %), again attributed to systematic difference in soil water potential between the PDI and VGM soil hydraulic models during dry soil conditions (see Fig. 4.1). Similarly, evapotranspiration from the PDI model exceeded that from the VGM model, except in the P46_VGM exercise. The total evaporative fraction consistently exceeded the water input. The differences between the soil hydraulic models were comparable in magnitude to those resulting from different scenarios.
Transpiration patterns varied by experiments. In both models, the lower PWP (P38_VGM and P38_PDI) resulted in transpiration rates similar to the reference scenario. In contrast, higher PWP (P46_VGM and P46_PDI) increased transpiration by 23 % for VGM and by 18 % for PDI compared to the reference. With no irrigation applied, transpiration decreased by 27 – 15 %, respectively, compared to the reference, while additional irrigation increased transpiration by 26 % to 9 %, respectively. Using the PDI model, P46_PDI affected transpiration most compared to the other experiments, followed by DI_PDI, while using the VGM model reversed this order with water addition (DI_VGM) having a stronger impact than the greater PWP (P46_VGM).
Bare soil evaporation was generally comparable (or slightly greater) to the reference model for P38_VGM and P38_PDI. In the P46_VGM and P46_PDI experiments, evaporation was also similar to the reference but slightly lower. No irrigation (NI_VGM and NI_PDI) reduced evaporation (VGM: 52 % and PDI: 30 %) whereas additional irrigation increased evaporation by 61 % for VGM and 42 % for PDI compared to the reference.

4.5 DISCUSSION

This study provides clear evidence that the selection of the soil hydraulic model and the permanent wilting point (PWP) have substantially affected simulations of the water balance under dry conditions. The variations influence simulated dynamics of soil water content and matric potential as well as the energy balance. In the subsequent sections, we will summarize these impacts and provide examples of their broader implications.

4.5.1 *The soil hydraulic model strongly impacts soil water modelling amounts and dynamics*

The comparison between the VGM and the PDI models revealed distinct differences in their ability to simulate soil moisture dynamics, particularly under dry conditions. The MBE showed that the PDI model consistently produced values below zero in contrast to the VGM model with positive and smaller errors. The PDI MBEs were, however, more consistent and varied less throughout the experiments. The overall hydrological model's performance during water-limited conditions was found to be suboptimal, largely due to issues with the parametrization of the water retention models. In particular, small changes in soil moisture in the VGM model resulted in disproportionately large changes in matric potential. While acknowledging limitations, Peters et al. (2024) highlight the "advancements of PDI over traditional concepts" in simulating soil water process particularly under dry conditions.

The most striking behavioural discrepancy was observed in the VGM model, which frequently reached the PWP, resulting in reduced dynamics and a disconnection from the observed soil moisture behaviour. This loss of dynamics in the VGM model was especially problematic in long-term simulations as the hydrological model's tendency to reach the PWP limits its ability to accurately represent the soil's response to fluctuating moisture conditions. Moreover, this limitation suggested plant wilting when it was actually not observed. However, when analysing monthly windows, particularly in October and September, the VGM model demonstrated greater stability, with less pronounced dynamics losses. This indicates that the VGM model performs more reliably under humid conditions but struggles to reproduce soil moisture dynamics during dry periods or in arid regions (Peters et al., 2021).

The PDI model demonstrated better agreement with observed soil moisture dynamics, particularly in its ability to capture drying processes. The differences between the two reference models were especially evident in matric potential with greater divergence in the drier ranges of the water retention curve while remaining at similar water content values. These results are consistent with Dettmann et al. (2019), who found a better representation of hydraulic conductivities and soil water content over the hole pressure head range during evaporation experiments using PDI. Performances were nearly equal near saturation between VGM and PDI, but functions of the latter for soil water content and saturated hydraulic conductivity demonstrated greater flexibility at dry conditions when the separation of hydraulic conductivity into capillary and film conductivity started playing a critical role.

The PDI model provided a more realistic representation of ecological

conditions required for a healthy and functional windbreak system. In contrast, the VGM model suggested that non-irrigated trees would remain in the wilting range, a condition under which they would not survive unless deep-root development occurred beyond the modelled depth, which is considering the species and field site conditions unlikely. Despite extensive parameter fitting to observations, the VGM model exhibited a persistent bias in MP near the PWP, whereas the PDI model effectively eliminated this issue. Additionally, we would like to point out that we used exactly the same parameters for VGM and PDI. However, the interpretability of parameters between models, especially of θ_r changes (Peters et al., 2024). Hence, deriving parameters specifically for the PDI model, most likely further improves the model performance under dry conditions. These results underscore the importance of selecting an appropriate model tailored to the specific conditions and objectives of the study.

4.5.2 *The permanent wilting point influences modelling results under dry conditions*

The PDI model exhibited a more stable MBE across the PWP experiments, indicating lower sensitivity in this humidity range compared to the VGM model. This supports again that the PDI model delivered more consistent performance in drier conditions where soil moisture is critically low. Increasing the PWP from 4.2 to 4.6 did not significantly affect the MBE for either the PDI or VGM models. This indicates that a higher PWP, which corresponds to more water availability for plants, does not substantially alter the numerical precision as reflected in the mass balance error. Overall, PWP influences on soil water behaviour were less pronounced in the PDI model compared to the VGM model, particularly under the relatively dry conditions studied here, indicating again the PDI model's greater stability. This finding suggests that the soil hydraulic models are more sensitive to reductions in water availability than to increases, emphasizing the importance of accurately capturing low moisture conditions in hydrological modelling.
A key observation concerns the timing of PWP occurrence in the VGM model (Fig. 4.5). The PWP was reached at different times across soil depths in the VGM model, yet the timing of P38_VGM and P46_VGM was surprisingly similar, despite the latter having greater water availability. Potential transpiration is governed by water near the surface whereas plants draw water from different soil depths. When reaching the PWP in the topsoil and thus restricting further water extraction for evaporation, the plants continue draining the lower cell but at a higher rate as long as there is still water available. Rainfall and transpiration water was not enough (no deep infiltration) to omit this occurrence, which led to the strong deviation in the final water balances, particularly in the storage change.

The increase in PWP from 4.2 to 4.6 provided more water for plant uptake, resulting in larger ET and infiltration for P46. While the impact of PWP changes on water balance processes was less pronounced in the experiments than the differences between the soil hydraulic models, they should not be neglected. For crop growth simulations under water stress, Yao et al. (2020) calibrated the PWP parameter based on field observations of soil water content and aboveground biomass (after initially measuring it in soil samples) and point out the potential to introduce large simulation errors under water stress conditions.

4.5.3 *Spectral methods for model evaluation and practical implications*

Using spectral methods for model evaluation, we found supporting evidence that a) spectral methods provide a much more differentiated view on the strengths and weaknesses of the model at different time scales as compared to the usual evaluation of residuals in the time domain, and that b) the PDI model allowed for a better fit of the available soil moisture and matric potential observations. The spectral analysis gave detailed insights into strengths and weakness of the model used and differences between experiments. The performance divergence in the different frequencies may not be surprising, but can be clearly quantified using signal decomposition (Fig. 4.6 and 4.7). For instance, we could show that the trend signal was the key driver for determining the overall NSE of the model and that the model struggled capturing the precipitation events in both timing and amplitude. Further, the role of each frequency band in explaining the overall variance between observations and simulations became evident (Fig. 4.7). Stallone et al. (2020) provide a detailed overview of limitations and pitfalls of this analysis method and summarize examples for its usage mostly in geophysics, but also e.g. in atmospheric and oceanographic studies. A major issue is associated with spikes and jumps in the original time series as they can have a substantial impact on the decomposition, and special care is required if used in "precursory" analyses, The strong rainfall event in the end of October can be considered as a spike as its influence is visible throughout the frequency bands (Fig. 4.6). Since we are comparing observed and simulated time series that both contain the spike, the influence on the decomposition should be the same and not affect our results.

Besides the rather methodological aspects discussed above, we want to outline some of their practical implications.
All three factors, namely the choice of the variable of interest (volumetric water content or matric potential), choice of soil hydraulic model, and chosen value of the PWP, strongly influence the simulation results. This has implications for irrigation strategies, particularly regarding

duration and severity of water stress. For instance, using the matric potential simulations, plant water stress started in the reference run in the second depth in mid-February, whereas using the water content in the end of December. Assuming an irrigation of 60 mm per week, this increases the irrigation demand to 360 mm, which is almost 50 % of the yearly precipitation in the area. Using volumetric water content as target variable for managing irrigation adds uncertainty as it is strongly affected by the choice of the soil hydraulic model, which determines at which value soil water content plant stress begins. For the reference run, the PDI model does not reach the PWP in either water content or matric potential. The VGM model simulated a water stress period lasting for approximately 50 days, resulting in a similar increased irrigation demand as the previous example. Lastly, the PWP uncertainties add to the timing of the water stress, shifting it depending on the threshold chosen but also affecting dynamics in general.

The choice of the soil hydraulic model also substantially affected simulated transpiration rates, overland flow, and hydraulic conductivities (Fig. 4.8). Therefore, these sensitivities should also be compared to sensitivities in other modelling compartments. McMillan et al. (2011) investigated the precipitation input error by using a rainfall error model and the suitability of a multiplicative error formulation to correct the model output. Loritz et al. (2022) demonstrate how sap flow measurements improved transpiration simulations of the same model used in the study here. They demonstrated how both storage predictions and dynamics were affected, especially during dry conditions. Combining and weighing of these uncertainties against each other may give an indication of the "severity" and need for improvement of each factor. Novick et al. (2022) found that including parameters such as hydraulic conductivity, field capacity and wilting point increased the variance of the simulated gross primary productivity to 22-53 %. Furthermore, Weihermüller et al. (2021) highlighted the importance of pedotransfer functions in soil hydrological modelling. The choice of the model used also affected simulated water fluxes, and uncertainties in e.g. ET may reach 10 % per year and respective uncertainties exceeded uncertainties across soil types (Paschalis et al., 2022).

Adding water in form of irrigation (Ref) improved the alignment of the hydrological model output (NI) with observations, which experienced both precipitation and irrigation. This adjustment shifted the system from water- to energy-limited (Hoffmeister et al., 2024), resulting in increased simulated evapotranspiration with irrigation: 550 mm (Ref_VGM) or 731 mm (DI_VGM) compared to 370 mm (NI_VGM). The choice of the soil hydraulic model plays also a crucial role as ET estimates vary substantially with 758 mm (Ref_PDI), 625 mm (NI_PDI), 870 mm (DI_PDI), where also differences between irrigation

managements in ET were smaller compared to the VGM.
Compared to the widely used VGM soil water retention model, also the PDI model simulated a larger water availability in soil to foster plant transpiration, which resulted in a 30 % (200 mm) increase in transpiration during a simulation period of half a year.
Furthermore, the increase in PWP from 4.2 to 4.6 provided more water for plant uptake, resulting in larger ET (550 $\rightarrow$ 634 VGM, 758 $\rightarrow$ 847 PDI), however, only arising from increased in transpiration as evaporation slightly decreased simultaneously. This highlights how the PWP acts as a critical threshold dividing energy input into latent heat (ET) and sensible heat (Hohenegger and Stevens, 2018).
The alterations in both the PWP and the soil hydraulic model will not only induce a substantial shift in the water balance, but also exert a marked effect on the energy balance by increasing the latent heat flux and reducing the sensible heat flux by an equivalent amount. Therefore, a switch from VGM to PDI (or in PWPs) will probably strongly affect modelling of land-surface-atmosphere exchange and climate. A hypersensitive coupling regime has been observed when air temperatures increase at a greater rate than soil water content declines and a simple energy-balance model indicated that this phenomenon occurs when a strong drop in evaporative cooling occurs, which is shortly before the soil water content reaches the PWP (Hsu et al., 2024).

4.6 CONCLUSIONS

This study highlights the importance of adopting a dynamic model evaluation in the spectral domain for hydrological assessments. Such an approach is particularly advantageous because it mitigates the impact of unavoidable biases and effectively detects changes across various time scales. The additional use of cEEMD as an analytical tool enables the removal of noise and trends without requiring prior assumptions, and informs on phase shifts and amplitude mismatches between observations and simulations. However, it is particularly sensitive to abrupt changes in time series data.
The findings indicate that hydrological model sensitivities and constraints are predominantly influenced by soil characterization rather than by changes in management practices. It is essential to recognize that this sensitivity may represent an "artificial" error, as soil properties in real-world scenarios do not change to the same extent as they do in our virtual experiments. The choice of soil hydraulic model has a substantial impact on modelling results, even affecting land-surface-atmosphere exchange.
Furthermore, the assumption of a constant PWP is strong, especially considering that the PWP even for sunflowers can vary significantly (ranging from 3.8 to 4.6), which may result in a nearly 10 % difference

in volumetric soil water content. This underscores the importance of carefully considering soil characterization when setting up a process-based model such as Catflow. If appropriate data were available to select hydraulic models and parameters with confidence, the accuracy of these models in real-world scenarios would be enhanced, which is of high importance for the simultaneous assessment of several components, including yields, erosion, biodiversity, shading and water availability at the AFS field scale.

Part V

SUMMARY AND DISCUSSION

In the following part, I summarize the key findings and discuss the results of the separate chapters in light of the objectives stated in the introduction. I derive practical implications from the findings and propose opportunities for development and further research.

5 SUMMARY AND DISCUSSION

In sections 2 – 4, two AFS field studies and one AFS modelling study were presented. In the following sections 5.1 – 5.3, I summarize and combine the key findings of the different studies and place them in the literature context. While I focus on summarizing soil water-plant interactions in 5.1 (objective I), I reflect in 5.2 on their observation through measurements and modelling (objective II and III), respectively, and will end this chapter with some practical impacts (5.3).

5.1 IMPACT OF AGROFORESTRY SYSTEMS ON SOIL-WATER-PLANT INTERACTIONS

This section is sorted by soil water-plant interactions (Fig. 1.2) that were closely observed together. Similar to the introduction, soil-related aspects are mentioned first, before moving on to soil-water and plant aspects. The processes (black) and the methods used to observe them (blue) are named in the marginal comments.

Soil carbon and nutrient accumulation
soil samples across field analysed for soil C and N

The data sets obtained in all three AFS (chapter 2 and 3) revealed an accumulation of carbon (C) and nitrogen (N) in the vicinity of the trees. In chapter 2, C and N increased with decreasing distance to the windbreak structure. This can be attributed to increasing amounts of leaf litter and old roots, but also interaction with fungi, all promoting elevated C input as well as nitrogen fixation in the soil (Nygren et al., 2012; Jackson et al., 2017; Dold et al., 2019; Mayer et al., 2022). Alder trees are know to be a nitrogen-fixing species (Claessens et al., 2010), which is a very useful trait for the crops in its vicinity that potentially benefit from the elevated soil nitrogen contents for nourishment and plant growth.
In Malawi, in both AFS treatments (Gliricidia-maize), soil C content was higher than in the control. This effect was, however, stronger in the site that had overall a lower soil C content. Soils with a high initial C contents are closer to a "C saturation", and therefore, less efficient in storing more C, showing a smaller response to C addition (Stewart et al., 2008; Hanegraaf et al., 2009; Iwasaki et al., 2017).
Another form of C sequestration is through biomass accumulation. Single trees may not sequester as much C as forested landscapes but exceed C storage of monocultural units (chapter 2). For instance, the windbreak studied in chapter 2 may store up to 238 kg CO_2 equivalent per metre of windbreak in total biomass. For comparison, Sheppard et al. (2024) estimated that a poplar windbreak also in the Western

Cape region of South Africa could store up to 198.5 kg CO_2 equivalent per metre of windbreak in aboveground biomass.

C influence on soil structure and stability

soil samples across field analysed for soil C, pedogenic oxides, density fractions

Elevated soil C and pedogenic oxides were linked to stronger aggregate stability in the AFS treatment (chapter 3; Barthès et al., 2008). The C added to the soil accumulated mostly in the more stable occluded light fraction (oLF) and heavy fraction (HF), which are less sensitive to destruction, indicating sufficient free mineral surfaces for stable C binding (Castellano et al., 2015). The AFS (Gliricidia-maize) treatment enhanced therefore aggregate stability and C storage, which in turn influences the soil hydraulic properties. This was more pronounced in the location with generally lower initial soil C content, and observed treatment differences in other characteristics could only be attributed to soil C influences if they were specific to this site. Otherwise other factors might be the key for shaping the respective parameter.

Soil structure influence on soil hydraulic properties

soil samples across field analysed for bulk density, porosity and saturated hydraulic conductivity

At the site with treatment differences in soil C accumulation (Makoka, Malawi, chapter 3), bulk density was accordingly lower and porosity higher in the AFS site. For the latter, the results were, however, not as clear as differences lay within the error margins. At the same time, saturated hydraulic conductivity and PAW were higher in the AFS soil compared to the control, both indicating enhanced water resupply to and water retention in the soil profile. The latter potentially compensating the lesser rainfall amount received due to interception. Data from Chitedze, Malawi (chapter 3) showed no treatment-differences in soil C accumulation and no substantial differences in any of the above mentioned parameters. In contrast to Makoka, Malawi, the data from South Africa (chapter 2) showed, despite elevated soil C, a slightly lower porosity and saturated hydraulic conductivity values in the vicinity of the windbreak compared to upslope within the blackberry field. Literature on the influence of soil C on saturated hydraulic conductivity is also not consistent. While Lado et al. (2004) and Fu et al. (2015) found saturated hydraulic conductivity increases in soil of high organic matter, Nemes et al. (2005) observed negative correlations between the two parameters, which they suggested could be due to organic matter improving water retention in some soil types.

Infiltration

soil water content in different depths and saturated hydraulic conductivity from soil samples

Precipitation reaching the soil surface is divided by the soil infiltrability into water remaining at the surface and water entering the soil. This is of critical importance for the water supply of plants. Saturated hydraulic conductivity in the South African AFS was much higher (302.3 mm h^{-1} ±191.3 mm h^{-1}) than the maximum precipitation intensity (max 82.6 mm h^{-1}) providing favourable conditions for infiltration and rapid percolation. It was, however, slightly lower at the windbreak than in the crop possibly due to erosion of fine materials during intense rainfall events.

In Makoka, Malawi (chapter 3) infiltration occurred more rapid and almost immediate in the deeper soil in the AFS compared to the control. The higher saturated hydraulic conductivity in the AFS (difference approx. 123 mm h^{-1}) is potentially caused by an elevated C content. Concurrent increases in soil water content at greater depths indicate the presence of macropores caused by root structures and enhanced biological activity in the AFS. This is in line with Chirwa et al. (2003), who observed higher infiltration rates in their AFS treatment as compared to monocropping. Similarly, Anderson et al. (2009) documented in a buffer strip study improved infiltration due to the rooting system in the AFSs compared to a control.

Surface runoff and erosion

precipitation, soil water content, nutrients across slope

Water at the soil surface remains, depending on the terrain, either ponding or forms surface runoff potentially creating soil erosion.
The field data from the South African site (chapter 2) indicated that the tree row acted, besides its role as windbreak, also as buffer for surface runoff, and therefore, also for potential erosion of material further downslope. On the one hand, this was evident during some of the rainfall events where storage change to a depth of 80 cm exceeded the measured precipitation input. On the other hand, C and N accumulated close to the trees and decreased with increasing distance to them, potentially arising from both accumulation by the trees and by erosion from higher parts of the slope. The lower saturated hydraulic conductivity values at the windbreak could also be an indication of erosion of fine materials downslope being intercepted by the trees.
In Malawi, saturated hydraulic conductivity was similar at both sites and unsaturated hydraulic conductivity decreased quickly with decreasing soil water content. A high-intensity rainfall event on rather dry soil could lead to infiltration saturation. However, due to the absence of strong topographical gradients, the water remains between the maize ridges and can infiltrate on their banks and continue to infiltrate at the rate of redistribution until depleted. Storage change after precipitation events remained generally quite high for a longer period of time, confirming this behaviour.
The advantage of introducing trees into agricultural fields for the reduction of surface runoff is also acknowledged in the field experimental as well as modelling literature (Richet et al., 2017; Jacobs et al., 2022; Rosier et al., 2023; Rosier et al., 2024).

Water availability

matric potential, soil water content and soil water retention curve from samples

No indication for substantial water stress in the AFSs was found. The crops had in general sufficient water to support healthy plant growth. The Gliricidia treatments in Malawi (chapter 3) were spared from severe water stress due to sufficient water availability, whereas the AFS management in South Africa (chapter 2) counteracted a crop water deficit. The latter was supported by the modelling experiments, who confirmed that without irrigation the blackberry crops would be

in a water deficit risking production. In Makoka, Malawi (chapter 3), the AFS with substantially more C content, also had a higher plant available soil water storage. However, the effect of soil C increases on soil water retention remains still unclear in the literature with contradicting findings reviewed by Minasny and McBratney (2018).
Water stress occurrence due to competition, can be mitigated by different strategies. In chapter 2, the crops are being irrigated on water stress risk days. In chapter 3, the Gliricidia plants are being coppiced at ground level during growing season of the maize. Such shoot pruning during the cropping season may reduce water uptake by trees, and thus, competition (Schroth, 1999). Further options to reduce competition are, for example, root pruning (basically ripping a line which severes the roots) mechanical barriers utilising metal or plastic sheets sunk into the soil to prevent roots from interacting (e.g. Ong et al., 1991).

Microclimate
precipitation, wind speed and direction, relative humidity

Trees in the landscape alter the microclimate in their surroundings via several processes. The findings of chapter 2 revealed that the windbreak acts as a buffer to reduce high wind speed occurring especially in the hot summer months in the Western Cape region, South Africa. This reduction in wind speed has a substantial effect on evapotranspiration (ET). In an example calculation, we demonstrated that a combination of sun and wind shading may reduce actual ET to 54 % of the potential ET, meaning in this specific example a reduction from 10.8 mm d^{-1} to 5.8 mm d^{-1} on a clear-sky day. This can substantially influence overall water availability and may result in e.g. a lower irrigation demand. However, the absence of sunlight may of course also have negative effects on plant growth.
In a nearby vineyard, Veste et al. (2020) observed a 20 % reduction in wind speed behind the windbreak in comparison to an open field. Based on Hintermaier-Erhard and Zech (1997) and Häckel (1999), a reduction in wind speed of up to 70 % can be expected on the leeward side of such a structure, depending most of all on its density, protecting the soil from wind erosion and promoting soil health (Shao, 2008; Shi et al., 2018).

Precipitation and interception
precipitation, soil water content below crown and in field

Single trees but also the windbreak canopy have an impact on the precipitation distribution by intermitting or retarding rain drops falling down. Several observations were made during the field studies that were related to interception. In chapter 2, a higher fraction of the total precipitation reached the soil in the crops as opposed to below the windbreak. The difference of approximately 10 %, corresponding to 26.5 mm, was supported by the literature for similar tree species (Muthuri et al., 2004). The model in chapter 4 estimated interception to be 3.5 - 8.6 % of the total precipitation based on the leaf area index multiplied with an empirical interception storage, which provided

satisfactory estimates in previous studies (e.g. Zehe et al., 2001). Both, the field and modelled estimates of interception, were substantially lower compared to literature values for e. g. temperate closed-canopy deciduous broadleaf forests of 22 % of yearly rainfall (Dingman, 2015). Windbreak branches experience more movement due to the strong wind exposure of most branches, resulting in less storage capacity on the leaves.
Similary, the AFSs in Makoka, Malawi (chapter 3) with larger maize crop and larger leaves compared to the control coincided with approximately 14 % less precipitation reaching the soil. Nazari et al. (2020) found that maize canopy may reduce total water input to the soil by 11-19 %, which closely aligns with our observations.
Rainfall interception reduces on the one hand, the kinetic energy of rainfall reaching the surface and therefore potentially protects the soil structure. On the other hand, it also reduces the amount of water reaching the soil, and therefore, available for vegetation below the canopy. While Tietjen et al. (2010) found interception-induced throughfall patterns to influence local infiltration and soil moisture, Fischer-Bedtke et al. (2023) related throughfall patterns rather to soil moisture dynamics and soil water storage changes. Interception is dependent on tree species, tree arrangement and the season.

This section has summarized the findings of the individual studies related to the soil-water-plant interactions in AFSs, which were introduced earlier and also illustrated in figure 1.2. Challenged by the width of information and factors involved in ecohydrology (Guswa et al., 2020), it is critical to use interdisciplinary methods to be able to get a full picture of AFSs benefits and limitations.

5.2 COMPREHENSIVE FRAMEWORKS AND LIMITATIONS OF THE STUDY

Using the common tools of one discipline alone was not sufficient to fully disentangle the relationships between the involved actors. In the following, I will give some examples and "lessons learned" why encompassing several disciplines to move forward in this field of research is critical.

5.2.1 *Challenges related to soil-water-plant measurements*

Capturing dominant processes and state variables in the ecohydrological context is a demanding task. The acquisition of useful and high-quality data is impeded not only by scale issues, but also by the fact that common hydrological approaches and concepts might not suffice to capture the complex interactions.

Example for synergy potential of interdisciplinary methods

Taking the studied AFS in Makoka, Malawi (chapter 3) as an example: If we had to solely rely on the samples taken for standard soil physical characteristics (bulk density, hydraulic conductivity, retention curve) and the soil water monitoring (which is often only volumentric water content and not including matric potential (Novick et al., 2022), we would have been able to observe treatment and site differences between the two plots in soil water dynamics. However, due to the collaboration with soil scientists we were able to relate our observations and especially the differences to key soil aspects, such as soil C accumulation and soil structure (density fractionation). The marginal notes in the previous section (section 5.1) summarise the wide variety of measurements used or required for investigating the different processes involved and this list does not claim to be complete.

Challenges in ecohydrological monitoring

Due to the multitude of fluxes and storages of interest in ecohydrology, it is not straightforward to setup a comprehensive measurement system. No off-the-shelf solutions exist that plainly allow plug-and-play installation in the field largely due to the "limited size of an environmental sensing market and the diversity of needs" (Guswa et al., 2020). Furthermore, there is a gap between research needs and the availability of observational technologies required to support hypothesis validation in catchments of interest (Beven et al., 2020) and no established standards for sensor communication exist (Guswa et al., 2020).

One challenge common to both modelling and monitoring is the difficulty of different scales. Ecohydrological processes occur from very small spatial scales, such as molecular level, to much larger scales and it remains mostly unclear how to interpolate from small spatial and temporal scales to larger scales or vice versa. However, it has been shown that localized processes impact large scale responses (Blöschl and Sivapalan, 1995; Bergström and Graham, 1998; Asbjornsen et al., 2011; Fan et al., 2019; Ward and Packman, 2019; Beven et al., 2020).

Beven et al. (2020) stated a challenge that I have also faced several times: The difficulty or rather impossibility of controlling the boundary conditions, which makes it difficult to work on "perceptual understanding and model formulations". It was very difficult to relate one observation (independently of samples or of time series) to precisely one process as indicated by the example above. With the help of additional data we could, through a procedure of exclusion, eliminate certain factors and a hypothesis be formulated for the most probable cause of the observed phenomena. Notwithstanding the constant feeling that some data were missing to clearly prove or reject the hypothesis. This is supported by Beven et al. (2018) who considered the collection of new data on fluxes and storages as a strategy to reduce uncertainties (Beven et al., 2020).

To achieve that it is critical to work in several dimensions sim-

ultaneously and to include measurements of different disciplines as indicated by the example above while finding the "sweet spot" between cost (time, personnel, equipment) and gain of information and thus new insights.

Sensor limitations

Additionally, each device has its own limitation. Soil water content is not measured directly but only by inferring from dielectrical parameters. For instance, a common way to monitor volumetric soil moisture is with time domain reflectometry (TDR) sensors (used in chapter 2 and 3), where the dielectric permittivity is related to soil water content. The measurement volume of TDR measurements is, however, much smaller than representative elementary volume of soil water storage (Zehe et al., 2010). As a result they include significant small-scale variability, spreading at the 10-meter scale potentially as much as across an entire catchment (Zehe et al., 2010; Mälicke et al., 2020). However, spatial soil moisture observations were shown to be rank-stable at small and large scales. Therefore, individual absolute numbers of soil water and specifically soil water storage may not be representative, they do, nevertheless, accurately reflect temporal dynamics (Mälicke et al., 2020). Here, matric potential sensors offer an advantage over soil water content because it allows for spatial interpolation between measurement locations (equipotential lines), which reduces the importance of an adequate representative measurement volume (Whalley et al., 2013).

Practical lessons learned from (un)successful monitoring sites

I learned a lot about practicalities surrounding soil water measurements during the studies mentioned before but especially during the Covid-19 pandemic, when instrumenting an AFS demonstration site near Karlsruhe due to enforced travel bans. We received too little useful data for drawing any conclusions about soil water dynamics but learned a lot about setting up measurement systems. Some of the challenges encountered are just inherent to working in the field, others, however, relate to the aforementioned drawbacks in technical development.

We encountered issues during the setup with mouse burrows and high root densities, which complicated proper installation of the equipment. The cable length connecting sensors with logging devices and power supply limited the distance to be covered. Partial shading of the solar panel due to fallen branches interrupted data collection along with field maintenance work, which accidentally cut the cables. Communication problems between sensors and loggers (despite using the same protocol) also produced some non-reproducible errors. The data that were obtained were also not always considered to be suitable for the designed tasks. For instance, we could not perform root water uptake calculations from soil moisture time series as the needed daily fluctuations in the signal were not apparent despite the close vicinity to the rooting system. A better measurement concept proved to be the setup in Malawi (chapter 3), where one logger and power supply

connected only a few sensors, preferably of one type, which can then be replicated to create greater coverage in a sort of "island" concept. Here, additional challenges arose due to the remoteness of field sites, where maintenance was not easily conducted, and the equipment's need to be guarded.
There is still a lot of room for improvements in the field of measurements. However, new concepts, systems and technologies are constantly developing an deliver promising outlooks to upgrade existing measurements.

5.2.2 *Modelling challenges of soil water dynamics under dry conditions*

As models are conceptual representations of some part of reality, they also face challenges in representing all key soil water-plant processes to properly represent soil water dynamics in AFSs.

Challenges and limitations of modelling soil water-plant interactions under dry conditions

During my work I encountered several challenges or issues regarding the feasibility of using a standard physically-based hydrological model for AFS modelling. The model proved to perform well in modelling precipitation events and respective surface runoff and subsurface flow paths (Hopp et al., 2009; Klaus and Zehe, 2010; Klaus and Zehe, 2011; Wienhöfer and Zehe, 2014; Loritz et al., 2017). It has been further developed for particle transport simulations and to capture erosion processes. Soil water-plant interactions always play a role in these processes, but are not the primary focus. Commonly, it was conceptualised that precipitation is the main driver of hydrological models, which strongly influenced model development. Leaving the precipitation-domain and moving towards dry conditions or semi-arid systems brings different elements of the hydrological cycle and landscape to the fore. For instance, the physically-based model in chapter 4 (likewise valid for most physically-based hydrological models) cannot expand the root system further than the tree crown or differentiate root density driven water uptake, because this was not important for precipitation-runoff-modelling but is essential for picturing sequential drying due to transpiration. The structure of the model used in chapter 4 is partially not set up in an ideal way to easily implement detailed plant structures. Beven et al. (2020) put it in a nutshell: "what is produced by a simulation depends on the structural assumptions of the model that produced it, and we have a mismatch between the complexity of the perceptual model of the relevant processes and the relative simplicity of current model structures". I will give a specific example from the model used in chapter 4, but other physically-based models function similarly. To include a windbreak into the model dimension, the "surface node" in the desired location is associated with a new land-use type, alongside basic parameters such as albedo, leaf area index, plant coverage, plant height and rooting depth. However, soil porosity and structure, which

is likely altered by roots and organic matter introduction due to litter fall is not automatically updated. Furthermore, the crown and root zone do not spread horizontally as is the case in reality, and shading of light and wind from trees is not automatically considered but needs to be added manually by separate input files attached to the respective surface nodes.

Hence, working under dry conditions and focusing on soil water-plant interactions opens up a new field for these type of models. I identified some weaknesses for the current state of the model that needs to be further developed in the future. Just as Novick et al. (2022) pointed out, environmental models are very sensitive to soil parameters, especially to the parametrisation of the water retention curve. Comparing two soil hydraulic models showed substantial differences, especially during water-limited conditions (chapter 4). Quite many studies compared pedotransfer functions (e.g. Weber et al., 2024) and their influence on simulated water fluxes (Weihermüller et al., 2021), but much less compare different soil hydraulic models especially their influence on simulations (Dettmann et al., 2019; Peters et al., 2021). Most hydrological models use the Van Genuchten/Mualem (VGM; Van Genuchten, 1980; Mualem, 1976) soil hydraulic model without considering its limitations, especially under dry conditions the PDI model which includes non-capillary water would be a better option. I covered this topic in chapter 4 and could show how the soil hydraulic model choice substantially impacts the water balance. For instance, transpiration increased by 30 % or 200 mm with the Peters-Durner-Iden (PDI; Peters et al., 2024) compared to VGM soil hydraulic model. Considering that the yearly precipitation at the studied site is approximately 742 mm y^{-1} (Meadows, 2015), the difference in transpiration is significant (27 %). Also the duration of water stress (days with matric potential or water content below the PWP) varied substantially between the models with 50 days using the VGM opposed to none for the PDI, directly affecting water management decisions, e.g. irrigation amounts. Generally, Whalley et al. (2013) further pointed out that because of the strong soil texture and structure impacts on the soil water retention curve, matric potential cannot be easily estimated from soil water content measurements and should be measured directly.

Model sensitivity to soil hydraulic models

Another pitfall I encountered is the fixed permanent wilting point. As mentioned in the chapter 4, the PWP is a critical threshold deciding the cut-off limit for water availability for plants. Once the soil water content drops below the PWP, no more water is extracted. Instead of partitioning into latent and sensible heat flux, the incoming energy increases only the sensible heat flux, raising the temperature of the environment. This energy shift can be quite substantial as the simulations with different PWPs in chapter 4 have shown with reductions in transpiration varying between 80 to 125 mm (depending on the soil hydrological model). Transpiring 100 mm less during half a year leads

Strong assumptions included by a fixed PWP in hydrological modelling

to a surplus of 24.5 MJ of energy impacting the energy balance.
Several studies have shown that assuming different PWPs is far from being unrealistic (Garg et al., 2020; Wiecheteck et al., 2020; Freitas et al., 2023). The strong assumption of the PWP being a static soil properties does not reflect any plant physiology or adaptation capability of plants to droughts or dry spells. It is rather more understood that PWP is a dynamic soil and plant specific variable. Considering that the PWP is widely used in hydrological and climate models, it is possible to imagine far-reaching consequences in prediction results associated to this rather strong assumption.

Recent developments in the field of ecohydrology consider now explicitly dynamics in "vegetation growth, root structure and plant physiology by integrating energy fluxes, water fluxes and storage together with vegetation dynamics to capture feedback between ecosystem productivity, hydrology and local climate" (Guswa et al., 2020). Implementation of sun and wind shading effects on plant growth and evapotranspiration will likely improve the representation of AFS through modelling.

5.3 PRACTICAL IMPLICATIONS (CHAPTER 2-4)

The thesis findings offer practical implications for on the one hand advancing scientific knowledge in soil water monitoring and modelling in combination with vegetation, and on the other hand, for a sustainable and optimized management of AFSs.

- A considerate combination of crops and tress can prevent or limit competition over resources as water and nutrients to a minimum without increasing work and maintenance load too much. Careful evaluation of further benefits likely outweigh minor additional costs (chapter 3, 4 and 5).
- Careful planning and testing of sensor networks is crucial for a successful acquisition of high-quality data. Interdisciplinary efforts allow for a comprehensive assessments of ecosystems such as AFS in different dimensions while remaining parsimonious (chapter 3, 4).
- The permanent wilting point is not a static property of the soil, but rather a dynamic soil and plant specific variable. Varying the PWP in the range of 3.8 to 4.6 in modelling experiments, resulted in reduced transpiration of 80-125 mm (depending on the soil hydraulic model). Acting as a divider between latent and sensible heat fluxes, this also substantially influences the energy balance (chapter 3).

- Taking non-capillary water flow into account by replacing the VGM soil hydraulic model with the PDI increased transpiration estimates by 30 % or 200 mm of a semi-arid AFSs over a period of half a year. Relating this to the yearly average precipitation of 742 mm (Stellenbosch, South Africa; Meadows, 2015), clearly demonstrates the substantial impact the mode choice has on modelling results and subsequent consequences. Additionally, the model choice substantially determined if and for how long vegetation experienced severe water stress (chapter 3).
- The latter two points have strong implications for management decisions, such as irrigation amounts or scheduling, which relate further to costs and resources necessary and reach as far as expected yields and subsequently overall productivity of a system. Also outside of the agricultural sector, accurate description of water balance components is crucial.

6

CONCLUDING REMARKS AND OUTLOOK

The goal of this thesis work is to improve understanding of the complex soil-water-plant processes and their acquisition in observations and modelling. Specifically, I focused on AFSs as a potentially beneficial agricultural development strategy to combat some of the challenges arising from climate change.

Impacts of trees on monoculture fields

The thesis work demonstrated the multifaceted impacts of trees on soil and water characteristics of monoculture agricultural fields. Trees contribute to soil fertility by accumulating nutrients and affect soil structure and stability. Root channels, increased biological activity, and improved soil stability collectively influence soil infiltration and water retention capacity. Additionally, trees influence microclimatic patterns by providing wind shelter and rainfall interception. While competition for resources such as water and nutrients can occur, judicious combination of trees and crops and management practises can minimise or even prevent these conflicts, optimising resource use efficiency.

Ecohydrological measurements of soil-water-plant interactions

To capture key soil-water-related processes in ecohydrology, this study employed interdisciplinary measurement methods, combining campaign-based sampling of soil physical properties to cover spatial variation with high-frequency hydrological monitoring for temporal dynamics. Successful data acquisition relies on careful planning and testing of equipment. Despite challenges related to technical limitations (accuracy and communication issues) and operational difficulties (maintenance needs and power outages), innovative designs and technological advances will improve ecohydrological measurements and data reliability.

Modelling challenges of soil water dynamics under dry conditions

The physically-based model faced difficulties in accurately representing soil drying processes and soil water variability related to rainfall events. The choice of the water retention parametrisation and the assumption of a constant PWP strongly influence water availability. These choices not only impact crop water availability with implications for water management, e.g. timing and amount of irrigation, but also determines partitioning into latent and sensible heat. If not enough water is available for evapotranspiration, incoming solar radiation

will transform only to sensible heat, which might lead particularly in land-surface models to further feedbacks.

One of the main challenges that emerged from my research is the dry conditions that the studies were conducted in. Considering that according to the World Desertification Atlas (Cherlet et al., 2018) approximately 40 % of the world are dry regions and fighting severe water limitations at least part times of the years, it is of critical importance to measure and simulate dominant process regarding the water fluxes correctly to be able to improve predictions and thus water management.

Achieving a complete picture of the water balance was a difficult endeavour throughout my studies. The most uncertainty arose from unreliable or not existent estimates of the transpiration. One way to quantify this was tested with the root water uptake estimates in chapter 2. However, the volumetric water content measurements did not yield very reliable results. Another way to go is the use of sap flow sensors. Sap flow data can be related to transpiration and have been proven to be useful in previous studies (e.g. Granier and Loustau, 1994; Dugas et al., 1994; Hassler et al., 2018; Loritz et al., 2022). Furthermore, differently combining existing sensors and testing newly developed measurement techniques to find more robust and reliable measurement systems is critically important especially for remote areas.

In this context, I would like to point out the importance and high value of long-term research trials such as the ones maintained in Malawi by ICRAF. As mentioned several times, AFS are slow growing and developing systems, just as much as changes in soil structure and texture also occur on long timescales. Therefore, it is critical to maintain well equipped and carefully established field trials running for long timespans.

Modelling of AFS systems should seek to couple important aspect such as wind and sun shielding effects, plant development, soil hydrology, and nutrient dynamics. The inclusion of distributed root water uptake not only from the column below the plant but also expanding horizontally into existent or newly developed modelling frameworks should also improve planning and management of AFSs. It also proved very important to consider possible shifts in dominant processes (e.g. soil water retention) and influences (e.g. PWP) in the modelling process when moving from wet to dry conditions, as key assumptions and concepts may not be universally valid.

Additionally, it could be interesting to look at the whole system more closely from the energy perspective. I have seen several aspects where this could be beneficial such as the irrigation seen as a mechanism shifting a system from water- to energy-limited conditions (chapter 2 and 4), windbreaks reducing the irrigation demand by reducing

evapotranspiration (chapter 2), or the influence of PWP on the energy balance (chapter 4), which substantially increases sensible heat fluxes. The matric potential concept seamlessly integrates into the energy perspective of the water-plant system. However, matric potential measurements are rare and I fully support the claim of Novick et al. (2022) promoting for more matric potential measurements. Recording both volumetric water content and matric potential has been extremely useful in the studies here.

Part VI

APPENDIX A

A

APPENDIX

A.1 APPENDIX OF CHAPTER 2

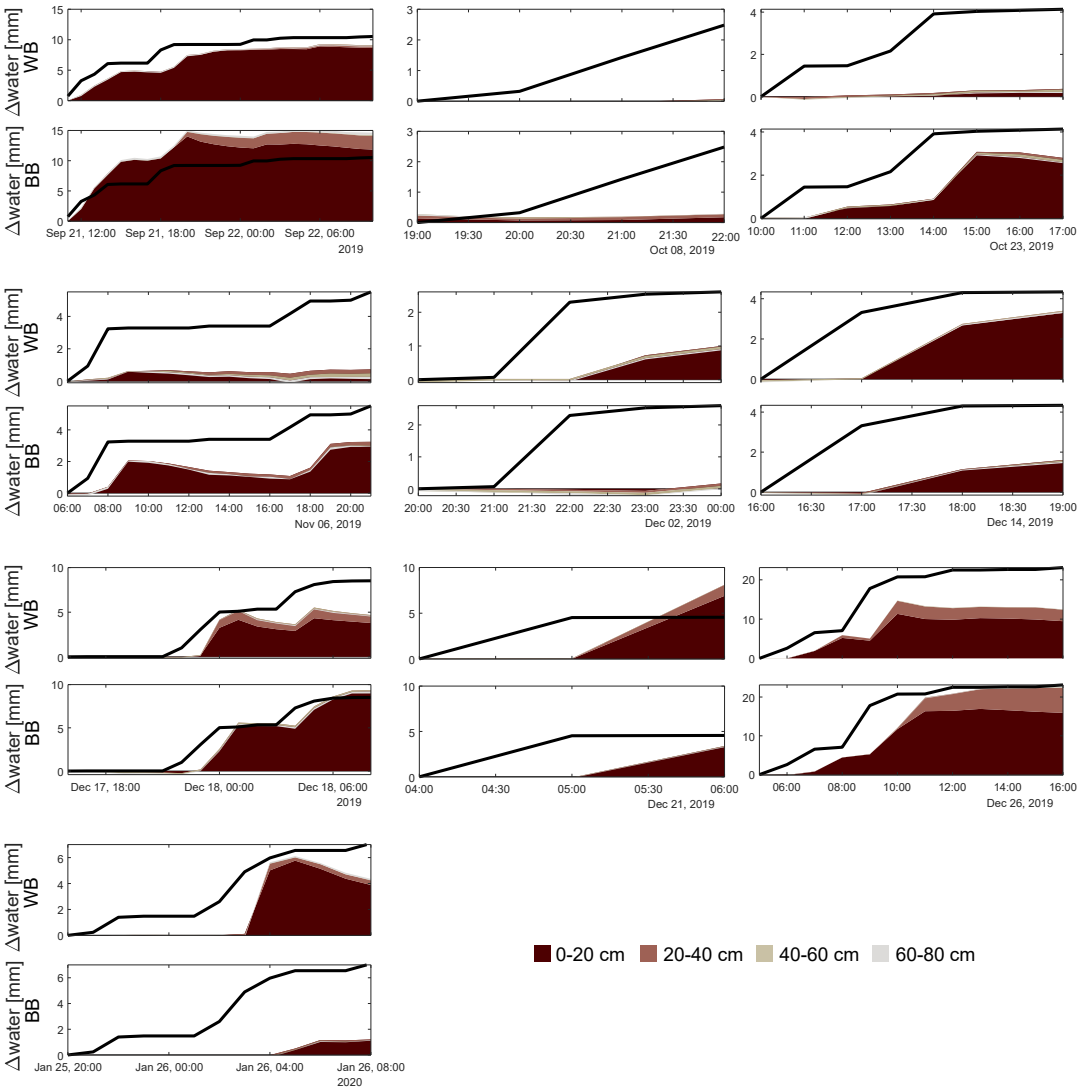

Figure A.1: Panels show cumulative precipitation (line) and cumulative soil water storage change of each sensor for all precipitation events not shown in figure 2, for both the windbreak (upper row) and the blackberry (lower row) location. The different colours represent the different depths of the sensors.

Table A.1: Laboratory analysis of three soil samples taken adjacently to the soil water content monitoring point near the windbreak at different depths. Abbreviations are: WB P = profile, WB = windbreak, BB = blackberries, E = east, M = middle, W = west, FC = field capacity, PWP = permanent wilting point, PAW = Plant-available water. The values of the three columns from the right are estimated using the PDI water retention model (Peters, 2014). The last four rows are averages of the windbreak and berry location at the two depths.(Further abbreviations: WC = water content, conct. = conductivity).

Location	Sample Depth $[m]$	Sat. hydr. conduct. $[\frac{mm}{h}]$	Organic matter [%]	Bulk density $[\frac{g}{cm^3}]$	Porosity	WC FC $[\frac{m^3}{m^3}]$	WC PWP $[\frac{m^3}{m^3}]$	PAW $[\frac{m^3}{m^3}]$
WB P	0.0	263.1	15.1	1.17	0.56	0.426	0.178	0.248
WB P	0.3	108.7	9.3	1.11	0.58	0.367	0.136	0.231
WB P	0.5	3.2	7.3	1.49	0.44	0.393	0.169	0.224
WB E	0.05	203.3	6.6	1.19	0.55	0.368	0.165	0.203
WB E	0.28	94.05	10.2	1.16	0.56	0.396	0.168	0.228
WB M	0.05	114.5	13.9	1.19	0.55	0.364	0.174	0.191
WB M	0.26	111.4	10.3	1.18	0.55	0.335	0.164	0.172
WB W	0.05	171.9	14.2	1.19	0.55	0.373	0.175	0.199
WB W	0.23	426.6	11.5	1.12	0.58	0.358	0.179	0.179
BB E	0.10	688.8	11.9	1.01	0.62	0.322	0.158	0.164
BB E	0.25	186.8	11.5	1.25	0.53	0.379	0.180	0.199
BB M	0.10	255.7	12.7	1.06	0.6	0.327	0.169	0.158
BB M	0.25	189.3	6.9	1.21	0.54	0.393	0.176	0.216
BB W	0.10	379.8	9.7	1.13	0.57	0.346	0.178	0.168
BB W	0.25	413.1	12.0	1.04	0.61	0.331	0.170	0.161
WB	0.05	163.2	11.6	1.19	0.55	0.369	0.171	0.197
WB	0.25	210.7	10.7	1.15	0.56	0.363	0.170	0.193
BB	0.05	441.4	11.4	1.07	0.60	0.332	0.168	0.164
BB	0.25	263.1	10.1	1.16	0.56	0.368	0.175	0.192

A.2 APPENDIX OF CHAPTER 3

Table A.2: Additional soil characteristics for both sites, separated according to site, treatment and sampling depth. Abbreviations are: PAW – plant-available water; Kf and Ksat – saturated hydraulic conductivity. The values in parentheses are standard errors of the mean. The numbers behind the site indicate: y – sampling year and n – sample size. The sampling year and size for the small cylinders are 2019 and 10 for Chitedze; and 2022 and 5 for Makoka. Sampling year and size of the big cylinders are 2022 and 3.

Site	Chitedze (y = 2019, n = 10)				Makoka (y = 2021, n=5)			
Treatment	Control		Gliricidia		Control	Gliricidia		
Depth [cm]	5	15	5	15	5	15	5	15
Bulk density	0.991	1.098	0.992	1.134	1.198	1.331	1.111	1.333
[g cm^{-3}]	(0.013)	(0.009)	(0.016)	(0.014)	(0.043)	(0.021)	(0.010)	(0.039)
Porosity [ ]					0.62	0.58	0.57	0.63
small cylind.					(0.02)	(0.02)	(0.02)	(0.03)
Porosity [ ] *	0.62	0.53	0.60	0.52	0.54	0.47	0.57	0.44
big cylinder	(0.01)	(0.01)	(0.01)	(0.01)	(0.04)	(0.04)	(0.04)	(0.02)
Ksat [mm h^{-1}]					502	244	869	454
small cylind.					(158)	(46)	(252)	(239)
Ksat [mm h^{-1}] **	452	149	458	89	595	42	310	254
big cylinder	(120)	(54)	(196)	(27)	(13)	(282)	(73)	(175)
PAW [vol. WC] *	18.8	19.0	20.9	21.0	19.8	18.0	19.2	19.0
	(1.7)	(0.6)	(0.7)	(0.5)	(2.0)	(0.6)	(1.9)	(0.6)

* from water retention curves

** not all samples included

Table A.3: Density fraction of C, N and C:N values into free light faction (fLF), the occulded light fraction (oLF) and heavy fraction (HF).

Density	Chitedze			Makoka		
fraction	C [g kg^{-1}]	N [g kg^{-1}]	C:N	C [g kg^{-1}]	N [g kg^{-1}]	C:N
oLF Control	2.17	0.10	22.53	0.71	0.03	23.63
fLF Control	1.10	0.07	16.59	0.44	0.02	18.43
HF Control	22.14	1.42	15.82	5.09	0.57	8.98
oLF Gliri	2.47	0.12	20.56	2.96	0.13	23.34
fLF Gliri	1.15	0.07	15.48	0.83	0.06	14.96
HF Gliri	23.51	1.54	15.27	11.10	1.14	9.76

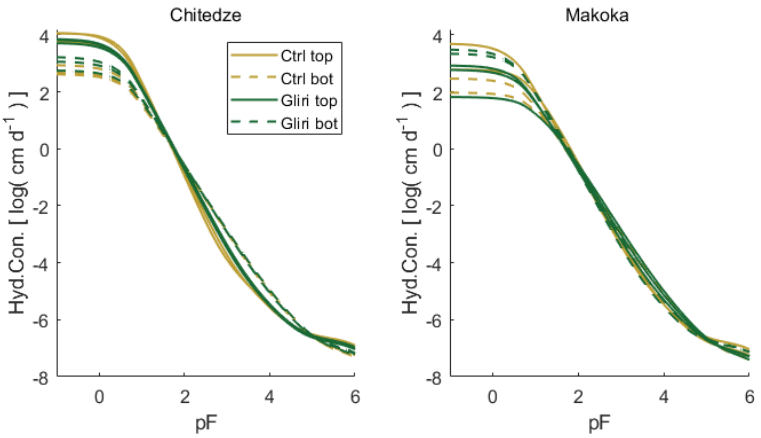

Figure A.2: Unsaturated hydraulic conductivity derived from water retention parameters and saturated hydraulic conductivity measured in the laboratory in the control (Ctrl = yellow) and the Gliricidia treatment (Gliri = green) at the sites Chitedze and Makoka (bot = bottom).

A.3 APPENDIX OF CHAPTER 4

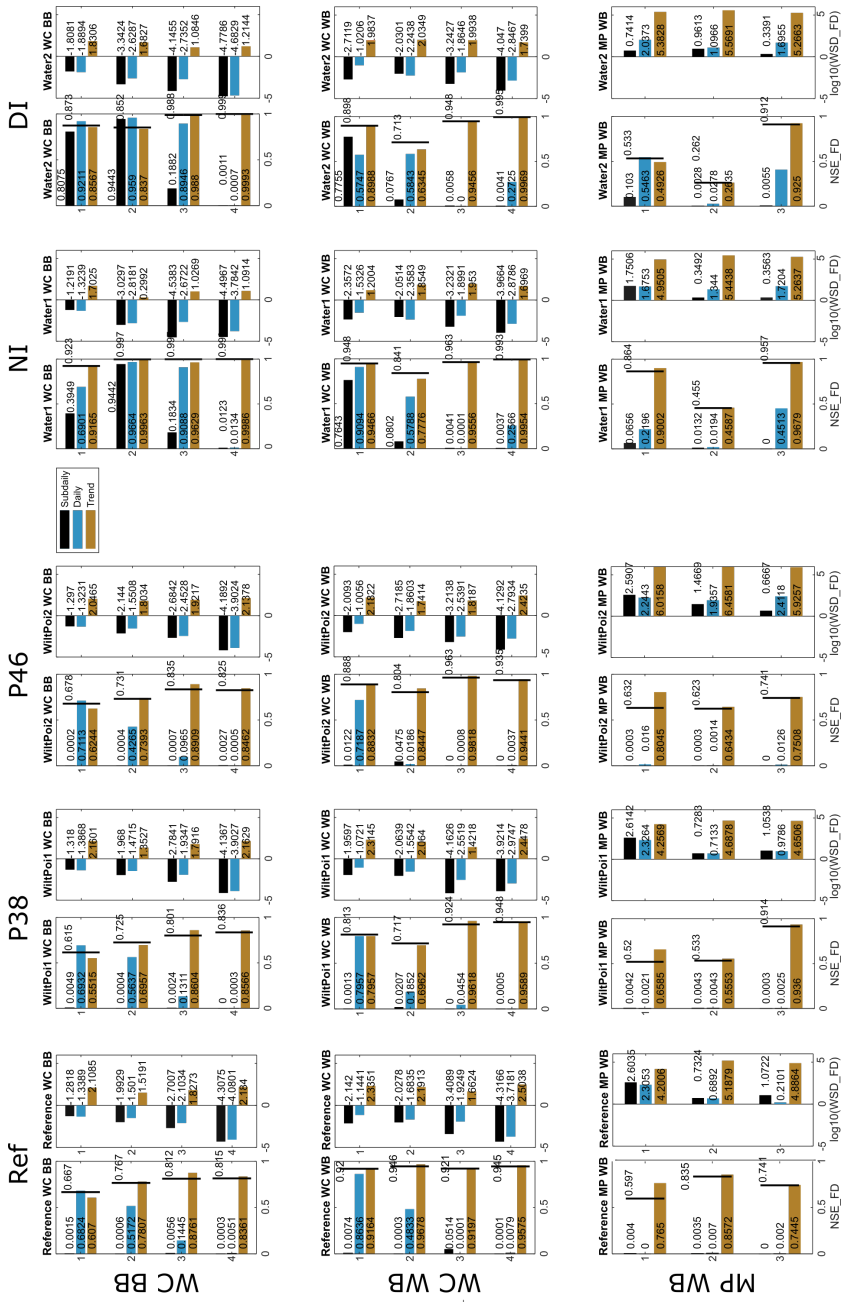

Figure A.3: Overview of all values of Nash-Sutcliff-Efficency (NSE) and Wasserstein Distance (WSD, on log-scale) of different modelling exercises (columns: reference run "Ref", runs with permanent wilting point of 3.8 "P38" and 4.6 "P46", run without irrigation "NI" and doubled irrigation "DI") utilizing the Van Genuchten/Mualem hydrological model. The model output time series of water content (WC) and matric potential (MP) at different locations (rows: windbreak WB and blackberry BB) were decomposed into empirical modes and the retrieved modes then added up into frequency categories (subdaily: blue, daily: orange and trend: yellow). Each subplot displays on the left-hand side the NSE values of the frequency domain in the above mentioned colour code and NSE of the time domain indicated by the vertical bars. WSD are presented for each frequency category on the right-hand side of the subplots.

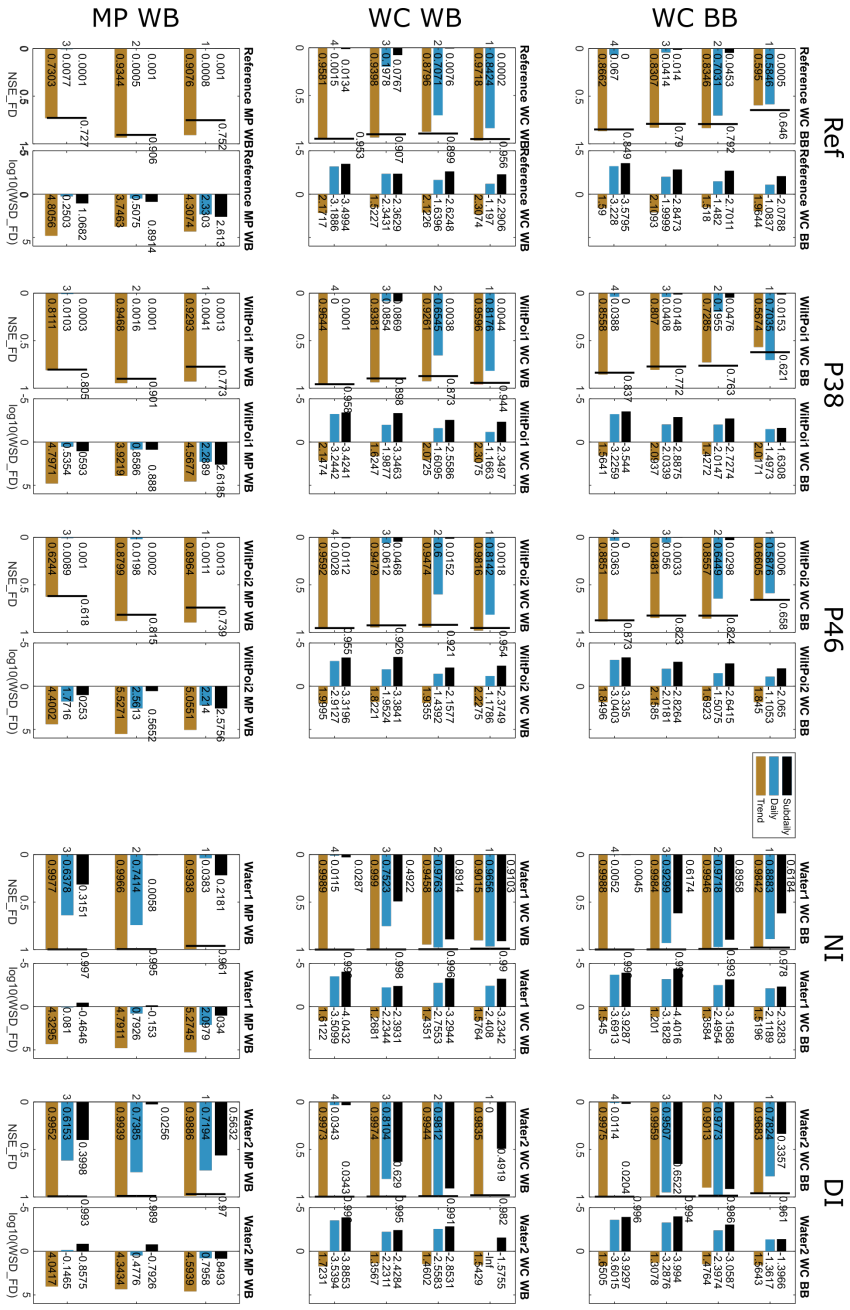

Figure A.4: Overview of all values of Nash-Sutcliff-Efficency (NSE) and Wasserstein Distance (WSD, on log-scale) of different modelling exercises (columns: reference run "Reference", runs with permanent wilting point of 3.8 "P38" and 4.6 "P46", run without irrigation "NI" and doubled irrigation "DI") utilizing the Peters-Durner-Iden hydrological model. The model output time series of water content (WC) and matric potential (MP) at different locations (rows: windbreak WB and blackberry BB) were decomposed into empirical modes and the retrieved modes then added up into frequency categories (subdaily: blue, daily: orange and trend: yellow). Each subplot displays on the left-hand side the NSE values of the frequency domain in the above mentioned colour code and NSE of the time domain indicated by the vertical bars. WSD are presented for each frequency category on the right-hand side of the subplots.

BIBLIOGRAPHY

Akinnifesi, F. K., W. Makumba and F. R. Kwesiga (2006). 'Sustainable maize production using Gliricidia/Maize intercropping in Southern Malawi'. In: *Experimental Agriculture* 42.4, pp. 441–457. DOI: 10.1017/S0014479706003814.

Akinnifesi, F. K., O. C. Ajayi, G. Sileshi, P. W. Chirwa and J. Chianu (2010). 'Fertiliser trees for sustainable food security in the maize-based production systems of East and Southern Africa. A review'. In: *Agronomy for Sustainable Development* 30.3, pp. 615–629. DOI: 10.1051/agro/2009058.

Akinnifesi, F. K., W. Makumba, G. Sileshi, O. C. Ajayi and D. Mweta (2007). 'Synergistic effect of inorganic N and P fertilizers and organic inputs from Gliricidia sepium on productivity of intercropped maize in Southern Malawi'. In: *Plant and Soil* 294.1-2, pp. 203–217. DOI: 10.1007/s11104-007-9247-z.

Albrecht, A. and S. T. Kandji (2003). 'Carbon sequestration in tropical agroforestry systems'. In: *Agriculture, Ecosystems & Environment* 99.1-3, pp. 15–27. DOI: 10.1016/S0167-8809(03)00138-5.

Allen, R. G., L. S. Pereira, D. Raes and M. Smith (1998). *Crop Evapotranspiration – Guidelines for Computing Crop Water Requirements. FAO Irrigation and drainage paper 56*. Rome, Italy: Food and Agriculture Organization of the United Nations.

Anderson, J. M. and J. S. I. Ingram (1990). 'Tropical Soil Biology and Fertility: A Handbook of Methods.' In: *The Journal of Ecology* 78.2, p. 547. DOI: 10.2307/2261129.

Anderson, S. H., R. P. Udawatta, T. Seobi and H. E. Garrett (2009). 'Soil water content and infiltration in agroforestry buffer strips'. In: *Agroforestry Systems* 75.1, pp. 5–16. DOI: 10.1007/s10457-008-9128-3.

Arnold, S., S. Attinger, K. Frank and A. Hildebrandt (2009). 'Uncertainty in parameterisation and model structure affect simulation results in coupled ecohydrological models'. In: *Hydrology and Earth System Sciences* 13.10, pp. 1789–1807. DOI: 10.5194/hess-13-1789-2009.

Asap final report (2023). *ASAP: Agroforestry in Southern Africa - New pathways of innovative land use systems under a changng climate : final report/Verbundschlussbericht : Laufzeit/life time: 01.12.2018-30.11.2022*. Freiburg. DOI: 10.2314/KXP:1912940949.

Asbjornsen, H., G. R. Goldsmith, M. S. Alvarado-Barrientos, K. Rebel, F. P. Van Osch, M. Rietkerk, J. Chen, S. Gotsch, C. Tobon, D. R. Geissert, A. Gomez-Tagle, K. Vache and T. E. Dawson (2011). 'Ecohydrological advances and applications in plant-water relations

research: a review'. In: *Journal of Plant Ecology* 4.1-2, pp. 3–22. DOI: 10.1093/jpe/rtr005.

Asgarzadeh, H., M. R. Mosaddeghi, A. A. Mahboubi, A. Nosrati and A. R. Dexter (2010). 'Soil water availability for plants as quantified by conventional available water, least limiting water range and integral water capacity'. In: *Plant and Soil* 335.1-2, pp. 229–244. DOI: 10.1007/s11104-010-0410-6.

Atsivor, L., G. N. Dowuona and S. G. Adiku (2001). 'Farming system-induced variability of some soil properties in a sub-humid zone of Ghana'. In: *Plant and Soil* 236, pp. 83–90. DOI: 10.1023/A:1011907420292.

Bagnall, D. K. et al. (2022). 'Carbon-sensitive pedotransfer functions for plant available water'. In: *Soil Science Society of America Journal* 86.3, pp. 612–629. DOI: 10.1002/saj2.20395.

Baptista, M. D., S. J. Livesley, E. G. Parmehr, M. Neave and M. Amati (2018). 'Variation in leaf area density drives the rainfall storage capacity of individual urban tree species'. In: *Hydrological Processes* 32.25, pp. 3729–3740. DOI: 10.1002/hyp.13255.

Barthès, B. G., E. Kouakoua, M. C. Larré-Larrouy, T. M. Razafimbelo, E. F. de Luca, A. Azontonde, C. S. Neves, P. L. de Freitas and C. L. Feller (2008). 'Texture and sesquioxide effects on water-stable aggregates and organic matter in some tropical soils'. In: *Geoderma* 143.1-2, pp. 14–25. DOI: 10.1016/j.geoderma.2007.10.003.

Bayala, J. and I. Prieto (2019). 'Water acquisition, sharing and redistribution by roots: applications to agroforestry systems'. In: *Plant and Soil*. DOI: 10.1007/s11104-019-04173-z.

Beedy, T. L., S. S. Snapp, F. K. Akinnifesi and G. W. Sileshi (2010). 'Impact of Gliricidia sepium intercropping on soil organic matter fractions in a maize-based cropping system'. In: *Agriculture, Ecosystems and Environment* 138.3-4, pp. 139–146. DOI: 10.1016/j.agee.2010.04.008.

Bergström, S. and L. Graham (1998). 'On the scale problem in hydrological modelling'. In: *Journal of Hydrology* 211.1-4, pp. 253–265. DOI: 10.1016/S0022-1694(98)00248-0.

Beven, K. J., W. P. Aspinall, P. D. Bates, E. Borgomeo, K. Goda, J. W. Hall, T. Page, J. C. Phillips, M. Simpson, P. J. Smith, T. Wagener and M. Watson (2018). 'Epistemic uncertainties and natural hazard risk assessment – Part 2: What should constitute good practice?' In: *Natural Hazards and Earth System Sciences* 18.10, pp. 2769–2783. DOI: 10.5194/nhess-18-2769-2018.

Beven, K., A. Asadullah, P. Bates, E. Blyth, N. Chappell, S. Child, H. Cloke, S. Dadson, N. Everard, H. J. Fowler, J. Freer, D. M. Hannah, K. Heppell, J. Holden, R. Lamb, H. Lewis, G. Morgan, L. Parry and T. Wagener (2020). 'Developing observational methods to drive future hydrological science: Can we make a start as a community?' In: *Hydrological Processes* 34.3, pp. 868–873. DOI: 10.1002/hyp.13622.

Beven, K. and P. Germann (2013). 'Macropores and water flow in soils revisited'. In: *Water Resources Research* 49.6, pp. 3071–3092. DOI: 10.1002/wrcr.20156.

Blair, N., R. Faulkner, A. Till and P. Poulton (2006). 'Long-term management impacts on soil C, N and physical fertility'. In: *Soil and Tillage Research* 91.1-2, pp. 30–38. DOI: 10.1016/j.still.2005.11.002.

Blöschl, G. and M. Sivapalan (1995). 'Scale issues in hydrological modelling: A review'. In: *Hydrological Processes* 9.3-4, pp. 251–290. DOI: 10.1002/hyp.3360090305.

Bodner, G., A. Nakhforoosh and H.-P. Kaul (2015). 'Management of crop water under drought: a review'. In: *Agronomy for Sustainable Development* 35.2, pp. 401–442. DOI: 10.1007/s13593-015-0283-4.

Bogena, H. R., A. Weuthen and J. A. Huisman (2022). 'Recent Developments in Wireless Soil Moisture Sensing to Support Scientific Research and Agricultural Management'. In: *Sensors* 22.24, p. 9792. DOI: 10.3390/s22249792.

Bogie, N. A., R. Bayala, I. Diedhiou, R. P. Dick and T. A. Ghezzehei (2018). 'Alteration of soil physical properties and processes after ten years of intercropping with native shrubs in the Sahel'. In: *Soil and Tillage Research* 182, pp. 153–163. DOI: 10.1016/j.still.2018.05.010.

Bohn Reckziegel, R., E. Larysch, J. P. Sheppard, H.-P. Kahle and C. Morhart (2021). 'Modelling and Comparing Shading Effects of 3D Tree Structures with Virtual Leaves'. In: *Remote Sensing* 13.3, p. 532. DOI: 10.3390/rs13030532.

Bohn Reckziegel, R., J. P. Sheppard, H.-P. Kahle, E. Larysch, H. Spiecker, T. Seifert and C. Morhart (2022). 'Virtual pruning of 3D trees as a tool for managing shading effects in agroforestry systems'. In: *Agroforestry Systems* 96.1, pp. 89–104. DOI: 10.1007/s10457-021-00697-5.

Bréda, N. J. J. (2008). 'Leaf Area Index'. In: *General Ecology: Encyclopedia of ecology*. Ed. by S. E. Jorgensen and B. D. Fath. Vol. 3. Oxford: Elsevier, pp. 2148–2154.

Bronick, C. and R. Lal (2005). 'Soil structure and management: a review'. In: *Geoderma* 124.1-2, pp. 3–22. DOI: 10.1016/j.geoderma.2004.03.005.

Brown, P and A Young (1965). *The physical environment of Central Malawi with special reference to soils and agriculture*. Zomba: Govt Printer.

Bruzzese, E (1998). 'The biology of blackberry in south-eastern Australia'. In: *Plant Protection Quarterly* 13.4, pp. 160–162.

Budyko, M. I. (1974). *Climate and life*. Orlando, FL: Academic Press, p. 508.

Burgess, P. J. and A. Rosati (2018). 'Advances in European agroforestry: results from the AGFORWARD project'. In: *Agroforestry Systems* 92.4, pp. 801–810. DOI: 10.1007/s10457-018-0261-3.

Burgess, P., A. Graves, S. G. de Jalón, J. Palma, C. Dupraz and M. van Noordwijk (2019). 'Modelling agroforestry systems'. In: June, pp. 209–238. DOI: 10.19103/as.2018.0041.13.

Burgess, S. S. O. (2011). 'Can hydraulic redistribution put bread on our table?' In: *Plant and Soil* 341.1-2, pp. 25–29. DOI: 10.1007/s11104-010-0638-1.

Burgess, S. S. O., M. A. Adams, N. C. Turner and C. K. Ong (1998). 'The redistribution of soil water by tree root systems'. In: *Oecologia* 115.3, pp. 306–311. DOI: 10.1007/s004420050521.

Calders, K., G. Newnham, A. Burt, S. Murphy, P. Raumonen, M. Herold, D. Culvenor, V. Avitabile, M. Disney, J. Armston and M. Kaasalainen (2015). 'Nondestructive estimates of above-ground biomass using terrestrial laser scanning'. In: *Methods in Ecology and Evolution* 6.2, pp. 198–208. DOI: 10.1111/2041-210X.12301.

Campi, P., A. Palumbo and M. Mastrorilli (2009). 'Effects of tree windbreak on microclimate and wheat productivity in a Mediterranean environment'. In: *European Journal of Agronomy* 30.3, pp. 220–227. DOI: 10.1016/j.eja.2008.10.004.

Castellano, M. J., K. E. Mueller, D. C. Olk, J. E. Sawyer and J. Six (2015). 'Integrating plant litter quality, soil organic matter stabilization, and the carbon saturation concept'. In: *Global Change Biology* 21.9, pp. 3200–3209. DOI: 10.1111/gcb.12982.

Celia, M. A., E. T. Bouloutas and R. L. Zarba (1990). 'A general mass-conservative numerical solution for the unsaturated flow equation'. In: *Water Resources Research* 26.7, pp. 1483–1496. DOI: 10.1029/WR026i007p01483.

Chagas Torres, L., T. Keller, R. Paiva de Lima, C. Antônio Tormena, H. Veras de Lima and N. Fabíola Balazero Giarola (2021). 'Impacts of soil type and crop species on permanent wilting of plants'. In: *Geoderma* 384, p. 114798. DOI: https://doi.org/10.1016/j.geoderma.2020.114798.

Chaplot, V. and M. Cooper (2015). 'Soil aggregate stability to predict organic carbon outputs from soils'. In: *Geoderma* 243-244, pp. 205–213. DOI: 10.1016/j.geoderma.2014.12.013.

Cherlet, M., C. Hutchinson, J. Reynolds, J. Hill, S. Sommer and G. von Maltitz (Eds.) (2018). *World Atlas of Desertification*. Luxembourg: Publication Office of the European Union. DOI: 10.2760/06292.

Chirwa, P. W., C. R. Black, C. K. Ong and J. A. Maghembe (2003). 'Tree and crop productivity in gliricidia/maize/pigeonpea cropping systems in southern Malawi'. In: *Agroforestry Systems* 59.3, pp. 265–277. DOI: 10.1023/B:AGFO.0000005227.69260.f9.

Chirwa, P. W., P. K. R. Nair and P. Nkedi-Kizza (1994). 'Pattern of soil moisture depletion in alley cropping under semiarid conditions in Zambia'. In: *Agroforestry Systems* 26.2, pp. 89–99. DOI: 10.1007/BF00707008.

Chirwa, P. W., C. K. Ong, J. Maghembe and C. R. Black (2007). 'Soil water dynamics in cropping systems containing Gliricidia sepium, pigeonpea and maize in southern Malawi'. In: *Agroforestry Systems* 69.1, pp. 29–43. DOI: 10.1007/s10457-006-9016-7.

Claessens, H., A. Oosterbaan, P. Savill and J. Rondeux (2010). 'A review of the characteristics of black alder (Alnus glutinosa (L.) Gaertn.) and their implications for silvicultural practices'. In: *Forestry* 83.2, pp. 163–175. DOI: 10.1093/forestry/cpp038.

Cleugh, H. A. (1998). 'Effects of windbreaks on airflow, microclimates and crop yields'. In: *Agroforestry Systems* 41.1, pp. 55–84. DOI: 10.1023/A:1006019805109.

Climate-Data.org (2024). *Stellenbosch Climate (South Africa)*. URL: https://de.climate-data.org/africa/south-africa/western-cape/stellenbosch-6770/ (visited on 24/01/2022).

DIN EN ISO 17892-1:2022-08 (2022). *DIN EN ISO 17892-1:2022-08, Geotechnische Erkundung und Untersuchung - Laborversuche an Bodenproben - Teil 1: Bestimmung des Wassergehalts (ISO 17892-1:2014+ Amd 1:2022); Deutsche Fassung EN ISO 17892-1:2014 + A1:2022*. DOI: 10.31030/3364115.

Dalland, A., P. I. Våje, R. B. Matthews and B. R. Singh (1993). 'The potential of alley cropping in improvement of cultivation systems in the high rainfall areas of Zambia. III. Effects on soil chemical and physical properties'. In: *Agroforestry Systems* 21.2, pp. 117–132. DOI: 10.1007/BF00705224.

Davis, S. D. and H. A. Mooney (1986). 'Water use patterns of four co-occurring chaparral shrubs'. In: *Oecologia* 70.2, pp. 172–177. DOI: 10.1007/BF00379236.

De Schutter, O. (2012). 'Agroecology, a tool for the realization of the right to food'. In: *Agroecology and Strategies for Climate Change*. Ed. by E. Lichtfouse. Dordrecht, The Netherlands: Springer, pp. 1–16.

Dearing, J. A., A. K. Braimoh, A. Reenberg, B. L. Turner and S. van der Leeuw (2010). 'Complex Land Systems: the Need for Long Time Perspectives to Assess their Future'. In: *Ecology and Society* 15.4. DOI: 10.5751/ES-03645-150421.

Demir, G., A. J. Guswa, J. Filipzik, J. C. Metzger, C. Römermann and A. Hildebrandt (2024). 'Root water uptake patterns are controlled by tree species interactions and soil water variability'. In: *Hydrology and Earth System Sciences* 28.6, pp. 1441–1461. DOI: 10.5194/hess-28-1441-2024.

Dettmann, U., M. Bechtold, T. Viohl, A. Piayda, L. Sokolowsky and B. Tiemeyer (2019). 'Evaporation experiments for the determination of hydraulic properties of peat and other organic soils: An evaluation of methods based on a large dataset'. In: *Journal of Hydrology* 575.May, pp. 933–944. DOI: 10.1016/j.jhydrol.2019.05.088.

Dingman, S. L. (2015). *Physical Hydrology*. Third. Long Grove, Illinois: Waveland Pr Inc, p. 643.

Dixon, J., A. Gulliver and D. Gibbon (2001). *Farming systems and poverty: Improving farmers' livelihoods in a changing world*. Ed. by M. Hall. Rome and Washington D.C.: Food & Agriculture Organization of the United Nations (FAO).

Dold, C., A. L. Thomas, A. J. Ashworth, D. Philipp, D. K. Brauer and T. J. Sauer (2019). 'Carbon sequestration and nitrogen uptake in a temperate silvopasture system'. In: *Nutrient Cycling in Agroecosystems* 114.1, pp. 85–98. DOI: 10.1007/s10705-019-09987-y.

Domec, J.-C., J. M. Warren, F. C. Meinzer, J. R. Brooks and R. Coulombe (2004). 'Native root xylem embolism and stomatal closure in stands of Douglas-fir and ponderosa pine: mitigation by hydraulic redistribution'. In: *Oecologia* 141.1, pp. 7–16. DOI: 10.1007/s00442-004-1621-4.

Douville, H., K. Raghavan, J. Renwick, R. Allan, P. Arias, M. Barlow, R. Cerezo-Mota, A. Cherchi, T. Gan, J. Gergis, D. Jiang, A. Khan, W. Pokam Mba, D. Rosenfeld, J. Tierney and O. Zolina (2021). 'Water Cycle Changes'. In: *Climate Change 2021 – The Physical Science Basis. Contribution of Working Group I to the Sixth Assessment Report of the Intergovernmental Panel on Climate Change*. Ed. by V. Masson-Delmotte, P. Zhai, A. Pirani, S. Connors, C. Péan, S. Berger, N. Caud, Y. Chen, L. Goldfarb, M. Gomis, M. Huang, K. Leitzell, E. Lonnoy, J. Matthews, T. Maycock, T. Waterfield, O. Yelekçi, R. Yu and B. Zhou. Cambridge, United Kingdom and New York, NY, USA: Cambridge University Press, pp. 1055–1210. DOI: 10.1017/9781009157896.010.

Dugas, W., M. Heuer, D. Hunsaker, B. Kimball, K. Lewin, J. Nagy and M. Johnson (1994). 'Sap flow measurements of transpiration from cotton grown under ambient and enriched CO2 concentrations'. In: *Agricultural and Forest Meteorology* 70.1-4, pp. 231–245. DOI: 10.1016/0168-1923(94)90060-4.

Durner, W., K. Germer, C. Jackisch, I. Andrä, K. Schulz, M. Schiedung, J. Haller-Jans, J. Schneider, J. Jaquemotte, P. Helmer, L. Lotz, T. Gräff, A. Bauer, I. Hahn, M. Sanda, M. Kumpan, J. Dorner, G. de Rooij, S. Wessel-Bothe, L. Kottmann and S. Schittenhelm (2017). 'Feldstudie zur Bodenfeuchtesensorik'. In: *17. Gumpensteiner Lysimetertagung : Lysimeterforschung - Möglichkeiten und Grenzen ; 09. und 10. Mai 2017 HBLFA Raumberg-Gumpenstein ; Bericht*, pp. 227–234.

Dyck, S. and G. Peschke (1995). *Grundlagen der Hydrologie*. 3., stark bearb. Aufl. Literaturangaben. Berlin: Verl. für Bauwesen.

Ehret, U. and E. Zehe (2011). 'Series distance – an intuitive metric to quantify hydrograph similarity in terms of occurrence, amplitude and timing of hydrological events'. In: *Hydrology and Earth System Sciences* 15.3, pp. 877–896. DOI: 10.5194/hess-15-877-2011.

Everson, C. S., T. M. Everson and W. van Niekerk (2009). 'Soil water competition in a temperate hedgerow agroforestry system in South

Africa'. In: *Agroforestry Systems* 75.3, pp. 211–221. DOI: 10.1007/s10457-008-9174-x.

Fan, Y., M. Clark, D. M. Lawrence, S. Swenson, L. E. Band, S. L. Brantley, P. D. Brooks, W. E. Dietrich, A. Flores, G. Grant, J. W. Kirchner, D. S. Mackay, J. J. McDonnell, P. C. D. Milly, P. L. Sullivan, C. Tague, H. Ajami, N. Chaney, A. Hartmann, P. Hazenberg, J. McNamara, J. Pelletier, J. Perket, E. Rouholahnejad-Freund, T. Wagener, X. Zeng, E. Beighley, J. Buzan, M. Huang, B. Livneh, B. P. Mohanty, B. Nijssen, M. Safeeq, C. Shen, W. van Verseveld, J. Volk and D. Yamazaki (2019). 'Hillslope Hydrology in Global Change Research and Earth System Modeling'. In: *Water Resources Research* 55.2, pp. 1737–1772. DOI: 10.1029/2018WR023903.

Fauchereau, N., S. Trzaska, M. Rouault and Y. Richard (2003). 'Rainfall variability and changes in Southern Africa during the 20th century in the global warming context'. In: *Natural Hazards* 29.2, pp. 139–154. DOI: 10.1023/A:1023630924100.

Feifel, M., W. Durner, T. L. Hohenbrink and A. Peters (2024). 'Effects of improved water retention by increased soil organic matter on the water balance of arable soils: A numerical analysis'. In: *Vadose Zone Journal* 23.1, pp. 1–13. DOI: 10.1002/vzj2.20302.

Fischer-Bedtke, C., J. C. Metzger, G. Demir, T. Wutzler and A. Hildebrandt (2023). 'Throughfall spatial patterns translate into spatial patterns of soil moisture dynamics – empirical evidence'. In: *Hydrology and Earth System Sciences* 27.15, pp. 2899–2918. DOI: 10.5194/hess-27-2899-2023.

Fredlund, D., A. Xing and S. Huang (1994). 'Predicting the permeability function for unsaturated soils using the soil-water characteristic curve'. In: *Canadian Geotechnical Journal* 31.4, pp. 533–546. DOI: 10.1139/t94-062.

Freitas, E. M. de, T. N. B. Vital, G. F. C. Guimarães, F. A. da Silveira, C. N. Gomes and F. F. da Cunha (2023). 'Determination of the Permanent Wilting Point of Physalis peruviana L.' In: *Horticulturae* 9.8, p. 873. DOI: 10.3390/horticulturae9080873.

Frouz, J., P. Dvorščík, A. Vávrová, O. Doušová, Š. Kadochová and L. Matějíček (2015). 'Development of canopy cover and woody vegetation biomass on reclaimed and unreclaimed post-mining sites'. In: *Ecological Engineering* 84, pp. 233–239. DOI: 10.1016/j.ecoleng.2015.09.027.

Fu, T., H. Chen, W. Zhang, Y. Nie, P. Gao and K. Wang (2015). 'Spatial variability of surface soil saturated hydraulic conductivity in a small karst catchment of southwest China'. In: *Environmental Earth Sciences* 74.3, pp. 2381–2391. DOI: 10.1007/s12665-015-4238-5.

Gaiser, T., K. Stahr, M. Bernard and B. T. Kang (2012). 'Changes in soil organic carbon fractions in a tropical Acrisol as influenced by the addition of different residue materials'. In: *Agroforestry Systems* 86.2, pp. 185–195. DOI: 10.1007/s10457-011-9417-0.

García-Orenes, F., C. Guerrero, J. Mataix-Solera, J. Navarro-Pedreño, I. Gómez and J. Mataix-Beneyto (2005). 'Factors controlling the aggregate stability and bulk density in two different degraded soils amended with biosolids'. In: *Soil and Tillage Research* 82.1, pp. 65–76. DOI: 10.1016/j.still.2004.06.004.

Garg, A., S. Bordoloi, S. P. Ganesan, S. Sekharan and L. Sahoo (2020). 'A relook into plant wilting: observational evidence based on unsaturated soil–plant-photosynthesis interaction'. In: *Scientific Reports* 10.1, pp. 1–15. DOI: 10.1038/s41598-020-78893-z.

Ghausi, S. A., Y. Tian, E. Zehe and A. Kleidon (2023). 'Radiative controls by clouds and thermodynamics shape surface temperatures and turbulent fluxes over land'. In: *Proceedings of the National Academy of Sciences* 120.29. DOI: 10.1073/pnas.2220400120.

Golchin, A., J. Baldock, P. Clarke, T. Higashi and J. Oades (1997). 'The effects of vegetation and burning on the chemical composition of soil organic matter of a volcanic ash soil as shown by 13C NMR spectroscopy. II. Density fractions'. In: *Geoderma* 76.3-4, pp. 175–192. DOI: 10.1016/S0016-7061(96)00103-6.

Gómez-Delgado, F., O. Roupsard, G. Le Maire, S. Taugourdeau, A. Pérez, M. Van Oijen, P. Vaast, B. Rapidel, J. M. Harmand, M. Voltz, J. M. Bonnefond, P. Imbach and R. Moussa (2011). 'Modelling the hydrological behaviour of a coffee agroforestry basin in Costa Rica'. In: *Hydrology and Earth System Sciences* 15.1, pp. 369–392. DOI: 10.5194/hess-15-369-2011.

Graf-Rosenfellner, M., A. Cierjacks, B. Kleinschmit and F. Lang (2016). 'Soil formation and its implications for stabilization of soil organic matter in the riparian zone'. In: *CATENA* 139, pp. 9–18. DOI: 10.1016/j.catena.2015.11.010.

Graham, C. B. and H. S. Lin (2011). 'Controls and Frequency of Preferential Flow Occurrence: A 175-Event Analysis'. In: *Vadose Zone Journal* 10.3, pp. 816–831. DOI: 10.2136/vzj2010.0119.

Granier, A. and D Loustau (1994). 'Measuring and modelling the transpiration of a maritime pine canopy from sap-flow data'. In: *Agricultural and Forest Meteorology* 71.1-2, pp. 61–81. DOI: 10.1016/0168-1923(94)90100-7.

Groenevelt, P. H., C. D. Grant and S. Semetsa (2001). 'A new procedure to determine soil water availability'. In: *Soil Research* 39.3, p. 577. DOI: 10.1071/SR99084.

Guderle, M. and A. Hildebrandt (2015). 'Using measured soil water contents to estimate evapotranspiration and root water uptake profiles – a comparative study'. In: *Hydrology and Earth System Sciences* 19.1, pp. 409–425. DOI: 10.5194/hess-19-409-2015.

Guderle, M., D. Bachmann, A. Milcu, A. Gockele, M. Bechmann, C. Fischer, C. Roscher, D. Landais, O. Ravel, S. Devidal, J. Roy, A. Gessler, N. Buchmann, A. Weigelt and A. Hildebrandt (2018). 'Dynamic niche partitioning in root water uptake facilitates efficient

water use in more diverse grassland plant communities'. In: *Functional Ecology* 32.1. Ed. by K. Field, pp. 214–227. DOI: 10.1111/1365-2435.12948.

Guest, G., R. M. Bright, F. Cherubini and A. H. Strømman (2013). 'Consistent quantification of climate impacts due to biogenic carbon storage across a range of bio-product systems'. In: *Environmental Impact Assessment Review* 43, pp. 21–30. DOI: 10.1016/j.eiar.2013.05.002.

Guswa, A. J., D. Tetzlaff, J. S. Selker, D. E. Carlyle-Moses, E. W. Boyer, M. Bruen, C. Cayuela, I. F. Creed, N. van de Giesen, D. Grasso, D. M. Hannah, J. E. Hudson, S. A. Hudson, S. Iida, R. B. Jackson, G. G. Katul, T. Kumagai, P. Llorens, F. Lopes Ribeiro, B. Michalzik, K. Nanko, C. Oster, D. E. Pataki, C. A. Peters, A. Rinaldo, D. Sanchez Carretero, B. Trifunovic, M. Zalewski, M. Haagsma and D. F. Levia (2020). 'Advancing ecohydrology in the 21st century: A convergence of opportunities'. In: *Ecohydrology* 13.4, pp. 1–14. DOI: 10.1002/eco.2208.

Häckel, H. (1999). *Farbatlas Wetterphänomene*. Eugen Ulmer.

Hanegraaf, M. C., E. Hoffland, P. J. Kuikman and L. Brussaard (2009). 'Trends in soil organic matter contents in Dutch grasslands and maize fields on sandy soils'. In: *European Journal of Soil Science* 60.2, pp. 213–222. DOI: 10.1111/j.1365-2389.2008.01115.x.

Hartge, K. H. and R. Horn (2009). *Die physikalische Untersuchung von Böden*. Stuttgart, Germany: E. Schweizerbart'sche Verlagsbuchhandlung.

Hassler, S. K., R. Bohn Reckziegel, B. du Toit, S. Hoffmeister, F. Kestel, A. Kunneke, R. Maier and J. P. Sheppard (2024a). 'Hydrological, pedological, dendrological and meteorological measurements in a blackberry-alder agroforestry system in South Africa'. In: *GFZ Data Services*. DOI: https://doi.org/10.5880/fidgeo.2023.028.

Hassler, S. K., R. Bohn Reckziegel, B. du Toit, S. Hoffmeister, F. Kestel, A. Kunneke, R. Maier and J. P. Sheppard (2024b). 'Multivariate characterisation of a blackberry–alder agroforestry system in South Africa: hydrological, pedological, dendrological and meteorological measurements'. In: *Earth System Science Data* 16.9, pp. 3935–3948. DOI: 10.5194/essd-16-3935-2024.

Hassler, S. K., M. Weiler and T. Blume (2018). 'Tree-, stand- and site-specific controls on landscape-scale patterns of transpiration'. In: *Hydrology and Earth System Sciences* 22.1, pp. 13–30. DOI: 10.5194/hess-22-13-2018.

Herbst, M., C. Eschenbach and L. Kappen (1999). 'Water use in neighbouring stands of beech (Fagus sylvatica L.) and black alder (Alnus glutinosa (L.) Gaertn.)' In: *Annals of Forest Science* 56.2, pp. 107–120. DOI: 10.1051/forest:19990203.

Hildebrandt, A. and E. A. B. Eltahir (2007). 'Ecohydrology of a seasonal cloud forest in Dhofar: 2. Role of clouds, soil type, and rooting

depth in tree-grass competition'. In: *Water Resources Research* 43.11, pp. 1–13. DOI: 10.1029/2006WR005262.

Hillel, D. (2004). *Introduction to environmental soil physics*. Amsterdam: Elsevier Acad. Press.

Hintermaier-Erhard, G. and W. Zech (1997). *Wörterbuch der Bodenkunde*. Stuttgart: Enke.

Hoffmeister, S., R. Bohn Reckziegel, B. du Toit, S. K. Hassler, F. Kestel, R. Maier, J. P. Sheppard and E. Zehe (2024). 'Hydrological and pedological effects of combining Italian alder and blackberries in an agroforestry windbreak system in South Africa'. In: *Hydrology and Earth System Sciences* 28.17, pp. 3963–3982. DOI: 10.5194/hess-28-3963-2024.

Hohenegger, C. and B. Stevens (2018). 'The role of the permanent wilting point in controlling the spatial distribution of precipitation'. In: *Proceedings of the National Academy of Sciences* 115.22, pp. 5692–5697. DOI: 10.1073/pnas.1718842115.

Hopp, L., C. Harman, S. L. E. Desilets, C. B. Graham, J. J. McDonnell and P. A. Troch (2009). 'Hillslope hydrology under glass: confronting fundamental questions of soil-water-biota co-evolution at Biosphere 2'. In: *Hydrology and Earth System Sciences* 13.11, pp. 2105–2118. DOI: 10.5194/hess-13-2105-2009.

Hsieh, J. J. C., W. H. Gardner and G. S. Campbell (1972). 'Experimental Control of Soil Water Content in the Vicinity of Root Hairs'. In: *Soil Science Society of America Journal* 36.3, pp. 418–421. DOI: 10.2136/sssaj1972.03615995003600030017x.

Hsu, H., P. A. Dirmeyer and E. Seo (2024). 'Exploring the Mechanisms of the Soil Moisture-Air Temperature Hypersensitive Coupling Regime'. In: *Water Resources Research* 60.7, pp. 1–12. DOI: 10.1029/2023WR036490.

ISO 11277:2002 (2002). *Soil quality — Determination of particle size distribution in mineral soil material — Method by sieving and sedimentation — Technical Corrigendum 1*.

IUSS Working Group WRB (2022). *World Reference Base for Soil Resources. International soil classification system for naming soils and creating legends for soil maps*. Vienna, Austria.

IUSS Working Group (2014). *World Reference Base for Soil Resources. World Soil Resources Reports 106*, pp. 1–191.

Ikerra, S. T., J. A. Maghembe, P. C. Smithson and R. J. Buresh (2001). 'Dry-season sesbania fallows and their influence on nitrogen availability and maize yields in Malawi'. In: *Agroforestry Systems* 52.1, pp. 13–21. DOI: 10.1023/A:1010772520991.

Ikerra, S. T., J. A. Maghembe, P. C. Smithson and R. J. Buresh (1999). 'Soil nitrogen dynamics and relationships with maize yields in a gliricidia-maize intercrop in Malawi'. In: *Plant and Soil* 211.2, pp. 155–164. DOI: 10.1023/A:1004636501488.

Iwasaki, S., Y. Endo and R. Hatano (2017). 'The effect of organic matter application on carbon sequestration and soil fertility in upland fields of different types of Andosols'. In: *Soil Science and Plant Nutrition* 63.2, pp. 200–220. DOI: 10.1080/00380768.2017.1309255.

Jackisch, C., L. Angermann, N. Allroggen, M. Sprenger, T. Blume, J. Tronicke and E. Zehe (2017). 'Form and function in hillslope hydrology: In situ imaging and characterization of flow-relevant structures'. In: *Hydrology and Earth System Sciences* 21.7, pp. 3749–3775. DOI: 10.5194/hess-21-3749-2017.

Jackisch, C., S. Knoblauch, T. Blume, E. Zehe and S. K. Hassler (2020). 'Estimates of tree root water uptake from soil moisture profile dynamics'. In: *Biogeosciences* 17.22, pp. 5787–5808. DOI: 10.5194/bg-17-5787-2020.

Jackson, R. B., K. Lajtha, S. E. Crow, G. Hugelius, M. G. Kramer and G. Piñeiro (2017). 'The Ecology of Soil Carbon: Pools, Vulnerabilities, and Biotic and Abiotic Controls'. In: *Annual Review of Ecology, Evolution, and Systematics* 48.1, pp. 419–445. DOI: 10.1146/annurev-ecolsys-112414-054234.

Jacobs, S. R., H. Webber, W. Niether, K. Grahmann, D. Lüttschwager, C. Schwartz, L. Breuer and S. D. Bellingrath-Kimura (2022). 'Modification of the microclimate and water balance through the integration of trees into temperate cropping systems'. In: *Agricultural and Forest Meteorology* 323, p. 109065. DOI: https://doi.org/10.1016/j.agrformet.2022.109065.

Jahn, R., H. Blume, V. Asio, O. Spaargaren and P. Schád (2006). *Guidelines for soil description*. Tech. rep. Rome, Italy: FAO.

Jarvis, N. J. (2007). 'A review of non-equilibrium water flow and solute transport in soil macropores: principles, controlling factors and consequences for water quality'. In: *European Journal of Soil Science* 58.3, pp. 523–546. DOI: 10.1111/j.1365-2389.2007.00915.x.

Jarvis, N. (1989). 'A simple empirical model of root water uptake'. In: *Journal of Hydrology* 107.1-4, pp. 57–72. DOI: 10.1016/0022-1694(89)90050-4.

Jarvis, P. G. (1976). 'The interpretation of the variations in leaf water potential and stomatal conductance found in canopies in the field'. In: *Philosophical Transactions of the Royal Society of London. B, Biological Sciences* 273.927, pp. 593–610. DOI: 10.1098/rstb.1976.0035.

Johansson, T. (1999). 'Dry matter amounts and increment in 21- to 91-year-old common alder and grey alder and some practical implications'. In: *Canadian Journal of Forest Research* 29.11, pp. 1679–1690. DOI: 10.1139/x99-126.

Jose, S. (2009). 'Agroforestry for ecosystem services and environmental benefits: an overview'. In: *Agroforestry Systems* 76.1, pp. 1–10. DOI: 10.1007/s10457-009-9229-7.

Kantorovich, L. V. (1960). 'Mathematical Methods of Organizing and Planning Production'. In: *Management Science* 6, pp. 366–422.

Kay, S., J. Crous-Duran, S. García de Jalón, A. Graves, J. H. Palma, J. V. Roces-Díaz, E. Szerencsits, R. Weibel and F. Herzog (2018). 'Landscape-scale modelling of agroforestry ecosystems services in Swiss orchards: a methodological approach'. In: *Landscape Ecology* 33.9, pp. 1633–1644. DOI: 10.1007/s10980-018-0691-3.

Kerr, A. (2012). 'Drought resilience of maize-legume agroforestry systems in Malawi'. PhD thesis. UC Berkeley Electron.

Kirsten, M., R. Mikutta, C. Vogel, A. Thompson, C. W. Mueller, D. N. Kimaro, H. L. Bergsma, K. H. Feger and K. Kalbitz (2021). 'Iron oxides and aluminous clays selectively control soil carbon storage and stability in the humid tropics'. In: *Scientific Reports* 11.1, pp. 1–12. DOI: 10.1038/s41598-021-84777-7.

Klaus, J. and E. Zehe (2011). 'A novel explicit approach to model bromide and pesticide transport in connected soil structures'. In: *Hydrology and Earth System Sciences* 15.7, pp. 2127–2144. DOI: 10.5194/hess-15-2127-2011.

Klaus, J. and E. Zehe (2010). 'Modelling rapid flow response of a tile-drained field site using a 2D physically based model: assessment of 'equifinal' model setups'. In: *Hydrological Processes* 24.12, pp. 1595–1609. DOI: 10.1002/hyp.7687.

Korwar, G. R. and G. D. Radder (1994). 'Influence of root pruning and cutting interval ofLeucaena hedgerows on performance of alley croppedrabi sorghum'. In: *Agroforestry Systems* 25.2, pp. 95–109. DOI: 10.1007/BF00705670.

Kosugi, K. (1996). 'Lognormal Distribution Model for Unsaturated Soil Hydraulic Properties'. In: *Water Resources Research* 32.9, pp. 2697–2703. DOI: 10.1029/96WR01776.

Kuyah, S., C. W. Whitney, M. Jonsson, G. W. Sileshi, I. Öborn, C. W. Muthuri and E. Luedeling (2019). 'Agroforestry delivers a win-win solution for ecosystem services in sub-Saharan Africa. A meta-analysis'. In: *Agronomy for Sustainable Development* 39.5. DOI: 10.1007/s13593-019-0589-8.

Kwesiga, F., F. K. Akinnifesi, P. L. Mafongoya, M. H. McDermott and A. Agumya (2003). 'Agroforestry research and development in southern Africa during the 1990s: Review and challenges ahead'. In: *Agroforestry Systems* 59.3, pp. 173–186. DOI: 10.1023/B:AGFO.0000005222.68054.38.

Lado, M., A. Paz and M. Ben-Hur (2004). 'Organic Matter and Aggregate-Size Interactions in Saturated Hydraulic Conductivity'. In: *Soil Science Society of America Journal* 68.1, pp. 234–242. DOI: 10.2136/sssaj2004.2340.

Lal, R. (2020). 'Soil organic matter and water retention'. In: *Agronomy Journal* 112.5, pp. 3265–3277. DOI: 10.1002/agj2.20282.

Lal, R., J. Bouma, E. Brevik, L. Dawson, D. J. Field, B. Glaser, R. Hatano, A. E. Hartemink, T. Kosaki, B. Lascelles, C. Monger, C. Muggler, G. M. Ndzana, S. Norra, X. Pan, R. Paradelo, L. B. Reyes-Sánchez, T. Sandén, B. R. Singh, H. Spiegel, J. Yanai and J. Zhang (2021). 'Soils and sustainable development goals of the United Nations: An International Union of Soil Sciences perspective'. In: *Geoderma Regional* 25, e00398. DOI: 10.1016/j.geodrs.2021.e00398.

Leakey, R. R. (1996). 'Definition of Agroforestry Revisited'. In: *Agrofor. Today* 8.5. DOI: 10.1016/B978-0-12-805356-0.00001-5.

Leffler, A. J., M. S. Peek, R. J. Ryel, C. Y. Ivans and M. M. Caldwell (2005). 'Hydraulic redistribution through the root system of senesced plants'. In: *Ecology* 86.3, pp. 633–642. DOI: 10.1890/04-0854.

Littmann, T. and M. Veste (2008). 'Evapotranspiration, transpiration and dewfall'. In: *Arid Dune Ecosystems: The Nizzana Sands in the Negev Desert*. Ed. by S.-W. Breckle, A. Yair and M. Veste. Berlin/Heidelberg, Germany: Springer, pp. 183–200.

Loritz, R., M. Bassiouni, A. Hildebrandt, S. K. Hassler and E. Zehe (2022). 'Leveraging sap flow data in a catchment-scale hybrid model to improve soil moisture and transpiration estimates'. In: *Hydrology and Earth System Sciences* 26.18, pp. 4757–4771. DOI: 10.5194/hess-26-4757-2022.

Loritz, R., S. K. Hassler, C. Jackisch, N. Allroggen, L. Van Schaik, J. Wienhöfer and E. Zehe (2017). 'Picturing and modeling catchments by representative hillslopes'. In: *Hydrology and Earth System Sciences* 21.2, pp. 1225–1249. DOI: 10.5194/hess-21-1225-2017.

Loritz, R., M. Hrachowitz, M. Neuper and E. Zehe (2021). 'The role and value of distributed precipitation data in hydrological models'. In: *Hydrology and Earth System Sciences* 25.1, pp. 147–167. DOI: 10.5194/hess-25-147-2021.

Lützow, M. V., I. Kögel-Knabner, K. Ekschmitt, E. Matzner, G. Guggenberger, B. Marschner and H. Flessa (2006). 'Stabilization of organic matter in temperate soils: mechanisms and their relevance under different soil conditions – a review'. In: *European Journal of Soil Science* 57.4, pp. 426–445. DOI: 10.1111/j.1365-2389.2006.00809.x.

Maier, R., H. Schack-Kirchner, B. I. Nyoka and F. Lang (2023). 'Gliricidia intercropping supports soil organic matter stabilization at Makoka Research Station, Malawi'. In: *Geoderma Regional* 35, e00730. DOI: 10.1016/j.geodrs.2023.e00730.

Makate, C., M. Makate, N. Mango and S. Siziba (2019). 'Increasing resilience of smallholder farmers to climate change through multiple adoption of proven climate-smart agriculture innovations. Lessons from Southern Africa'. In: *Journal of Environmental Management* 231.August 2018, pp. 858–868. DOI: 10.1016/j.jenvman.2018.10.069.

Makumba, W., F. K. Akinnifesi and B. H. Janssen (2009). 'Spatial rooting patterns of gliricidia, pigeon pea and maize intercrops

and effect on profile soil N and P distribution in southern Malawi'. In: *African Journal of Agricultural Research* 4.4, pp. 278–288.

Makumba, W., F. K. Akinnifesi, B. Janssen and O. Oenema (2007). 'Long-term impact of a gliricidia-maize intercropping system on carbon sequestration in southern Malawi'. In: *Agriculture, Ecosystems & Environment* 118.1-4, pp. 237–243. DOI: 10.1016/j.agee.2006.05.011.

Makumba, W., B. Janssen, O. Oenema, F. K. Akinnifesi, D. Mweta and F. Kwesiga (2006). 'The long-term effects of a gliricidia–maize intercropping system in Southern Malawi, on gliricidia and maize yields, and soil properties'. In: *Agriculture, Ecosystems & Environment* 116.1-2, pp. 85–92. DOI: 10.1016/j.agee.2006.03.012.

Mälicke, M., S. K. Hassler, T. Blume, M. Weiler and E. Zehe (2020). 'Soil moisture: Variable in space but redundant in time'. In: *Hydrology and Earth System Sciences* 24.5, pp. 2633–2653. DOI: 10.5194/hess-24-2633-2020.

Malunga, I., J. J. Lelei and W. Makumba (2017). 'Effect of Mineral Nitrogen and Legume Intercrops on Maize (Zea Mays L.) Nitrogen Uptake, Nutrient Use Efficiency and Yields in Chitedze and Zomba, Malawi'. In: *Sustainable Agriculture Research* 7.1, p. 64. DOI: 10.5539/sar.v7n1p64.

Manoj J, A., R. Loritz, F. Villinger, M. Mälicke, M. Koopaeidar, H. Göppert and E. Zehe (2024). 'Toward Flash Flood Modeling Using Gradient Resolving Representative Hillslopes'. In: *Water Resources Research* 60.6. DOI: 10.1029/2023WR036420.

Maurer, T. (1997). 'Physikalisch begründete zeitkontinuierliche Modellierung des Wassertransports in kleinen ländlichen Einzugsgebieten.' PhD thesis. Karlsruhe Institute of Technology. DOI: https://doi.org/10.5445/IR/65797.

Mayer, S., M. Wiesmeier, E. Sakamoto, R. Hübner, R. Cardinael, A. Kühnel and I. Kögel-Knabner (2022). 'Soil organic carbon sequestration in temperate agroforestry systems – A meta-analysis'. In: *Agriculture, Ecosystems & Environment* 323, p. 107689. DOI: 10.1016/j.agee.2021.107689.

Mbow, C., C. Rosenzweig, L. G. Barioni, T. G. Benton, M. Herrero, M. Krishnapillai, E. Liwenga, P. Pradhan, M. G. Rivera-Ferre, T. Sapkota, F. N. Tubiello and Y. Xu (2019). 'Food security'. In: *Climate Change and Land: an IPCC special report on climate change, desertification, land degradation, sustainable land management, food security, and greenhouse gas fluxes in terrestrial ecosystems*. Ed. by P. Shukla, J. Skea, E. C. Buendia, V. Masson-Delmotte, H.-O. Pörtner, D. Roberts, P. Zhai, R. Slade, S. Connors, R. van Diemen, M. Ferrat, E. Haughey, S. Luz, S. Neogi, M. Pathak, J. Petzold, J. Portugal Pereira, P. Vyas, E. Huntley, K. Kissick, M. Belkacemi and J. Malley. DOI: 10.1017/9781009157988.007.

Mbow, C., M. Van Noordwijk, E. Luedeling, H. Neufeldt, P. A. Minang and G. Kowero (2014). 'Agroforestry solutions to address food security and climate change challenges in Africa'. In: *Current Opinion in Environmental Sustainability* 6.1, pp. 61–67. DOI: 10.1016/j.cosust.2013.10.014.

McMillan, H., B. Jackson, M. Clark, D. Kavetski and R. Woods (2011). 'Rainfall uncertainty in hydrological modelling: An evaluation of multiplicative error models'. In: *Journal of Hydrology* 400.1-2, pp. 83–94. DOI: 10.1016/j.jhydrol.2011.01.026.

McNaughton, K. (1988). 'Effects of windbreaks on turbulent transport and microclimate'. In: *Agriculture, Ecosystems & Environment* 22/23, pp. 17–39. DOI: 10.1016/0167-8809(88)90006-0.

Meadows, M. E. (2015). 'The Cape Winelands'. In: *Landscapes and Landforms of South Africa. World Geomorphological Landscapes*. Ed. by S. Grab and J. Knight. Springer, Cham., pp. 103–109. DOI: 10.1007/978-3-319-03560-4_12.

Mehra, O. P. and M. L. Jackson (1958). 'Iron Oxide Removal from Soils and Clays by a Dithionite-Citrate System Buffered with Sodium Bicarbonate'. In: *Clays and clay minerals (National Conference on Clays and Clay Minerals)* 7, 317–327. DOI: 10.1346/CCMN.1958.0070122.

Minasny, B. and A. B. McBratney (2018). 'Limited effect of organic matter on soil available water capacity'. In: *European Journal of Soil Science* 69.1, pp. 39–47. DOI: 10.1111/ejss.12475.

Montanarella, L., D. J. Pennock, N. McKenzie, M. Badraoui, V. Chude, I. Baptista, T. Mamo, M. Yemefack, M. S. Aulakh, K. Yagi, S. Y. Hong, P. Vijarnsorn, G. L. Zhang, D. Arrouays, H. Black, P. Krasilnikov, J. Sobocká, J. Alegre, C. R. Henriquez, M. d. L. Mendonça-Santos, M. Taboada, D. Espinosa-Victoria, A. AlShankiti, S. K. AlaviPanah, E. A. E. Mustafa Elsheikh, J. Hempel, M. C. Arbestain, F. Nachtergaele and R. Vargas (2016). 'World's soils are under threat'. In: *Soil* 2.1, pp. 79–82. DOI: 10.5194/soil-2-79-2016.

Mualem, Y. (1976). 'A new model for predicting the hydraulic conductivity of unsaturated porous media'. In: *Water Resources Research* 12.3, pp. 513–522. DOI: 10.1029/WR012i003p00513.

Muthuri, C. W., C. K. Ong, C. R. Black, B. M. Mati, V. W. Ngumi and M Van-Noordwijk (2004). 'Modelling the effects of leafing phenology on growth and water use by selected agroforestry tree species in semi-arid Kenya'. In: *Land Use and Water Resources Research* 4, pp. 1–11.

Mwangi, H. M., S. Julich, S. D. Patil, M. A. McDonald and K.-H. Feger (2016). 'Modelling the impact of agroforestry on hydrology of Mara River Basin in East Africa'. In: *Hydrological Processes* 30.18, pp. 3139–3155. DOI: 10.1002/hyp.10852.

Nabuurs, G., O. Masera, K. Andrasko, P. Benitez-Ponce, R. Boer, M. Dutschke, E. Elsiddig, J. Ford-Robertson, P. Frumhoff, T. Karjalainen, O. Krankina, W. Kurz, M. Matsumoto, W. Oyhantcabal,

N. Ravindranath, M. S. Sanchez and X. Zhang (2007). *Forestry*. Tech. rep. Cambridge, United Kingdom and New York, NY, USA.

Nabuurs, G.-J., R. Mrabet, A. Abu Hatab, M. Bustamante, H. Clark, P. Havlík, J. House, C. Mbow, K. Ninan, A. Popp, S. Roe, B. Sohngen and S. Towprayoon (2022). 'Agriculture, Forestry and Other Land Uses (AFOLU)'. In: *Climate Change 2022 - Mitigation of Climate Change. Contribution of Working Group III to the Sixth Assessment Report of the Intergovernmental Panel on Climate Change*. Ed. by P. Shukla, J. Skea, R. Slade, A. Al Khourdajie, R. van Diemen, D. McCollum, M. Pathak, S. Some, P. Vyas, R. Fradera, M. Belkacemi, A. Hasija, G. Lisboa, S. Luz and J. Malley. Cambridge, United Kingdom and New York, NY, USA: Cambridge University Press, pp. 747–860. DOI: 10.1017/9781009157926.009.

Nägeli, W. (1943). 'Untersuchungen über die Windverhältnisse im Bereich von Windschutzstreifen'. In: *Mitteilungen der Schweizerischen Anstalt für das forstliche Versuchswesen*. Ed. by H. Burger. Zürich: Beer, pp. 223–276.

Nair, P. K. R. (1993). *An introduction to agroforestry*. Kluwer Academic Publishers in cooperation with International Centre for Research in Agroforestry, p. 499.

Nair, P. K. R. (2012). 'Climate Change Mitigation: A Low-Hanging Fruit of Agroforestry'. In: *Agroforestry - The Future of Global Land Use. Advances in Agroforestry*. Ed. by P. Nair and D. Garrity. Vol. 9. Dordrecht: Springer, pp. 31–67. DOI: 10.1007/978-94-007-4676-3_7.

Nair, P. R. (2007). 'The coming of age of agroforestry'. In: *Journal of the Science of Food and Agriculture* 87.9, pp. 1613–1619. DOI: 10.1002/jsfa.2897.

Nash, J. E. and J. V. Sutcliffe (1970). 'River Flow Forecasting Through Conceptual Models Part I-a Discussion of Principles*'. In: *Journal of Hydrology* 10, pp. 282–290. DOI: 10.1016/0022-1694(70)90255-6. arXiv: arXiv:1011.1669v3.

Nazari, M., S. M. M. Sadeghi, J. T. Van Stan and M. R. Chaichi (2020). 'Rainfall interception and redistribution by maize farmland in central Iran'. In: *Journal of Hydrology: Regional Studies* 27, p. 100656. DOI: 10.1016/j.ejrh.2019.100656.

Ndebele, N. E., S. Grab and A. Turasie (2020). 'Characterizing rainfall in the south-western Cape, South Africa: 1841–2016'. In: *International Journal of Climatology* 40.4, pp. 1992–2014. DOI: 10.1002/joc.6314.

Nemes, A., W. J. Rawls and Y. A. Pachepsky (2005). 'Influence of Organic Matter on the Estimation of Saturated Hydraulic Conductivity'. In: *Soil Science Society of America Journal* 69.4, pp. 1330–1337. DOI: 10.2136/sssaj2004.0055.

Niang, I., O. Ruppel, M. Abdrabo, A. Essel, C. Lennard, J. Padgham and P. Urquhart (2014). 'Chapter 22 - Africa'. In: *Climate Change 2014: Impacts, Adaptation and Vulnerability - Contributions of the Work-*

ing Group II to the Fifth Assessment Report of the Intergovernmental Panel on Climate Change., pp. 1199–1265.

Nimmo, J. R. and K. C. Akstin (1988). 'Hydraulic Conductivity of a Sandy Soil at Low Water Content After Compaction by Various Methods'. In: *Soil Science Society of America Journal* 52.2, pp. 303–310. DOI: 10.2136/sssaj1988.03615995005200020001x.

Novick, K. A., D. L. Ficklin, D. Baldocchi, K. J. Davis, T. A. Ghezzehei, A. G. Konings, N. MacBean, N. Raoult, R. L. Scott, Y. Shi, B. N. Sulman and J. D. Wood (2022). 'Confronting the water potential information gap'. In: *Nature Geoscience* 15.3, pp. 158–164. DOI: 10.1038/s41561-022-00909-2.

Nygren, P., M. P. Fernández, J.-M. Harmand and H. A. Leblanc (2012). 'Symbiotic dinitrogen fixation by trees: an underestimated resource in agroforestry systems?' In: *Nutrient Cycling in Agroecosystems* 94.2-3, pp. 123–160. DOI: 10.1007/s10705-012-9542-9.

Odhiambo, H. O., C. K. Ong, J. D. Deans, J. Wilson, A. A. Khan and J. I. Sprent (2001). 'Roots, soil water and crop yield: Tree crop interactions in a semi-arid agroforestry system in Kenya'. In: *Plant and Soil* 235.2, pp. 221–233. DOI: 10.1023/A:1011959805622.

Olsson, L., H. Barbosa, S. Bhadwal, A. Cowie, K. Delusca, D. Flores-Renteria, K. Hermans, E. Jobbagy, W. Kurz, D. Li, D. J. Sonwa, L. Stringer, T. Crews, M. Dallimer, J. Eekhout, K. Erb, E. Haughey, R. Houghton, M. M. Iqbal, F. X. Johnson, W. K. Lee, J. Morton, F. G. Oliva, J. Petzold, M. Rahimi, F. Renou-Wilson, A. Tengberg, L. Verchot, K. Vincent, J. M. Moreno, C. Vera, A. S. Barau, L. Olsson, H. Barbosa, S. Bhadwal, A. Cowie, K. Delusca, D. Flores-Renteria, K. Hermans, E. Jobbagy, W. Kurz, D. Li, D. J. Sonwa and L. Stringer (2019). 'Land degradation'. In: *Climate Change and Land*. Cambridge University Press, pp. 345–436. DOI: 10.1017/9781009157988.006.

Ong, C., J. Corlett, R. Singh and C. Black (1991). 'Above and below ground interactions in agroforestry systems'. In: *Forest Ecology and Management* 45.1-4, pp. 45–57. DOI: 10.1016/0378-1127(91)90205-A.

Pachauri, R. K. (2012). 'Climate Change and Agroforestry'. In: *Agroforestry - The Future of Global Land Use. Advances in Agroforestry.* Ed. by P. Nair and D. Garrity. Vol. 9. Dordrecht: Springer, pp. 13–15. DOI: 10.1007/978-94-007-4676-3_4.

Pachepsky, Y. and W. Rawls (2003). 'Soil structure and pedotransfer functions'. In: *European Journal of Soil Science* 54.3, pp. 443–452. DOI: 10.1046/j.1365-2389.2003.00485.x.

Paradelo, R., F. van Oort and C. Chenu (2013). 'Water-dispersible clay in bare fallow soils after 80 years of continuous fertilizer addition'. In: *Geoderma* 200-201, pp. 40–44. DOI: 10.1016/j.geoderma.2013.01.014.

Paschalis, A., S. Bonetti, Y. Guo and S. Fatichi (2022). 'On the Uncertainty Induced by Pedotransfer Functions in Terrestrial Bio-

sphere Modeling'. In: *Water Resources Research* 58.9, pp. 1–18. DOI: 10.1029/2021WR031871.

Perrens, S. J. and K. K. Watson (1977). 'Numerical analysis of two-dimensional infiltration and redistribution'. In: *Water Resources Research* 13.4, pp. 781–790. DOI: 10.1029/WR013i004p00781.

Pertassek, T., A. Peters and W. Durner (2015). *HYPROP-FIT Software User's Manual, V.3.0*. Tech. rep. METER Group AG, p. 66.

Peters, A. (2014). 'Simple consistent models for water retention and hydraulic conductivity in the complete moisture range'. In: *Water Resources Research* 49.10, pp. 6765–6780. DOI: 10.1002/wrcr.20548.

Peters, A., W. Durner and S. Iden (2024). 'The PDI model system for parameterizing soil hydraulic properties'. In: *Vadose Zone Journal* 23.4, pp. 1–20. DOI: 10.1002/vzj2.20338.

Peters, A., T. L. Hohenbrink, S. C. Iden and W. Durner (2021). 'A Simple Model to Predict Hydraulic Conductivity in Medium to Dry Soil From the Water Retention Curve'. In: *Water Resources Research* 57.5. DOI: 10.1029/2020WR029211.

Philip, J. R. (1966). 'Plant Water Relations: Some Physical Aspects'. In: *Annual Review of Plant Physiology* 17.1, pp. 245–268. DOI: 10.1146/annurev.pp.17.060166.001333.

Plate, E. J. and E. Zehe (2008). *Hydrologie und Stoffdynamik kleiner Einzugsgebiete. Prozesse und Modelle*. Ed. by E. J. Plate and E. Zehe. Stuttgart, Germany: Schweizerbart'sche Verlagsbuchhandlung.

R. H. Brooks and A. T. Corey (1964). 'Hydraulic Properties of Porous Media and Their Relation to Drainage Design'. In: *Transactions of the ASAE* 7.1, pp. 0026–0028. DOI: 10.13031/2013.40684.

Ramachandran Nair, P. K., B. Mohan Kumar and V. D. Nair (2009). 'Agroforestry as a strategy for carbon sequestration'. In: *Journal of Plant Nutrition and Soil Science* 172.1, pp. 10–23. DOI: 10.1002/jpln.200800030.

Rasmussen, C., K. Heckman, W. R. Wieder, M. Keiluweit, C. R. Lawrence, A. A. Berhe, J. C. Blankinship, S. E. Crow, J. L. Druhan, C. E. Hicks Pries, E. Marin-Spiotta, A. F. Plante, C. Schädel, J. P. Schimel, C. A. Sierra, A. Thompson and R. Wagai (2018). 'Beyond clay: towards an improved set of variables for predicting soil organic matter content'. In: *Biogeochemistry* 137.3, pp. 297–306. DOI: 10.1007/s10533-018-0424-3.

Raumonen, P., M. Kaasalainen, Å. Markku, S. Kaasalainen, H. Kaartinen, M. Vastaranta, M. Holopainen, M. Disney and P. Lewis (2013). 'Fast automatic precision tree models from terrestrial laser scanner data'. In: *Remote Sensing* 5.2, pp. 491–520. DOI: 10.3390/rs5020491.

Raumonen, P. and M. Åkerblom (May 2022). *InverseTampere/TreeQSM: Version 2.4.1*. Version 2.4.1. DOI: 10.5281/zenodo.6539580.

Rawlins, S. L., W. R. Gardner and F. N. Dalton (1968). 'In Situ Measurement of Soil and Plant Leaf Water Potential'. In: *Soil Science*

Society of America Journal 32.4, pp. 468–470. DOI: 10.2136/sssaj1968.03615995003200040016x.

Rawls, W. J., Y. A. Pachepsky, J. C. Ritchie, T. M. Sobecki and H. Bloodworth (2003). 'Effect of soil organic carbon on soil water retention'. In: *Geoderma* 116.1-2, pp. 61–76. DOI: 10.1016/S0016-7061(03)00094-6.

Rawls, W., A. Nemes and Y. Pachepsky (2004). 'Effect of soil organic carbon on soil hydraulic properties'. In: *Development of Pedotransfer Functions in Soil Hydrology*. Vol. 30. Developments in Soil Science. Elsevier, pp. 95–114. DOI: https://doi.org/10.1016/S0166-2481(04)30006-1.

Ribeiro-Barros, A. I., M. J. Silva, I. Moura, J. C. Ramalho, C. Máguas-Hanson and N. S. Ribeiro (2017). 'The Potential of Tree and Shrub Legumes in Agroforestry Systems'. In: *Nitrogen in Agriculture*. Ed. by Amanullah and S. Fahad. Rijeka: IntechOpen. Chap. 12. DOI: 10.5772/intechopen.69995.

Richards, J. H. and M. M. Caldwell (1987). 'Hydraulic lift: Substantial nocturnal water transport between soil layers by Artemisia tridentata roots'. In: *Oecologia* 73.4, pp. 486–489. DOI: 10.1007/BF00379405.

Richards, L. A., R. B. Campbell and L. H. Healton (1950). 'Some Freezing Point Depression Measurements on Cores of Soil in Which Cotton and Sunflower Plants Were Wilted'. In: *Soil Science Society of America Journal* 14, pp. 47–50. DOI: 10.2136/sssaj1950.036159950014000C0011x.

Richards, L. A. and L. R. Weaver (1943). 'Fifteen-atomshpere percentage as related to the permanent wilting percentage'. In: *Soil Science* 56.5, pp. 331–340. DOI: 10.1097/00010694-194311000-00002.

Richet, J.-B., J.-F. Ouvry and M. Saunier (2017). 'The role of vegetative barriers such as fascines and dense shrub hedges in catchment management to reduce runoff and erosion effects: Experimental evidence of efficiency, and conditions of use'. In: *Ecological Engineering* 103, pp. 455–469. DOI: 10.1016/j.ecoleng.2016.08.008.

Rosenstock, T. S., I. K. Dawson, E. Aynekulu, S. Chomba, A. Degrande, K. Fornace, R. Jamnadass, A. Kimaro, R. Kindt, C. Lamanna, M. Malesu, K. Mausch, S. McMullin, P. Murage, N. Namoi, M. Njenga, I. Nyoka, A. M. Paez Valencia, P. Sola, K. Shepherd and P. Steward (2019). 'A Planetary Health Perspective on Agroforestry in Sub-Saharan Africa'. In: *One Earth* 1.3, pp. 330–344. DOI: 10.1016/j.oneear.2019.10.017.

Rosier, I., J. Diels, B. Somers and J. Van Orshoven (2023). 'The impact of vegetated landscape elements on runoff in a small agricultural watershed: A modelling study'. In: *Journal of Hydrology* 617, p. 129144. DOI: 10.1016/j.jhydrol.2023.129144.

Rosier, I., J. Diels, B. Somers and J. Van Orshoven (2024). 'Maximising runoff retention by vegetated landscape elements positioned

through spatial optimisation'. In: *Landscape and Urban Planning* 243, p. 104968. DOI: 10.1016/j.landurbplan.2023.104968.

Rubin, J. (1967). 'Numerical Method for Analyzing Hysteresis-Affected, Post-Infiltration Redistribution of Soil Moisture'. In: *Soil Science Society of America Journal* 31.1, pp. 13–20. DOI: 10.2136/sssaj1967.03615995003100010009x.

San-Miguel-Ayanz, J., D. de Rigo, G. Caudullo, T. Houston Durrant and A. Mauri, eds. (2016). *European atlas of forest tree species*. Luxembourg: Publications Office of the European Union. DOI: 10.2760/776635.

Savage, M. J., J. T. Ritchie, W. L. Bland and W. A. Dugas (1996). 'Lower Limit of Soil Water Availability'. In: *Agronomy Journal* 88.4, pp. 644–651. DOI: 10.2134/agronj1996.00021962008800040024x.

Schaefli, B and E Zehe (2009). 'Hydrological model performance and parameter estimation in the wavelet-domain'. In: *Hydrology and Earth System Sciences* 13.10, pp. 1921–1936. DOI: 10.5194/hess-13-1921-2009.

Schaik, L. van, J. Palm, J. Klaus, E. Zehe and B. Schröder (2014). 'Linking spatial earthworm distribution to macropore numbers and hydrological effectiveness'. In: *Ecohydrology* 7.2, pp. 401–408. DOI: 10.1002/eco.1358.

Scheffer, F. and P. Schachtschabel (1992). *Lehrbuch der Bodenkunde*. Stuttgart: Enke Verlag.

Schneider, C. L., S. Attinger, J.-O. Delfs and A. Hildebrandt (2010). 'Implementing small scale processes at the soil-plant interface – the role of root architectures for calculating root water uptake profiles'. In: *Hydrology and Earth System Sciences* 14.2, pp. 279–289. DOI: 10.5194/hess-14-279-2010.

Schroth, G. (1999). 'A review of belowground interactions in agroforestry, focussing on mechanisms and management options'. In: *Agroforestry Systems* 43, pp. 5–34. DOI: 10.1023/a:1026443018920.

Schumacher, J. and J. R. Christiansen (2020). 'LiDAR Applications to Forest-Water Interactions.' In: *Forest-water interactions*. Ed. by D. F. Levia, J. G. Canadell, S. Díaz, G. Heldmaier, R. B. Jackson, E.-D. Schulze, U. Sommer and D. A. Wardle. Vol. 240. Cham, Switzerland: Springer, pp. 87–112.

Schweizer, S. A., C. W. Mueller, C. Höschen, P. Ivanov and I. Kögel-Knabner (2021). 'The role of clay content and mineral surface area for soil organic carbon storage in an arable toposequence'. In: *Biogeochemistry* 156.3, pp. 401–420. DOI: 10.1007/s10533-021-00850-3.

Scott, H. D. (2000). *Soil physics: agricultural and environmental applications*. 1st ed. Ames, Iowa: Iowa State University Press.

Seibert, S. P., U. Ehret and E. Zehe (2016). 'Disentangling timing and amplitude errors in streamflow simulations'. In: *Hydrology and*

Earth System Sciences 20.9, pp. 3745–3763. DOI: 10.5194/hess-20-3745-2016.

Sekiya, N., H. Araki and K. Yano (2011). 'Applying hydraulic lift in an agroecosystem: Forage plants with shoots removed supply water to neighboring vegetable crops'. In: *Plant and Soil* 341.1-2, pp. 39–50. DOI: 10.1007/s11104-010-0581-1.

Seneviratne, S. I., T. Corti, E. L. Davin, M. Hirschi, E. B. Jaeger, I. Lehner, B. Orlowsky and A. J. Teuling (2010). 'Investigating soil moisture–climate interactions in a changing climate: A review'. In: *Earth-Science Reviews* 99.3, pp. 125–161. DOI: 10.1016/j.earscirev.2010.02.004.

Shao, Y., ed. (2008). *Physics and Modelling of Wind Erosion*. Vol. 37. Atmospheric and Oceanographic Sciences Library. Dordrecht: Springer Netherlands. DOI: 10.1007/978-1-4020-8895-7.

Sheppard, J. P., R. Bohn Reckziegel, L. Borrass, P. W. Chirwa, C. J. Cuaranhua, S. K. Hassler, S. Hoffmeister, F. Kestel, R. Maier, M. Mälicke, C. Morhart, N. P. Ndlovu, M. Veste, R. Funk, F. Lang, T. Seifert, B. du Toit and H.-P. Kahle (2020a). 'Agroforestry: An Appropriate and Sustainable Response to a Changing Climate in Southern Africa?' In: *Sustainability* 12.17, p. 6796. DOI: 10.3390/su12176796.

Sheppard, J. P., J. Chamberlain, D. Agúndez, P. Bhattacharya, P. W. Chirwa, A. Gontcharov, W. C. J. Sagona, H. long Shen, W. Tadesse and S. Mutke (2020b). 'Sustainable Forest Management Beyond the Timber-Oriented Status Quo: Transitioning to Co-production of Timber and Non-wood Forest Products—a Global Perspective'. In: *Current Forestry Reports* 6.1, pp. 26–40. DOI: 10.1007/s40725-019-00107-1.

Sheppard, J. P., E. Larysch, C. J. Cuaranhua, Z. Schindler, B. du Toit, G. F. Malherbe, A. Kunneke, C. Morhart, R. Bohn Reckziegel, T. Seifert and H.-P. Kahle (2024). 'Assessment of biomass and carbon storage of a Populus simonii windbreak located in the Western Cape Province, South Africa'. In: *Agroforestry Systems*. DOI: 10.1007/s10457-023-00940-1.

Shi, L., W. Feng, J. Xu and Y. Kuzyakov (2018). 'Agroforestry systems: Meta-analysis of soil carbon stocks, sequestration processes, and future potentials'. In: *Land Degradation and Development* 29.11, pp. 3886–3897. DOI: 10.1002/ldr.3136.

Sileshi, G. W., F. K. Akinnifesi, P. L. Mafongoya, E. Kuntashula and O. C. Ajayi (2020). 'Potential of Gliricidia-Based Agroforestry Systems for Resource-Limited Agroecosystems'. In: *Agroforestry for Degraded Landscapes*. Singapore: Springer Singapore, pp. 255–282. DOI: 10.1007/978-981-15-4136-0_9.

Sileshi, G. W., P. L. Mafongoya, F. K. Akinnifesi, E. Phiri, P. Chirwa, T. Beedy, W. Makumba, G. Nyamadzawo, J. Njoloma, M. Wuta, P. Nyamugafata and O. Jiri (2014). 'Agroforestry: Fertilizer Trees'. In:

Encyclopedia of Agriculture and Food Systems. Elsevier, pp. 222–234. DOI: 10.1016/B978-0-444-52512-3.00022-X.

Silvertown, J., Y. Araya and D. Gowing (2015). 'Hydrological niches in terrestrial plant communities: a review'. In: *Journal of Ecology* 103.1. Ed. by W. Cornwell, pp. 93–108. DOI: 10.1111/1365-2745.12332.

Singh, R. P., N. Saharan and C. K. Ong (1989). 'Above and below ground interactions in alley-cropping in semi-arid India'. In: *Agroforestry Systems* 9.3, pp. 259–274. DOI: 10.1007/BF00141088.

Siriri, D., J. Wilson, R. Coe, M. M. Tenywa, M. A. Bekunda, C. K. Ong and C. R. Black (2013). 'Trees improve water storage and reduce soil evaporation in agroforestry systems on bench terraces in SW Uganda'. In: *Agroforestry Systems* 87.1, pp. 45–58. DOI: 10.1007/s10457-012-9520-x.

Six, J, R. T. Conant, E. A. Paul and K Paustian (2002). 'Stabilization mechanisms of SOM implications for C saturation of soils.pdf'. In: *Plant and soil* 241.2, pp. 155–176. DOI: 10.1023/A:1016125726789. arXiv: 0005074v1 [arXiv:astro-ph].

Smith, M. M., G. Bentrup, T. Kellerman, K. MacFarland, R. Straight and L. Ameyaw (2021). 'Windbreaks in the United States: A systematic review of producer-reported benefits, challenges, management activities and drivers of adoption'. In: *Agricultural Systems* 187, p. 103032. DOI: 10.1016/j.agsy.2020.103032.

Stallone, A., A. Cicone and M. Materassi (2020). 'New insights and best practices for the successful use of Empirical Mode Decomposition, Iterative Filtering and derived algorithms'. In: *Scientific Reports* 10.1, p. 15161. DOI: 10.1038/s41598-020-72193-2.

Sternagel, A., R. Loritz, W. Wilcke and E. Zehe (2019). 'Simulating preferential soil water flow and tracer transport using the Lagrangian Soil Water and Solute Transport Model'. In: *Hydrology and Earth System Sciences* 23.10, pp. 4249–4267. DOI: 10.5194/hess-23-4249-2019.

Stewart, C. E., K. Paustian, R. T. Conant, A. F. Plante and J. Six (2008). 'Soil carbon saturation: Evaluation and corroboration by long-term incubations'. In: *Soil Biology and Biochemistry* 40.7, pp. 1741–1750. DOI: 10.1016/j.soilbio.2008.02.014.

Thomas, S. C. and A. R. Martin (2012). 'Carbon Content of Tree Tissues: A Synthesis'. In: *Forests* 3.2, pp. 332–352. DOI: 10.3390/f3020332.

Tietjen, B., F. Jeltsch, E. Zehe, N. Classen, A. Groengroeft, K. Schiffers and J. Oldeland (2010). 'Effects of climate change on the coupled dynamics of water and vegetation in drylands'. In: *Ecohydrology* 3.2, pp. 226–237. DOI: 10.1002/eco.70.

Torres, M. E., M. A. Colominas, G. Schlotthauer and P. Flandrin (2011). 'A complete ensemble empirical mode decomposition with adaptive noise'. In: *2011 IEEE International Conference on Acoustics, Speech and Signal Processing (ICASSP)*, pp. 4144–4147. DOI: 10.1109/ICASSP.2011.5947265.

Trisos, C., I. Adelekan, E. Totin, A. Ayanlade, J. Efitre, A. Gemeda, K. Kalaba, C. Lennard, C. Masao, Y. Mgaya, G. Ngaruiya, D. Olago, N. Simpson and S. Zakieldeen (2022). 'Africa'. In: *Climate Change 2022: Impacts, Adaptation and Vulnerability. Contribution of Working Group II to the Sixth Assessment Report of the Intergovernmental Panel on Climate Change*. Ed. by H.-O. Pörtner, D. Roberts, M. Tignor, E. Poloczanska, K. Mintenbeck, A. Alegría, M. Craig, S. Langsdorf, S. Löschke, V. Möller, A. Okem and B. Rama. Cambridge, UK and New York, NY, USA: Cambridge University Press, pp. 1285–1455. DOI: 10.1017/9781009325844.011.

Tumushabe, J. T. (2018). 'Climate Change, Food Security and Sustainable Development in Africa'. In: *The Palgrave Handbook of African Politics, Governance and Development*. Ed. by T. Oloruntoba, S.O., Falola. New York: Palgrave Macmillan US, pp. 853–868. DOI: 10.1057/978-1-349-95232-8_53.

University of Stellenbosch (2023). *Stellenbosch Weather*. URL: http://weather.sun.ca.za/ (visited on 03/04/2023).

Van Eimern, J., R. Karschon, L. A. Razumova and G. W. Robertson (1964). *Windbreaks and shelterbelts: report of a working group of the Commission for Agricultural Meteorology*. Tech. rep. World Meteorol. Org. Tech. Note No. 59, p. 191.

Van Genuchten, M. T. (1980). 'A Closed-form Equation for Predicting the Hydraulic Conductivity of Unsaturated Soils'. In: *Soil Science Society of America Journal* 44.5, pp. 892–898. DOI: 10.2136/sssaj1980.03615995004400050002x.

Van Noordwijk, M. and B. Lusiana (1998). 'WaNulCAS, a model of water, nutrient and light capture in agroforestry systems'. In: *Agroforestry Systems* 43.1-3, pp. 217–242. DOI: 10.1023/a:1026417120254.

Veste, M., T. Littmann, A. Kunneke, B. du Toit and T. Seifert (2020). 'Windbreaks as part of climate-smart landscapes reduce evapotranspiration in vineyards, Western Cape Province, South Africa'. In: *Plant, Soil and Environment* 66.No. 3, pp. 119–127. DOI: 10.17221/616/2019-PSE.

Villinger, F., R. Loritz and E. Zehe (2022). 'Physikalisch-basierte Simulation einer abgelaufenen Sturzflut mittels "repräsentativer Hänge" in einem ländlichen Einzugsgebiet'. In: *Hydrologie und Wasserbewirtschaftung* 66.6, pp. 286–297. DOI: 10.5675/HyWa_2022.6_1.

Ward, A. S. and A. I. Packman (2019). 'Advancing our predictive understanding of river corridor exchange'. In: *WIREs Water* 6.1, pp. 1–17. DOI: 10.1002/wat2.1327.

Weber, T. K. D., L. Weihermüller, A. Nemes, M. Bechtold, A. Degré, E. Diamantopoulos, S. Fatichi, V. Filipović, S. Gupta, T. L. Hohenbrink, D. R. Hirmas, C. Jackisch, Q. de Jong van Lier, J. Koestel, P. Lehmann, T. R. Marthews, B. Minasny, H. Pagel, M. van der Ploeg, S. A. Shojaeezadeh, S. F. Svane, B. Szabó, H. Vereecken, A. Verhoef, M. Young, Y. Zeng, Y. Zhang and S. Bonetti (2024).

'Hydro-pedotransfer functions: a roadmap for future development'. In: *Hydrology and Earth System Sciences* 28.14, pp. 3391–3433. DOI: 10.5194/hess-28-3391-2024.

Weihermüller, L., P. Lehmann, M. Herbst, M. Rahmati, A. Verhoef, D. Or, D. Jacques and H. Vereecken (2021). 'Choice of Pedotransfer Functions Matters when Simulating Soil Water Balance Fluxes'. In: *Journal of Advances in Modeling Earth Systems* 13.3, pp. 1–30. DOI: 10.1029/2020MS002404.

Werf, W. van der, K. Keesman, P. Burgess, A. Graves, D. Pilbeam, L. Incoll, K. Metselaar, M. Mayus, R. Stappers, H. van Keulen, J. Palma and C. Dupraz (2007). 'Yield-SAFE: A parameter-sparse, process-based dynamic model for predicting resource capture, growth, and production in agroforestry systems'. In: *Ecological Engineering* 29.4, pp. 419–433. DOI: 10.1016/j.ecoleng.2006.09.017.

Whalley, W. R., E. S. Ober and M. Jenkins (2013). 'Measurement of the matric potential of soil water in the rhizosphere'. In: *Journal of Experimental Botany* 64.13, pp. 3951–3963. DOI: 10.1093/jxb/ert044.

Wiecheteck, L. H., N. F. Giarola, R. P. de Lima, C. A. Tormena, L. C. Torres and A. L. de Paula (2020). 'Comparing the classical permanent wilting point concept of soil (-15,000 hPa) to biological wilting of wheat and barley plants under contrasting soil textures'. In: *Agricultural Water Management* 230, p. 105965. DOI: 10.1016/j.agwat.2019.105965.

Wienhöfer, J. and E. Zehe (2014). 'Predicting subsurface stormflow response of a forested hillslope – the role of connected flow paths'. In: *Hydrology and Earth System Sciences* 18.1, pp. 121–138. DOI: 10.5194/hess-18-121-2014.

Wilkes, P., A. Lau, M. Disney, K. Calders, A. Burt, J. Gonzalez de Tanago, H. Bartholomeus, B. Brede and M. Herold (2017). 'Data acquisition considerations for Terrestrial Laser Scanning of forest plots'. In: *Remote Sensing of Environment* 196, pp. 140–153. DOI: 10.1016/j.rse.2017.04.030.

Williams, J, R. Prebble, W. Williams and C. Hignett (1983). 'The influence of texture, structure and clay mineralogy on the soil moisture characteristic'. In: *Soil Research* 21.1, p. 15. DOI: 10.1071/SR9830015.

Wilson, M. H. and S. T. Lovell (2016). 'Agroforestry-The next step in sustainable and resilient agriculture'. In: *Sustainability (Switzerland)* 8.6. DOI: 10.3390/su8060574.

World Agroforestry (2023). *Worldwide 'open access' tree functional attributes and ecological database*. URL: http://db.worldagroforestry.org/ (visited on 14/08/2023).

World Food Programme (2019). *End-of-Season Update for 2018/19 and Overview of the Food Security Situation in 2019/20*.

Wu, J., W. Liu and C. Chen (2016). 'Below-ground interspecific competition for water in a rubber agroforestry system may enhance

water utilization in plants'. In: *Scientific Reports* 6. DOI: 10.1038/srep19502.

Yao, N., Y. Li, F. Xu, J. Liu, S. Chen, H. Ma, H. Wai Chau, D. L. Liu, M. Li, H. Feng, Q. Yu and J. He (2020). 'Permanent wilting point plays an important role in simulating winter wheat growth under water deficit conditions'. In: *Agricultural Water Management* 229.September 2019. DOI: 10.1016/j.agwat.2019.105954.

Zehe, E., U. Ehret, L. Pfister, T. Blume, B. Schröder, M. Westhoff, C. Jackisch, S. J. Schymanski, M. Weiler, K. Schulz, N. Allroggen, J. Tronicke, L. van Schaik, P. Dietrich, U. Scherer, J. Eccard, V. Wulfmeyer and A. Kleidon (2014). 'HESS Opinions: From response units to functional units: a thermodynamic reinterpretation of the HRU concept to link spatial organization and functioning of intermediate scale catchments'. In: *Hydrology and Earth System Sciences* 18.11, pp. 4635–4655. DOI: 10.5194/hess-18-4635-2014.

Zehe, E., T. Graeff, M. Morgner, A. Bauer and A. Bronstert (2010). 'Plot and field scale soil moisture dynamics and subsurface wetness control on runoff generation in a headwater in the Ore Mountains'. In: *Hydrology and Earth System Sciences* 14.6, pp. 873–889. DOI: 10.5194/hess-14-873-2010.

Zehe, E., T. Maurer, J. Ihringer and E. Plate (2001). 'Modeling water flow and mass transport in a loess catchment'. In: *Physics and Chemistry of the Earth, Part B: Hydrology, Oceans and Atmosphere* 26.7-8, pp. 487–507. DOI: 10.1016/S1464-1909(01)00041-7.

Zehe, E. and G. Blöschl (2004). 'Predictability of hydrologic response at the plot and catchment scales: Role of initial conditions'. In: *Water Resources Research* 40.10, pp. 1–21. DOI: 10.1029/2003WR002869.

Zehe, E. and C. Jackisch (2016). 'A Lagrangian model for soil water dynamics during rainfall-driven conditions'. In: *Hydrology and Earth System Sciences* 20.9, pp. 3511–3526. DOI: 10.5194/hess-20-3511-2016.

Zhang, X., G. Feng and X. Sun (2024). 'Advanced technologies of soil moisture monitoring in precision agriculture: A Review'. In: *Journal of Agriculture and Food Research* 18, p. 101473. DOI: 10.1016/j.jafr.2024.101473.

ACKNOWLEDGMENTS

There are so many people to whom I owe immense gratitude, as this work would not have been possible without their unwavering support and contributions. I am deeply thankful for both my professional and personal environments, which have been essential in shaping this journey.

To Prof. Dr. Erwin Zehe, thank you, Erwin, for the enriching discussions, your steadfast support of my ideas and plans, and your guidance during the challenges of COVID-19. You create a trust-based working environment that allowed me to explore and grow in many directions, and for that, I am truly grateful.

To Prof. Dr. Anke Hildebrandt, thank you, Anke, for your support as my "Koreferentin" and for being such an inspiring role model. I am eager for the possibility of collaborating with you more in the future!

To the ASAP team, thank you for your unwavering support across various tasks. A special thanks to Jon for coordinating the project and proofreading, and to Ben, Anton, Isaac, Mafongo, and Charles for helping with field site logistics, sharing your knowledge, and assisting with last-minute equipment needs and maintenance. This project would not have been possible without your dedication and expertise. I feel incredibly fortunate to have been part of this project, which allowed me to explore new parts of the world, work in fascinating ecosystems, and connect with so many amazing people.

To Sibylle and Rebekka, thank you for your adventurous spirit and the joy you brought to fieldwork. From your boundless creativity in finding solutions to your determination and persistence, especially in pushing through the trip to Malawi. Thank you for shared laughter and tears and for creating so many memorable moments, and of course also for sharing your knowledge and experience.

To Conrad, Mirko, and Jan, I am so grateful for your technical ingenuity. Thank you for teaching me all the creative ways to connect sensors, solder cables, manage power supplies and data transmission. Conrad, your endless discussions about field site advantages and sensor network setups were pivotal.

To all my colleagues and former colleagues in our group, thank

you for making daily work life so enjoyable and for the encouraging and supportive environment you create. To Raziye, thank you for your meticulous work in analysing samples and maintaining the lab equipment.

To my ”Lieblingsmenschen”, my family and my friends. Thank you for being my rock, my role models, and my source of endless inspiration and support!

THANK YOU! VIELEN DANK! BAIE DANKIE! ZIKOMO!

OWN PUBLICATIONS

FIRST AUTHOR; PEER-REVIEWED INTERNATIONAL PUBLICATIONS

Hoffmeister, S., Bohn Reckziegel, R., du Toit, B., Hassler, S. K., Kestel, F., Maier, R., Sheppard, J. P., and Zehe, E. (2024). "Hydrological and pedological effects of combining Italian alder and blackberries in an agroforestry windbreak system in South Africa." In: *Hydrology and Earth System Sciences* 28, pp. 3963–3982. https://doi.org/10.5194/hess-28-3963-2024.

Hoffmeister, S., Hassler, S. K., Lang, F., Maier, R., Nyoka, I., Zehe, E. "Influence of carbon input on soil physical and hydrological properties in two agroforestry systems in Malawi." Manuscript.

Hoffmeister, S., Wienhöfer, J. and Zehe, E. "The role of water retention and permanent wilting point parametrization in process-based modelling of soil water dynamics." Manuscript.

CO-AUTHOR; PEER-REVIEWED INTERNATIONAL PUBLICATIONS

Sheppard, J. P., Bohn Reckziegel, R., Borrass, L., Chirwa, P. W., Cuaranhua, C. J., Hassler, S. K., **Hoffmeister, S.**, Kestel, F., Maier, R., Mälicke, M., Morhart, C., Ndlovu, N. P., Veste, M., Funk, R., Lang, F., Seifert, T., du Toit, B., and Kahle, H.-P. (2020) "Agroforestry: An Appropriate and Sustainable Response to a Changing Climate in Southern Africa?" In: *Sustainability* 12, 17, pp. 6796, https://doi.org/10.3390/su12176796.

Hassler, S. K., Bohn Reckziegel, R., du Toit, B., **Hoffmeister, S.**, Kestel, F., Kunneke, A., Maier, R., and Sheppard, J. P. (2024) "Multivariate characterisation of a blackberry–alder agroforestry system in South Africa: hydrological, pedological, dendrological and meteorological measurements" In: *Earth Syst. Sci. Data* 16, 9, pp. 3935–3948, https://doi.org/10.5194/essd-16-3935-2024.

van Hateren, T. C., Jongen, H. J., Al-Zawaidah, H., Beemster, J. G. W., Boekee, J., Bogerd, L., Gao, S., Kannen, C., van Meerveld, I., de Lange, S. I., Linke, F., Pinto, R. B., Remmers, J. O. E., Ruijsch, J., Rusli, S. R., van de Vijsel, R. C., Aerts, J. P. M., Agoungbome, S. M. D., Anys, M., Blanco Ramírez, S., van Emmerik, T., Gallitelli, L., Chiquito Gesualdo, G., Gonzalez Otero, W., Hanus, S., He, Z., **Hoffmeister, S.**, Imhoff, R. O., Kerlin, T., Meshram, S. M., Meyer, J., Meyer Oliveira, A., Müller, A. C. T., Nijzink, R., Scheller, M., Schreyers, L., Sehgal, D., Tasseron, P. F.,

Teuling, A. J., Trevisson, M., Waldschläger, K., Walraven, B., Wannasin, C., Wienhöfer, J., Zander, M. J., Zhang, S., Zhou, J., Zomer, J. Y., and Zwartendijk, B. W. (2023) "Where should hydrology go? An early-career perspective on the next IAHS Scientific Decade" In: *Hydrol. Sci. J.* 68, 4, pp. 529–541, https://doi.org/10.1080/02626667.2023.2170754.

DECLARATION

Authors contributions:

Section 2: Hoffmeister, S., Bohn Reckziegel, R., du Toit, B., Hassler, S. K., Kestel, F., Maier, R., Sheppard, J. P., and Zehe, E. (2024). "Hydrological and pedological effects of combining Italian alder and blackberries in an agroforestry windbreak system in South Africa." In: *Hydrology and Earth System Sciences* 28, pp. 3963–3982. https://doi.org/10.5194/hess-28-3963-2024.

Svenja Hoffmeister (SH) was responsible for the primary writing, data analysis, and figure creation. SH, RBR, BdT, SKH, FK, RM and JPS designed their respective field methods, conducted the field work and initially analysed the acquired data. SH and SKH collected all soil water related data in the field and curated the data of all the authors. SH and EZ prepared the manuscript with contributions from all co-authors.

Section 3: Hoffmeister, S., Hassler, S. K., Lang, F., Maier, R., Nyoka, I., Zehe, E. "Influence of carbon input on soil physical and hydrological properties in two agroforestry systems in Malawi." Manuscript.

Svenja Hoffmeister (SH), SHK and RM designed the field work and collected the data. SH and SHK designed and wrote the manuscript outline. SH conducted the analyses and figures. RM, EZ, IN, FL support with their expertise on respective parts of the paper.

Section 4: Hoffmeister, S., Wienhöfer, J. and Zehe, E. "The role of water retention and permanent wilting point parametrization in process-based modelling of soil water dynamics." Manuscript.

Svenja Hoffmeister (SH), JW and EZ developed the ideas of the study and designed the manuscript outline. SH conducted the analyses and figures. SH, JW and EZ prepared the manuscript.

Eidesstattliche Versicherung gemäß § 13 Absatz 2 Satz 1 Ziffer 4 der Promotionsordnung des Karlsruher Instituts für Technologie (KIT) für die KIT-Fakultät für Bauingenieur-, Geo- und Umweltwissenschaften:

1. Bei der eingereichten Dissertation zu dem Thema *Soil water interactions in Southern African agroforestry systems* handelt es sich um meine eigenständig erbrachte Leistung.

2. Ich habe nur die angegebenen Quellen und Hilfsmittel benutzt und mich keiner unzulässigen Hilfe Dritter bedient. Insbesondere habe ich wörtlich oder sinngemäß aus anderen Werken übernommene Inhalte als solche kenntlich gemacht.

3. Die Arbeit oder Teile davon habe ich bislang nicht an einer Hochschule des In- oder Auslands als Bestandteil einer Prüfungs- oder Qualifikationsleistung vorgelegt.

4. Die Richtigkeit der vorstehenden Erklärungen bestätige ich.

5. Die Bedeutung der eidesstattlichen Versicherung und die strafrechtlichen Folgen einer unrichtigen oder unvollständigen eidesstattlichen Versicherung sind mir bekannt.

Ich versichere an Eides statt, dass ich nach bestem Wissen die reine Wahrheit erklärt und nichts verschwiegen habe.

Karlsruhe, 2025

Svenja-Maria Hoffmeister

COLOPHON

This document was typeset using the typographical look-and-feel classicthesis developed by André Miede. The style was inspired by Robert Bringhurst's seminal book on typography *"The Elements of Typographic Style"*. classicthesis is available for both LaTeX and LyX:

https://bitbucket.org/amiede/classicthesis/

Happy users of classicthesis usually send a real postcard to the author, a collection of postcards received so far is featured here:

http://postcards.miede.de/

Final Version as of 12th December 2025 (classicthesis v4.6).